INFRASTRUTTURE VIARIE IN SOTTERRANEO

CARATTERIZZAZIONE GEOTECNICA

Prof. Ing. Geol. Eugenio Castelli

ecastelli@units.it

EVALUATION OF ENGINEERING GEOLOGY DATA
INTACT ROCK
DISCONTINUITIES
SHEAR STRENGTH OF DISCONTINUITIES

Interaction 1,2
ROCK STRUCTURE / STRESS
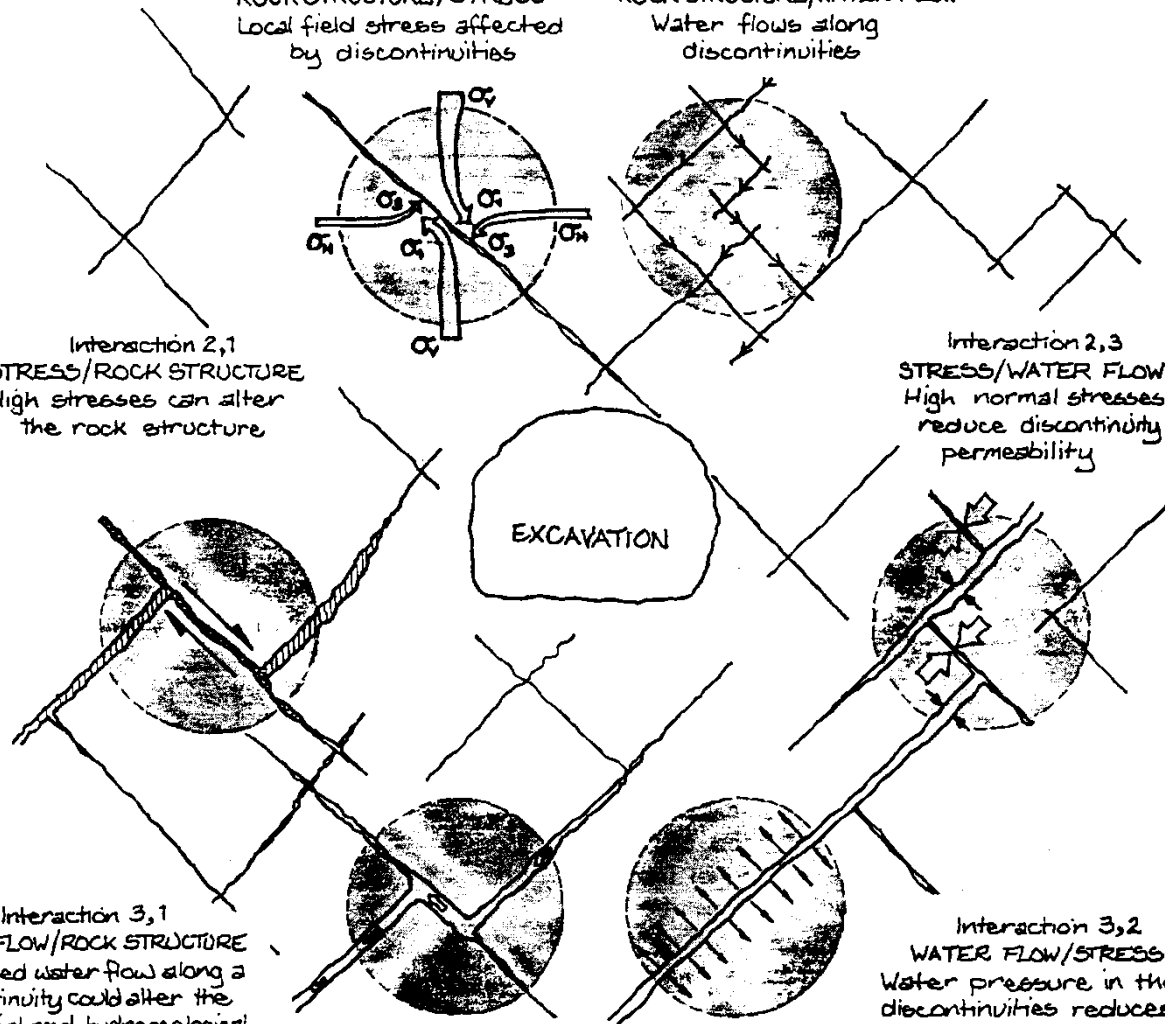Local field stress affected
by discontinuities

Interaction 1,3
ROCK STRUCTURE/WATER FLOW
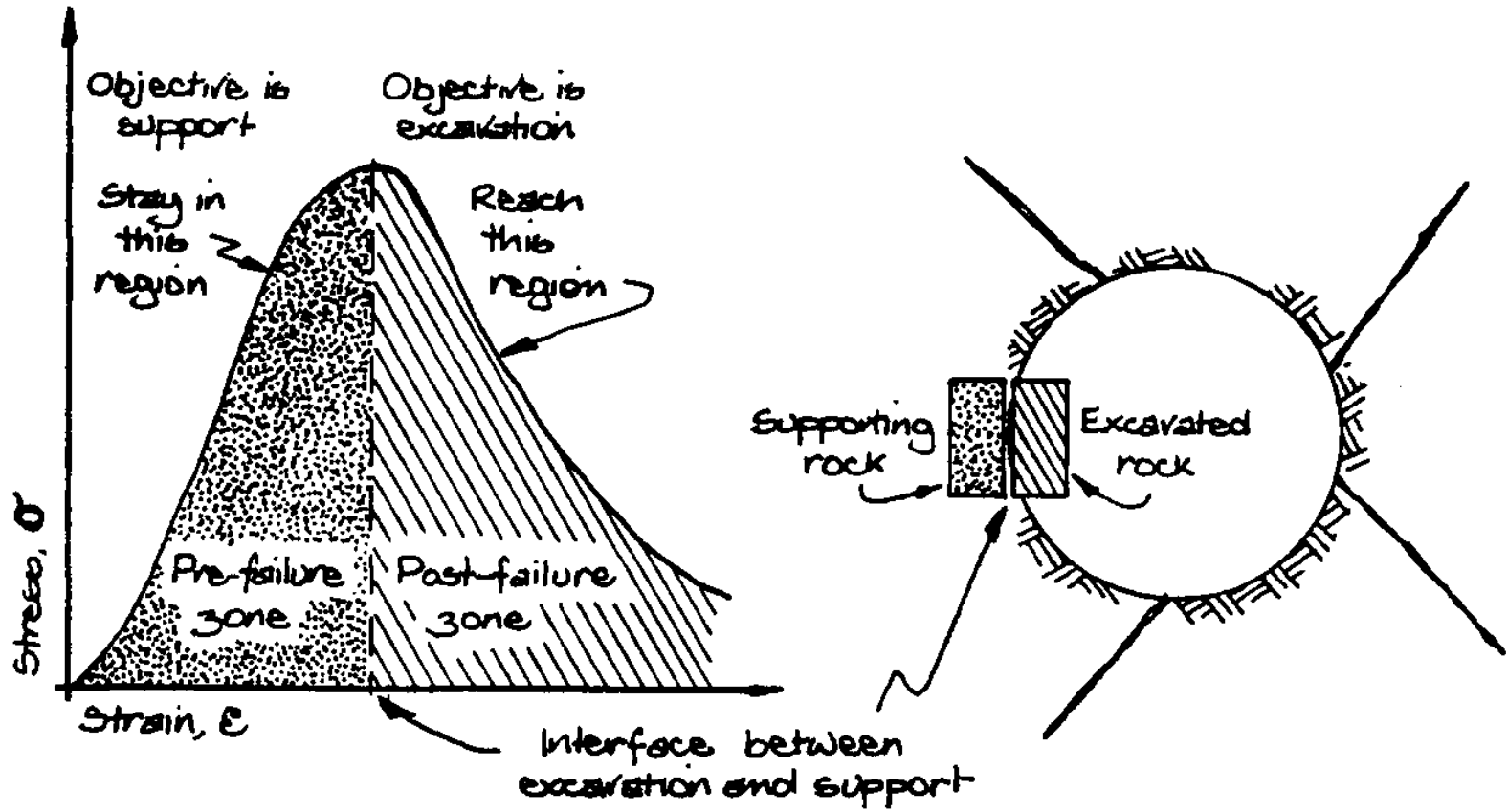Water flows along
discontinuities

Interaction 2,1
STRESS/ROCK STRUCTURE
High stresses can alter
the rock structure

Interaction 2,3
STRESS/WATER FLOW
High normal stresses
reduce discontinuity
permeability

EXCAVATION

Interaction 3,1
WATER FLOW/ROCK STRUCTURE
Continued water flow along a
discontinuity could alter the
mechanical and hydrogeological
properties

Interaction 3,2
WATER FLOW/STRESS
Water pressure in the
discontinuities reduces
the normal stress

Left diagram (stress-strain curve):

Stress, σ (vertical axis) vs Strain, ε (horizontal axis)

Objective is support

Objective is excavation

Stay in this region

Reach this region

Pre-failure zone

Post-failure zone

Interface between excavation and support

Right diagram (circular tunnel cross-section):

Supporting rock

Excavated rock

La progettazione geotecnica si sviluppa secondo le fasi di seguito elencate:

- Identificazione geologica e geotecnica del sito: ciò comporta la definizione del cosiddetto profilo geologico e geotecnico.
- Caratterizzazione geotecnica dell'ammasso roccioso: è finalizzata alla individuazione dei parametri utili alla progettazione dell'opera, in accordo al modello geotecnico scelto.
- Modellizzazione ed analisi: sono finalizzate alla previsione del comportamento tensio-deformativo dell'ammasso roccioso allo scavo, sia in assenza (condizioni intrinseche) che in presenza dei sostegni e degli interventi di stabilizzazione/rinforzo/consolidamento.
- Monitoraggio: è finalizzato alla misura delle grandezze (spostamenti, pressioni, livelli piezometrici, ecc.) da osservare in corso d'opera e alla verifica del complesso opera-ammasso roccioso, in esercizio.

2. OBIETTIVI DELLA CARATTERIZZAZIONE GEOTECNICA

In sintesi, si può affermare che il successo nella progettazione di una galleria dipende dall'abilità del progettista nel prevedere le condizioni dell'ammasso roccioso in profondità con particolare riguardo al comportamento tensio-deformativo ed alla risposta in presenza dei sostegni messi in atto durante la costruzione. Le condizioni reali dell'ammasso roccioso devono essere trasformate in un modello interpretativo, possibilmente semplice, collegando l'acquisizione dei dati relativi al sottosuolo e lo stesso modello con la realtà fisica.

Lo scopo della caratterizzazione geotecnica è dunque quello di individuare, lungo il tracciato scelto ed in coerenza con il modello geologico-strutturale ricostruito (capitolo 1):

- le zone omogenee interessate dallo scavo ed i parametri geotecnici che si prevede di utilizzare per il progetto e per il controllo dell'opera nel suo insieme ed in rapporto all'ammasso roccioso;
- il modello geotecnico che sarà utilizzato nei calcoli di progetto, con riferimento sia alle fasi di costruzione che alla fase definitiva;
- l'eventuale presenza di falde acquifere, i moti di filtrazione ed il regime delle pressioni neutre nella zona interessata dallo scavo.

A tal fine saranno eseguiti rilievi, indagini e prove che dovranno riguardare la parte del sottosuolo influenzata, direttamente o indirettamente, dalla costruzione della galleria e che ne determina il comportamento. Tali attività devono essere portate a termine in tempi utili alla compilazione del progetto. È tuttavia implicita nella impostazione che sarà data al progetto stesso, anche in relazione alla complessità della situazione geologica emersa dalle relative indagini, l'esigenza di verificare le ipotesi assunte sulla base delle osservazioni e dei dati che saranno raccolti nel corso dei lavori.
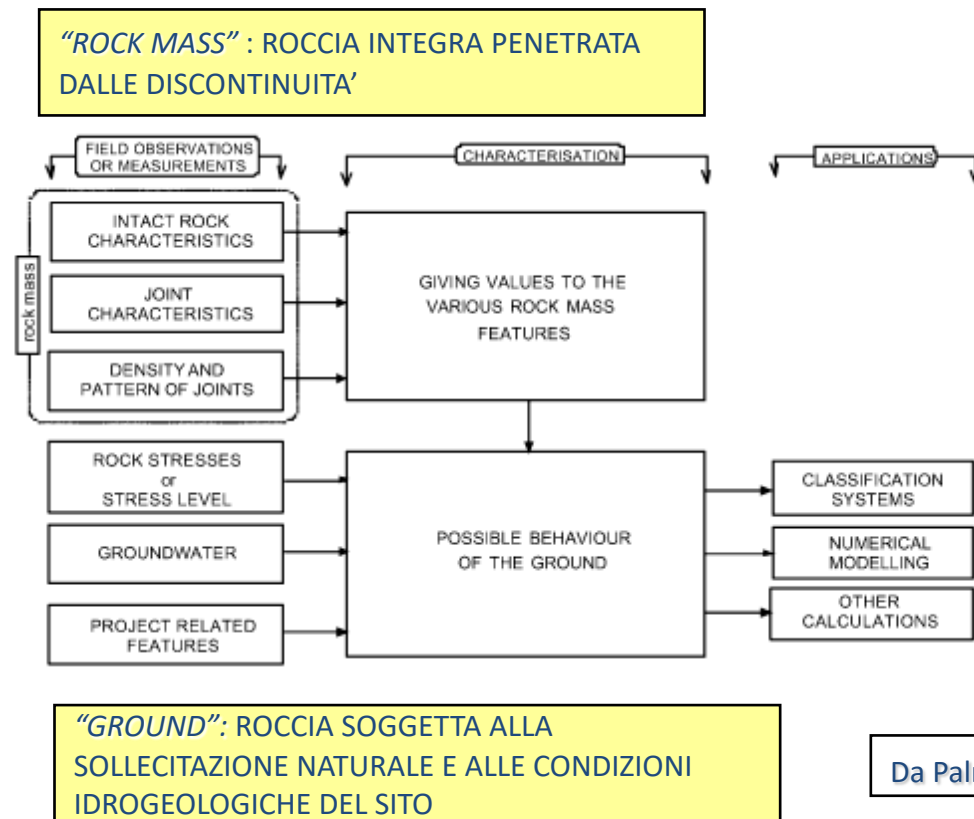
PRINCIPALI DIFFICOLTA' DEL PROGETTISTA

INCERTEZZA LEGATA ALLE DIFFICOLTA' TECNOLOGICHE ED ECONOMICHE NELL'INDAGARE L'AMMASSO ROCCIOSO
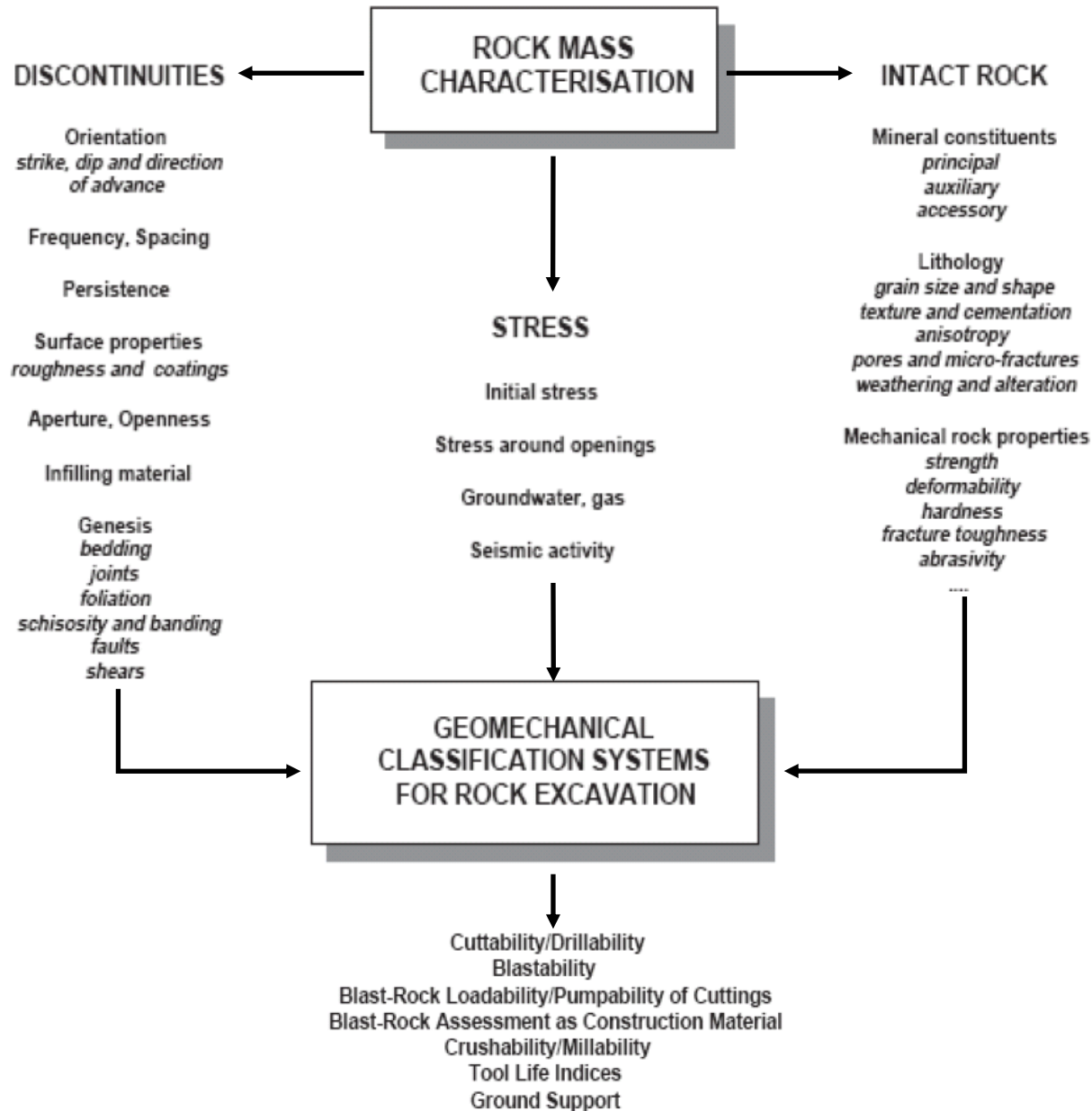
INCERTEZZA DEL MEZZO IN CUI VA AD OPERARE DOVUTO A:

1. ETEROGENEITA' STRUTTURALE

2. PRESENZA DI ACQUA E GAS

3. STATO TENSIONALE ORIGINARIO

"ROCK MASS" : ROCCIA INTEGRA PENETRATA DALLE DISCONTINUITA'

FIELD OBSERVATIONS OR MEASUREMENTS — CHARACTERISATION — APPLICATIONS

rock mass

INTACT ROCK CHARACTERISTICS

JOINT CHARACTERISTICS

DENSITY AND PATTERN OF JOINTS

GIVING VALUES TO THE VARIOUS ROCK MASS FEATURES

ROCK STRESSES or STRESS LEVEL

GROUNDWATER

PROJECT RELATED FEATURES

POSSIBLE BEHAVIOUR OF THE GROUND

CLASSIFICATION SYSTEMS

NUMERICAL MODELLING

OTHER CALCULATIONS

"GROUND": ROCCIA SOGGETTA ALLA SOLLECITAZIONE NATURALE E ALLE CONDIZIONI IDROGEOLOGICHE DEL SITO

Da Palmstrom (2002)

ROCK MASS CHARACTERISATION

DISCONTINUITIES

Orientation
*strike, dip and direction
of advance*

Frequency, Spacing

Persistence

Surface properties
roughness and coatings

Aperture, Openness

Infilling material

Genesis
*bedding
joints
foliation
schisosity and banding
faults
shears*

INTACT ROCK

Mineral constituents
*principal
auxiliary
accessory*

Lithology
*grain size and shape
texture and cementation
anisotropy
pores and micro-fractures
weathering and alteration*

Mechanical rock properties
*strength
deformability
hardness
fracture toughness
abrasivity
.....*

STRESS

Initial stress

Stress around openings

Groundwater, gas

Seismic activity

GEOMECHANICAL CLASSIFICATION SYSTEMS FOR ROCK EXCAVATION

Cuttability/Drillability
Blastability
Blast-Rock Loadability/Pumpability of Cuttings
Blast-Rock Assessment as Construction Material
Crushability/Millability
Tool Life Indices
Ground Support

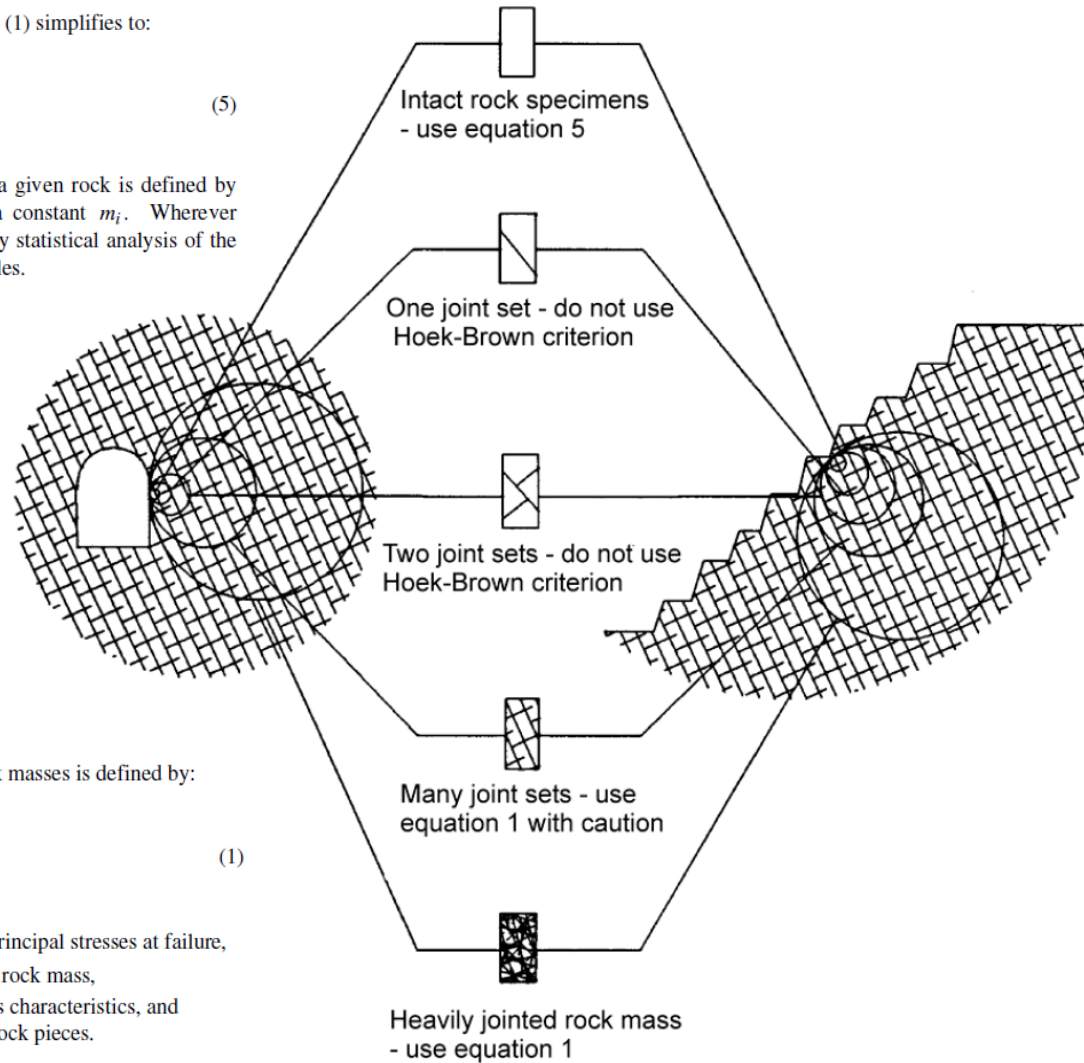|	Description	Strength characteristics	Strength testing	Theoretical considerations
	Hard intact rock	Brittle, elastic and generally isotropic	Triaxial testing of core specimens in laboratory relatively simple and inexpensive and results usually reliable	Theoretical behaviour of isotropic elastic brittle rock adequately understood for most practical applications
	Intact rock with single inclined discontinuity	Highly anisotropic, depending on shear strength and inclination of discontinuity	Triaxial testing of core with inclined joints difficult and expensive but results reliable. Direct shear testing of joints simple and inexpensive but results require careful interpretation	Theoretical behaviour of individual joints and of schistose rock adequately understood for most practical applications
	Massive rock with a few sets of discontinuities	Anisotropic, depending on number, shear strength and continuity of discontinuities	Laboratory testing very difficult because of sample disturbance and equipment size limitations	Behaviour of jointed rock poorly understood because of complex interaction of interlocking blocks
	Heavily jointed rock	Reasonably isotropic. Highly dilatant at low normal stress levels with particle breakage at high normal stress	Triaxial testing of undisturbed core samples extremely difficult due to sample disturbance and preparation problems	Behaviour of heavily jointed rock very poorly understood because of interaction of interlocking angular pieces
	Compacted rockfill	Reasonably isotropic. Less dilatant and lower shear strength than in situ jointed rock but overall behaviour generally similar	Triaxial testing simple but expensive because of large equipment size required to accommodate representative samples	Behaviour of compacted rockfill reasonably well understood from soil mechanics studies on granular materials
	Loose waste rock	Poor compaction and grading allow particle rotation and movement resulting in mobility of waste rock dumps	Triaxial or direct shear testing relatively simple but expensive because of large equipment size required	Behaviour of waste rock adequately understood for most applications

Figure 1 : Summary of range of rock mass characteristics

Intact rock properties

For the intact rock pieces that make up the rock mass, equation (1) simplifies to:

$$\sigma_1' = \sigma_3' + \sigma_{ci}\left(m_i \frac{\sigma_3'}{\sigma_{ci}} + 1 \right)^{0.5} \tag{5}$$

The relationship between the principal stresses at failure for a given rock is defined by two constants, the uniaxial compressive strength σ_{ci} and a constant m_i. Wherever possible the values of these constants should be determined by statistical analysis of the results of a set of triaxial tests on carefully prepared core samples.
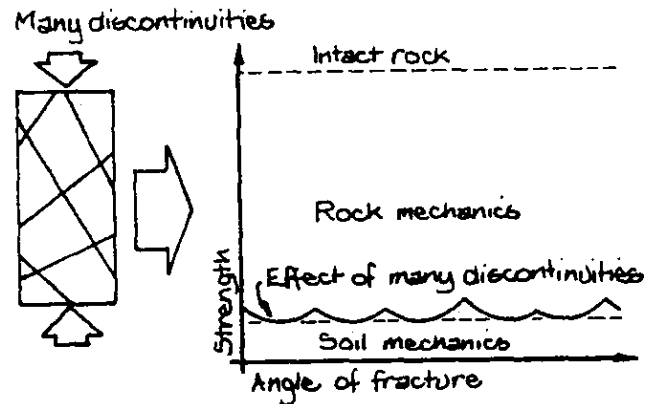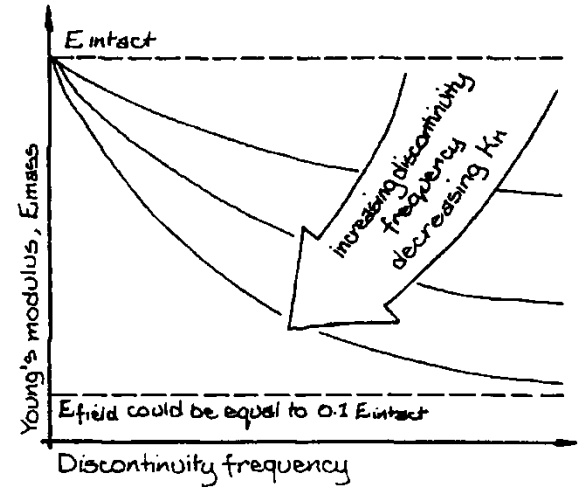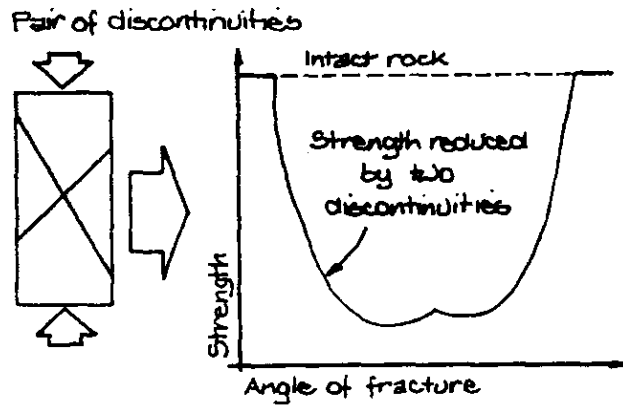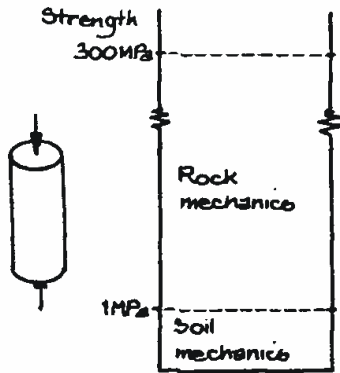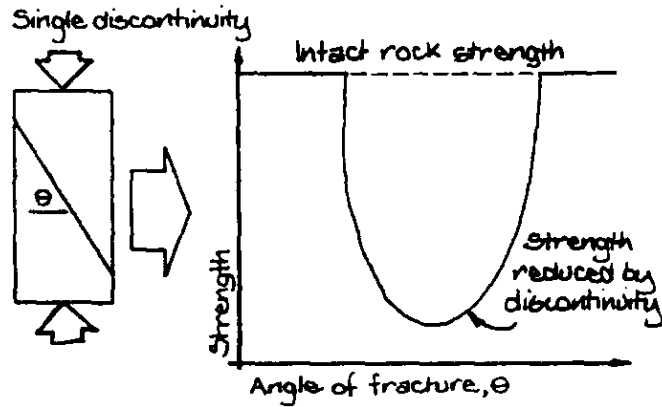
The Generalised Hoek-Brown failure criterion for jointed rock masses is defined by:

$$\sigma_1' = \sigma_3' + \sigma_{ci}\left(m_b \frac{\sigma_3'}{\sigma_{ci}} + s \right)^{a} \tag{1}$$

where σ_1' and σ_3' are the maximum and minimum effective principal stresses at failure,

    m_b is the value of the Hoek-Brown constant m for the rock mass,

    s and a are constants which depend upon the rock mass characteristics, and

    σ_{ci} is the uniaxial compressive strength of the intact rock pieces.

Intact rock specimens
- use equation 5

One joint set - do not use
Hoek-Brown criterion

Two joint sets - do not use
Hoek-Brown criterion

Many joint sets - use
equation 1 with caution

Heavily jointed rock mass
- use equation 1

Figure 5: Idealised diagram showing the transition from intact to a heavily jointed rock mass with increasing sample size.

Single discontinuity

Intact rock strength

Strength reduced by discontinuity

Strength

Angle of fracture, Θ

Strength

300MPa

Rock mechanics

1MPa

Soil mechanics

Pair of discontinuities

Intact rock

Strength reduced by two discontinuities

Strength

Angle of fracture

E intact

increasing discontinuity frequency decreasing Kn

Young's modulus, Emass

Efield could be equal to 0.1 Eintact

Discontinuity frequency

Many discontinuities

Intact rock

Rock mechanics

Effect of many discontinuities

Strength

Soil mechanics

Angle of fracture

MODELLO GEOTECNICO PER DESCRIZIONE AMMASSI ROCCIOSI

CONTINUO

DISCONTINUO

TERRENI SCIOLTI E ROCCE TENERE

LE DISCONTINUITA' SONO PARTE DETERMINANTE DEL MODELLO E SE NE DOVRA' SCEGLIERE UNA LEGGE COSTITUTIVA SODDISFACENTE

TIENE CONTO DELL'EFFETTO DELLE DISCONTINUITA' IN SENSO GLOBALE (CONTINUO EQUIVALENTE)

L'USO DI UN MODELLO O DELL'ALTRO DIPENDE DAL *RAPPORTO TRA SPAZIATURA DELLE DISCONTINUITÀ E DIMENSIONI DELLO SCAVO* PUO' ESSERVI UN CAMPO DI SOVRAPPOSIZIONE IN CUI PUÒ ESSERE UTILE *APPLICARE ENTRAMBI I MODELLI* E *CONFRONTARNE I RISULTATI*

Pseudo-continuum using continuum approach | Discontinuum approach | Continuum approach

Q = 0.1   Q = 100

FEM/FLAC | UDEC/3DEC | FEM/BEM

QUANTITATIVE DESCRIPTION OF DISCONTINUITIES IN ROCK MASSES

1. Rock material description
   A. Rock type
   B. Wall strength
   C. Weathering

2. Discontinuity description
   D. Type
   E. Orientation
   F. Roughness
   G. Aperture

3. Infilling
   H. Infilling type/Width

4. Rock mass description
   I. Spacing
   J. Persistence
   K. Number of sets
   L. Block size and shape

5. Groundwater
   M. Seepage

E: orientation α-dip dirn. ψ-dip

A: rock type

K: number of sets B, J_1, J_2

I: spacing $S_1 = S_{app} \sin\theta$ $S_{bedding}$

J: Persistence (*l*)

B: wall strength

H: filling type, width

D: discontinuity type: bedding, fault etc.

F: roughness (*i*)

L: block size/shape

M: seepage

G: aperture (open)

J_1

J_2

S_1

θ

α

ψ

N

B

$S_{bedding}$

l

S_{app}

Filling

Discontinuity Set

Discontinuity Set

Block size

Wall strength

Roughness

Persistence

Spacing

BOREHOLE   OR SCANLINE

Aperture

Dip and
dip direction

Seepage

Discontinuity Mapping

Scanline mapping

Window mapping

GENERAL INFORMATION

Seq. No. 7,4,8,9   Site A,N,Y,W,H,E,R,E   Date 1,0 0,3 7,6 (Day Month Year)   Operator A,C   Method of location 3

Co-ordinates or chainage (metres):   Northing or Chainage | Eastings | Elevation

1. By co-ordinates
2. Chainage
3. On attached map/drawing/photograph

Locality type 2   Size of locality 1   No. of supplementary sheets of discontinuity data 1,2   Sketch 1   Photograph 1   Slope dip 8,0   Dip direction 1,0,0

Remarks: 32 m high. Signs of instability. Some wedge failures have occured

1. Natural exposure
2. Construction excavation
3. Tunnel

1. >10 m²
2. 5 - 10 m²
3. 1 - 5 m²
4. <1 m²
5. Line survey

0. No.
1. Yes.

ROCK MATERIAL INFORMATION

Colour 1,1,9   Grain size 2   Compressive strength 4   Rock type GRANITE

1. Light 1. pinkish 1. pink 9. grey
2. Dark   2. reddish 2. red 10. black
          3. yellowish 3. yellow
          4. brownish 4. brown
          5. olive 5. olive
          6. greenish 6. green
          7. bluish 7. blue
          8. greyish 8. white

1. Very coarse (>60 mm)
2. Coarse (2 - 60mm)
3. Medium (60μ - 2mm)
4. Fine (2 - 60μ)
5. Very fine (<2μ)

1. Very weak – can be broken in the hand
2. Weak - crumbles under firm blows with a pick
3. Mod. strong – indents with a pick
4. Strong – breaks with single hammer blow
5. Very strong – requires several hammer blows to break

Qualifying terms to describe rock: Slightly weathered, moderately weathered on joints.

ROCK MASS INFORMATION

Fabric 1   Block size 2/3   State of weathering 2   No. of major discontinuity set 3

1. Blocky
2. Tabular
3. Columnar

1. Very large (>8m³)
2. Large (0.2 - 8m³)
3. Medium (0.008 - 0.2 m³)
4. Small (0.0002 - 0.008m³)
5. Very small (0.0002 m³)

1. Fresh
2. Slightly
3. Moderately
4. Highly
5. Completely
6. Residual soil

LINE SURVEYS TO DETERMINE DISCONTINUITY SPACINGS

	Plunge of line	Trend of line	Length of line (metres)	No. of fractures	Spacing	Remarks
Line 1	0,0	1,0	6,0	4,7	2/3	Base of slope
Line 2	0,0	1,0	4,8	4,0	2/3	Berm level
Line 3	8,0	1,0,0	3,2	5,0	2/3	Centre line of slope

Discontinuity spacing: 1. Ext. wide (<2m)   2. Very wide (600mm - 2m)   3. Wide (200 - 600mm)   4. Mod. wide (60 - 200 mm)   5. Mod. narrow (20 - 60mm)   6. Narrow (6 - 20mm)   7. Very narrow (<6mm)

Figure 2.10 - Example of Description Sheet for Rock Mass Survey

---

GENERAL INFORMATION

Seq. No. 7,9,8   Site A,N,Y,W,H,E,R,E   Date 1,0 0,3 7,6 (Day Month Year)   Operator A,C   Discontinuity data Sheet No. 2 of 1,2

NATURE AND ORIENTATION OF DISCONTINUITIES

Chainage or No.	Type	Dip	Dip direction	Persistence	Aperture	Infilling	Consistency	Roughness	Differentially weathered zone width mm	Waviness wavelength	Waviness amplitude	Water	Remarks
1, ,1,3	2	5,6	1,7,8	,3,5	4	4		2	1,5,0	2,0	0,5	1	
1, ,1,4	2	8,6	3,1,3	,1,5	5	2		–	,5,0	1,0	0,4	1	
1, ,1,5	2	8,6	2,3,5	,9	7	2		–	,2,0	–	–	1	
1, ,1,6	2	6,6	1,7,6	,7	6	6		5	,4,0	–	–	1	
1, ,1,7	2	8,4	2,4,6	,4,3	4	4		2	1,2,0	2,0	0,5	1	Shot hole shows 50mm movement
1, ,1,8	2	5,5	1,4,9	,2,4	5	2		–	,3,0	1,5	1,0	1	
1, ,1,9	1	4,4	,6,4	2,5,0	3	4		4	2,0,0	3,0	0,8	2	
1, ,2,0	2	9,0	1,4,4	,1,9	7	6		5	,2,0	0,5	0,5	1	
1, ,2,1	2	8,2	2,3,4	,3,3	4	2		–	1,0,0	1,5	0,3	1	
1, ,2,2	2	8,1	3,2	,4	7	2		–	,2,0	–	–	1	
1, ,2,3	2	6,2	1,4,4	,1,3	5	2		–	,5,0	1,0	0,5	1	
1, ,2,4	1	8,0	2,6,3	1,8,0	3	4		4	2,0,0	4,5	2,0	3	

Type	Dip, Dip direction	Persistence	Aperture	Nature of infilling	Consistency of infilling		Roughness	Waviness	Water
0. Fault zone	(Expressed in degrees)	(Expressed in metres)	1. Wide (>200 mm)	1. Clean	Soil strength	Rock strength	1. Polished	Express wavelength, amplitude in metres	1. Dry
1. Fault			2. Mod. wide (60 - 200mm)	2. Surface staining	1. Soft	5. Weak	2. Slickensided		2. Seepage
2. Joint			3. Mod. narrow (20 - 60mm)	3. Non - cohesive	2. Firm	6. Mod. strong	3. Smooth		3. Slight flow <0.1 l/sec
3. Cleavage			4. Narrow (6 - 20 mm)	4. Cohesive	3. Stiff	7. Strong	4. Rough		4. Mod. flow 0.1 - 1 l/sec
4. Schistosity			5. Very narrow (2 - 6 mm)	5. Cemented	4. Hard	8. Very strong	5. Defined ridges		5. High flow >0.1 l/sec
5. Shear			6. Ext. narrow (<2 mm)	6. Calcite			6. Small slope		
6. Fissure			7. Tight	7. Chlorite, talc			7. Very rough		
7. Tension crack				8. Others - specify					
8. Foliation									
9. Bedding									

Figure 2.11 - Example of Data Sheet for Discontinuity Survey
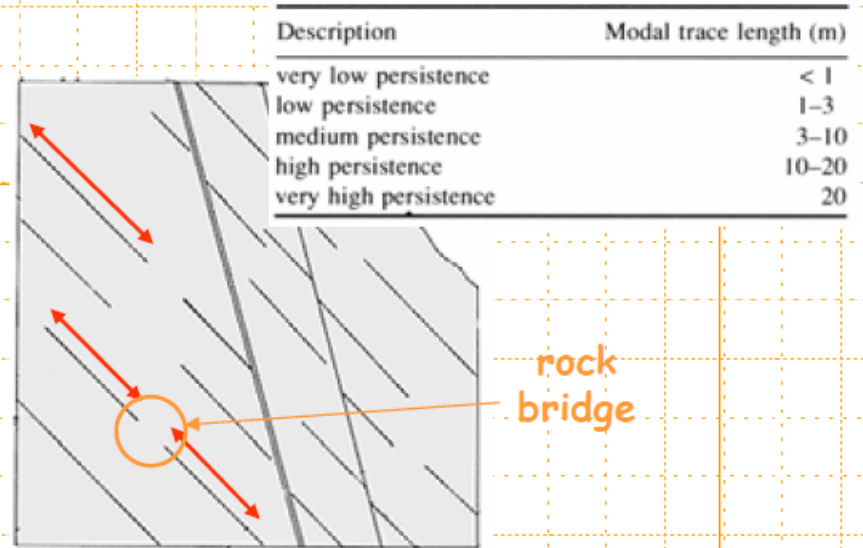
Stereonets – Pole Plots

Plotting dip and dip direction, pole plots provide an immediate visual depiction of pole **concentrations**. All **natural** discontinuities have a certain variability in their orientation that results in **scatter** of the pole plots. However, by contouring the pole plot, the most highly concentrated areas of poles, representing the **dominant** discontinuity sets, can be identified.
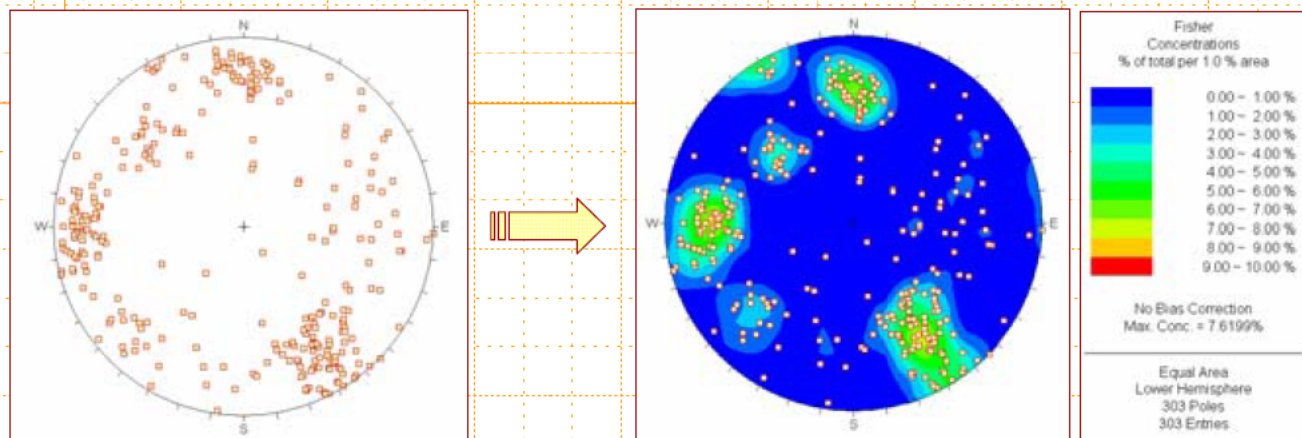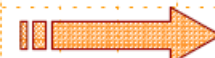

It must be remembered though, that it may be difficult to <u>distinguish</u> which set a particular discontinuity belongs to or that in some cases a <u>single</u> discontinuity may be the **controlling factor** as opposed to a set of discontinuities.

Discontinuity Persistence

Persistence refers to the areal extent or **size** of a discontinuity plane **within** a plane. Clearly, the persistence will have a major influence on the shear strength developed in the plane of the discontinuity, where the intact rock segments are referred to as 'rock bridges'.

Description	Modal trace length (m)
very low persistence	< 1
low persistence	1–3
medium persistence	3–10
high persistence	10–20
very high persistence	20

rock bridge

increasing persistence

Discontinuity Persistence

Together with spacing, discontinuity **persistence** helps to define the size of blocks that can slide from a rock face. Several procedures have been developed to calculate persistence by **measuring** their exposed **trace lengths** on a specified area of the face.
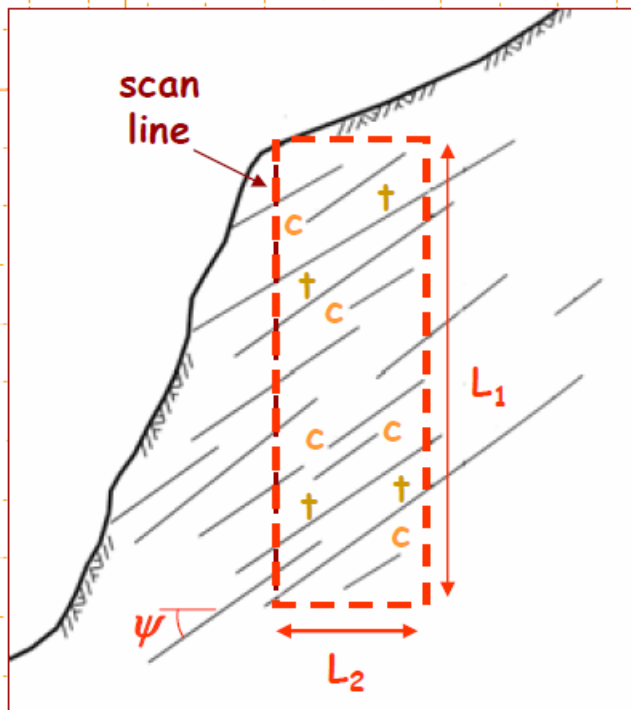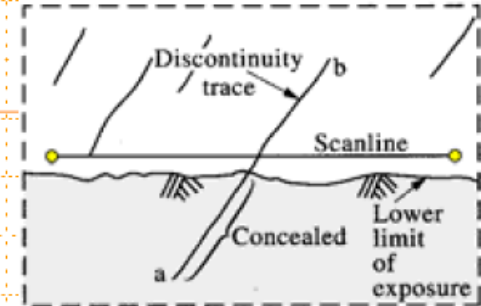
Step 1: define a mapping area on the rock face with dimensions L_1 and L_2.

Step 2: count the total number of discontinuities (N'') of a specific set with dip ψ in this area, and the numbers of these either contained within (N_c) or transecting (N_t) the mapping area defined.

For example, in this case:

$N'' = 14$

$N_c = 5$

$N_t = 4$

Discontinuity Persistence
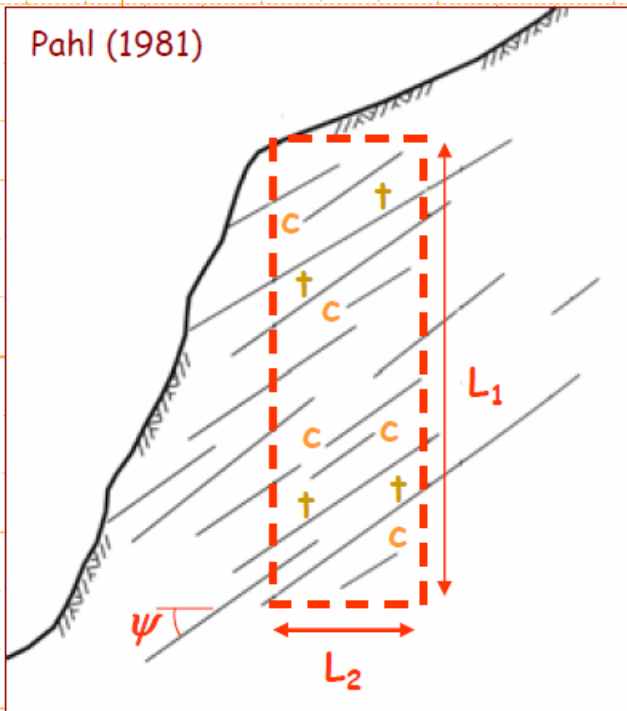
Pahl (1981)

Step 1: define a mapping area on the rock face with dimensions L_1 and L_2.

Step 2: count the total number of discontinuities (N'') of a specific set with dip ψ in this area, and the numbers of these either contained within (N_c) or transecting (N_t) the mapping area defined.

Step 3: calculate the approximate length, $\bar{l}$, of the discontinuities using the equations below.

$$m = \frac{(N_t - N_c)}{(N'' + 1)} \qquad H' = \frac{L_1 \cdot L_2}{(L_1 \cdot \cos\psi + L_2 \cdot \sin\psi)}$$

$$\bar{l} = H'\frac{(1 + m)}{(1 - m)}$$

Again, for this case:

If L_1 = 15 m, L_2 = 5 m and ψ = 35°, then H' = 4.95 m and m = -0.07. From this, the average length/persistence of the discontinuity set $\bar{l}$ = 4.3 m.

Discontinuity Spacing

Spacing is a key parameter in that it controls the block size distribution related to a potentially unstable mass (i.e. failure of a massive block or unravelling-type failure).
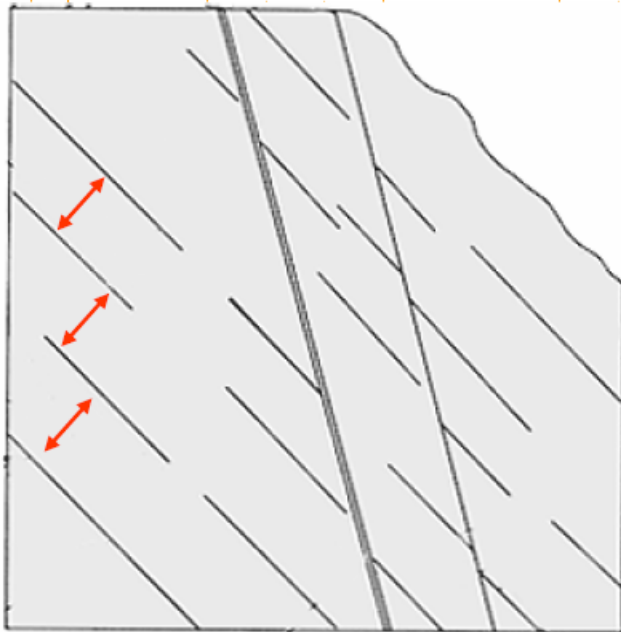
Discontinuity Shear Strength

Strength along a discontinuity surface is mostly provided by asperities. For shear failure to occur, the discontinuity surfaces must either dilate, allowing asperities to override one another, or shear through the asperities.
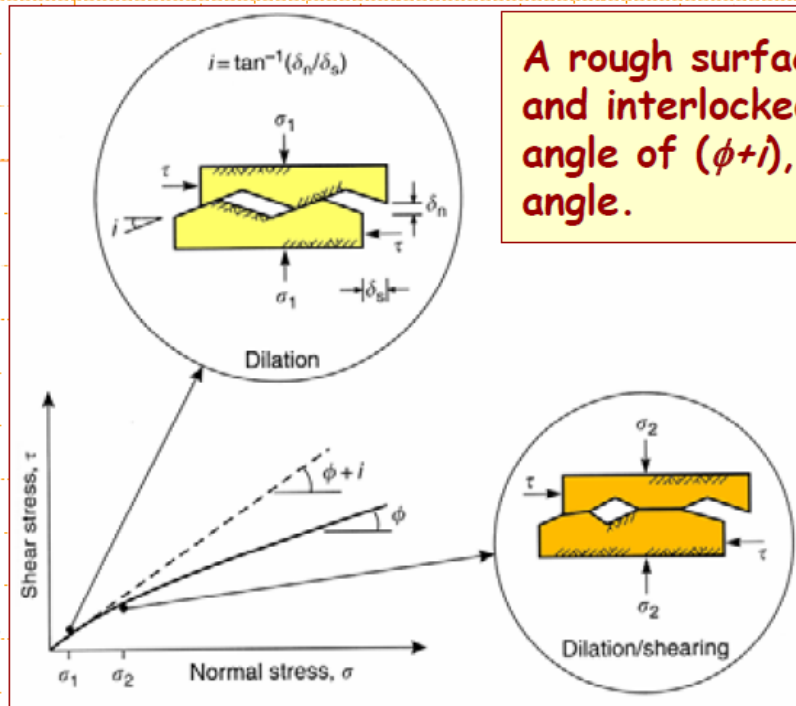
A rough surface that is initially undisturbed and interlocked will have a peak friction angle of ($\phi+i$), where i is the roughness angle.

As normal stresses increase, dilatancy is gradually reduced as a greater proportion of the asperities are damaged during shearing. Here, the friction angle progressively diminishes to a minimum value (residual friction).

Wyllie & Norrish (1996)

$i = \tan^{-1}(\delta_n/\delta_s)$

Dilation

Dilation/shearing

Shear stress, τ

Normal stress, σ

$\phi + i$

ϕ
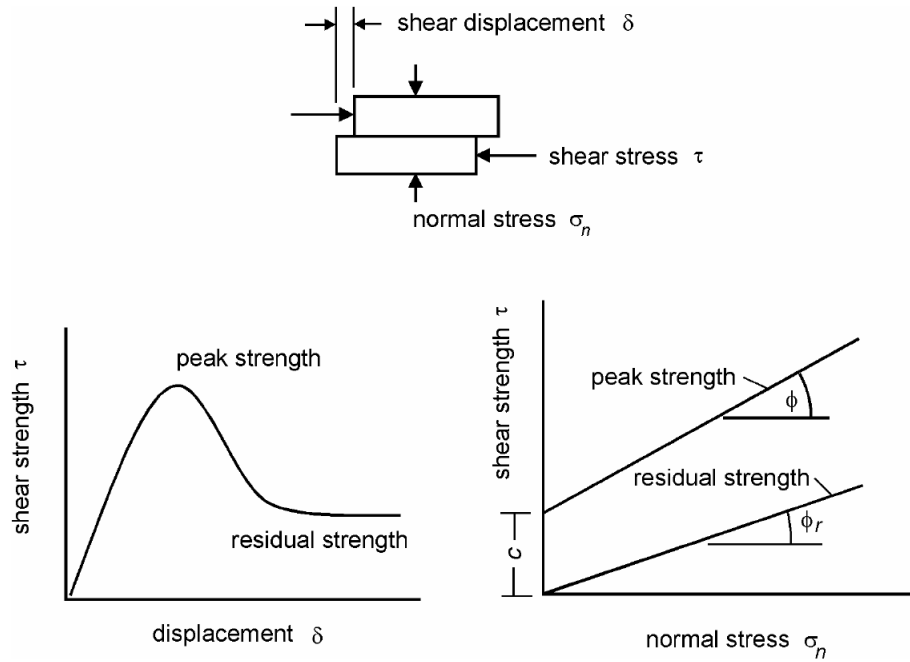
Figure 1: Shear testing of discontinuities
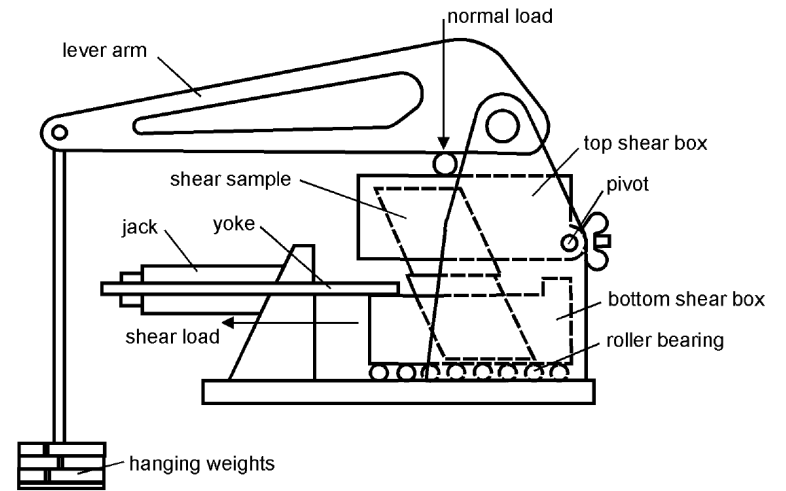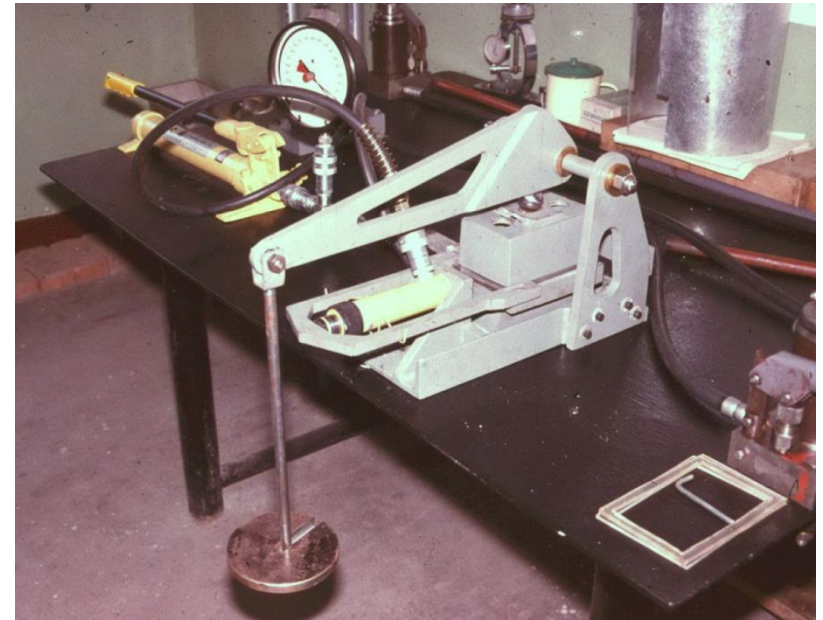
Figure 2: Diagrammatic section through shear machine used by Hencher and Richards (1982).

Patton (1966) demonstrated this influence by means of an experiment in which he carried out shear tests on 'saw-tooth' specimens such as the one illustrated in Figure 4. Shear displacement in these specimens occurs as a result of the surfaces moving up the inclined faces, causing dilation (an increase in volume) of the specimen.

The shear strength of Patton's saw-tooth specimens can be represented by:

$$\tau = \sigma_n \tan(\phi_b + i) \tag{4}$$

where ϕ_b is the basic friction angle of the surface and
         i is the angle of the saw-tooth face.
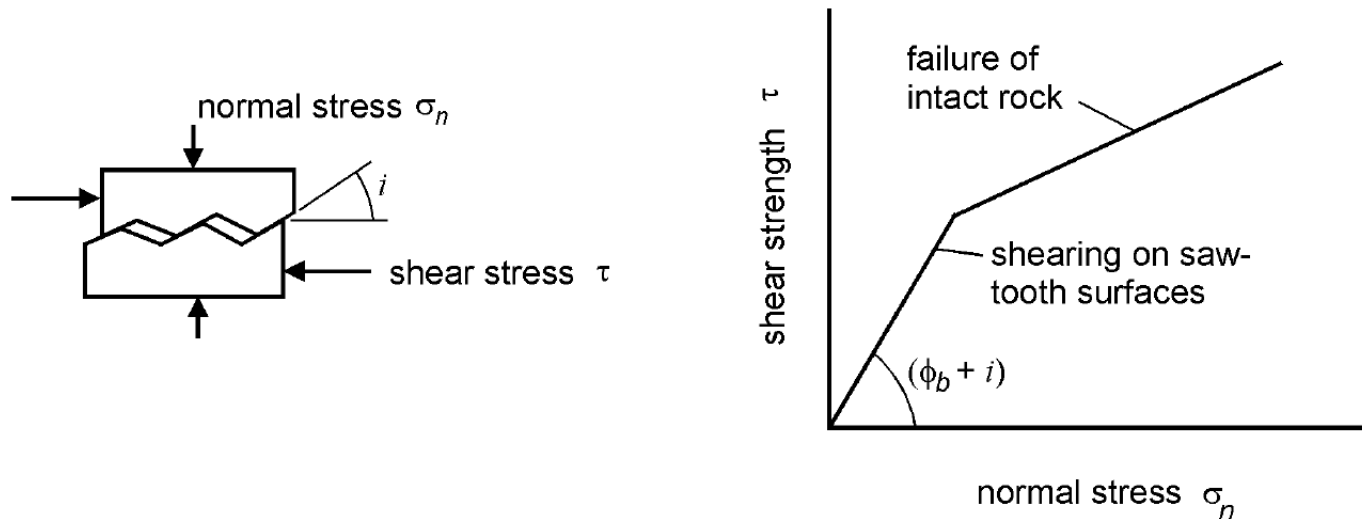
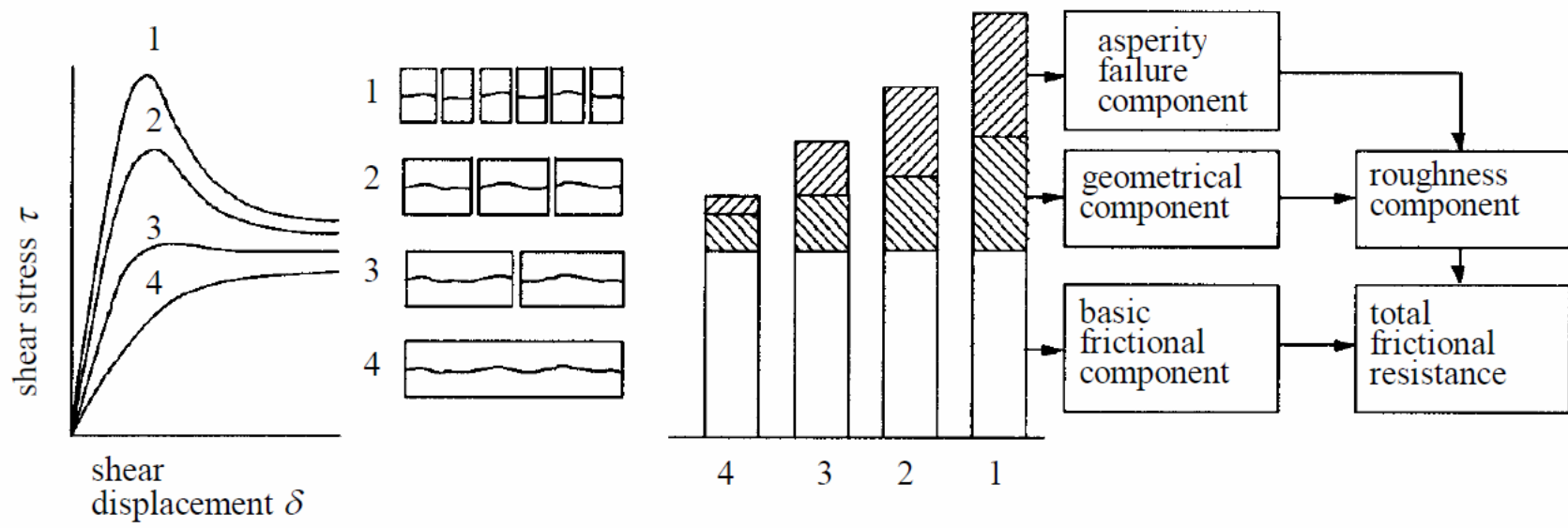Figure 4: Patton's experiment on the shear strength of saw-tooth specimens.

Figure 5.3: Influence of scale on the three components of the shear strength of a rough discontinuity. After Bandis (1990) and Barton and Bandis (1990).

Barton's estimate of shear strength

Equation (4) is valid at low normal stresses where shear displacement is due to sliding along the inclined surfaces. At higher normal stresses, the strength of the intact material will be exceeded and the teeth will tend to break off, resulting in a shear strength behaviour which is more closely related to the intact material strength than to the frictional characteristics of the surfaces.

While Patton's approach has the merit of being very simple, it does not reflect the reality that changes in shear strength with increasing normal stress are gradual rather than abrupt. Barton (1973, 1976) studied the behaviour of natural rock joints and proposed that equation (4) could be re-written as:

$$\tau = \sigma_n \tan\left(\phi_b + JRC \log_{10}\left(\frac{JCS}{\sigma_n}\right)\right) \tag{5}$$

where JRC is the joint roughness coefficient and
            JCS is the joint wall compressive strength .

Barton developed his first non-linear strength criterion for rock joints (using the basic friction angle ϕ_b) from analysis of joint strength data reported in the literature. Barton and Choubey (1977), on the basis of their direct shear test results for 130 samples of variably weathered rock joints, revised this equation to

$$\tau = \sigma_n \tan\left(\phi_r + JRC \log_{10}\left(\frac{JCS}{\sigma_n}\right)\right) \tag{6}$$

Where ϕ_r is the residual friction angle
Barton and Choubey suggest that ϕ_r can be estimated from

$$\phi_r = (\phi_b - 20) + 20(r/R) \tag{7}$$

where r is the Schmidt rebound number wet and weathered fracture surfaces and R is the Schmidt rebound number on dry unweathered sawn surfaces.

Field estimates of *JRC*

The joint roughness coefficient *JRC* is a number that can be estimated by comparing the appearance of a discontinuity surface with standard profiles published by Barton and others. One of the most useful of these profile sets was published by Barton and Choubey (1977) and is reproduced in Figure 5.

The appearance of the discontinuity surface is compared visually with the profiles shown and the *JRC* value corresponding to the profile which most closely matches that of the discontinuity surface is chosen. In the case of small scale laboratory specimens, the scale of the surface roughness will be approximately the same as that of the profiles illustrated. However, in the field the length of the surface of interest may be several metres or even tens of metres and the *JRC* value must be estimated for the full scale surface.

An alternative method for estimating *JRC* is presented in Figure 6.

Field estimates of *JCS*

Suggested methods for estimating the joint wall compressive strength were published by the ISRM (1978). The use of the Schmidt rebound hammer for estimating joint wall compressive strength was proposed by Deere and Miller (1966), as illustrated in Figure 7.

Influence of scale on *JRC* and *JCS*

On the basis of extensive testing of joints, joint replicas, and a review of literature, Barton and Bandis (1982) proposed the scale corrections for *JRC* defined by the following relationship:

$$JRC_n = JRC_o \left(\frac{L_n}{L_o} \right)^{-0.02 JRC_o} \tag{8}$$

where JRC_o, and L_o (length) refer to 100 mm laboratory scale samples and JRC_n, and L_n refer to in situ block sizes.

Because of the greater possibility of weaknesses in a large surface, it is likely that the average joint wall compressive strength (*JCS*) decreases with increasing scale. Barton and Bandis (1982) proposed the scale corrections for *JCS* defined by the following relationship:

$$JCS_n = JCS_o \left(\frac{L_n}{L_o} \right)^{-0.03 JRC_o} \tag{9}$$

where JCS_o and L_o (length) refer to 100 mm laboratory scale samples and JCS_n and L_n refer to in situ block sizes.

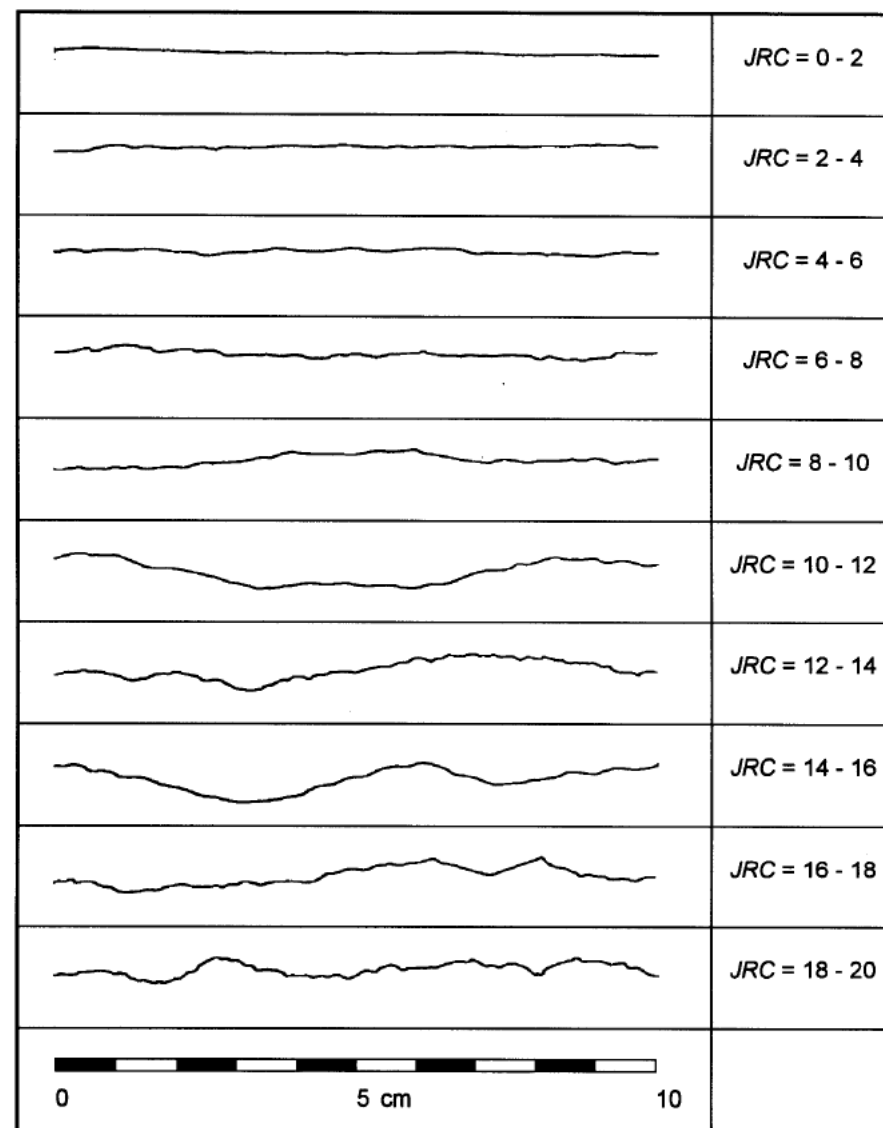|	
	JRC = 0 - 2
	JRC = 2 - 4
	JRC = 4 - 6
	JRC = 6 - 8
	JRC = 8 - 10
	JRC = 10 - 12
	JRC = 12 - 14
	JRC = 14 - 16
	JRC = 16 - 18
	JRC = 18 - 20

0   5 cm   10

Figure 5: Roughness profiles and corresponding *JRC* values (After Barton and Choubey 1977).
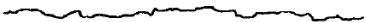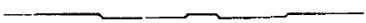
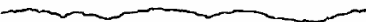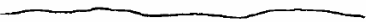| Description	Profile	J_r	JRC 200mm	JRC 1 m
Rough		4	20	11
Smooth		3	14	9
Slickensided				
Stepped		2	11	8
Rough		3	14	9
Smooth		2	11	8
Slickensided				
Undulating		1.5	7	6
Rough		1.5	2.5	2.3
Smooth		1.0	1.5	0.9
Slickensided				
Planar		0.5	0.5	0.4

Figure 5.2: Relationship between J_r in the Q system and JRC for 200 mm and 1000 mm samples (After Barton, 1987).

Figure 6: Alternative method for estimating *JRC* from measurements of surface roughness amplitude from a straight edge (Barton 1982).

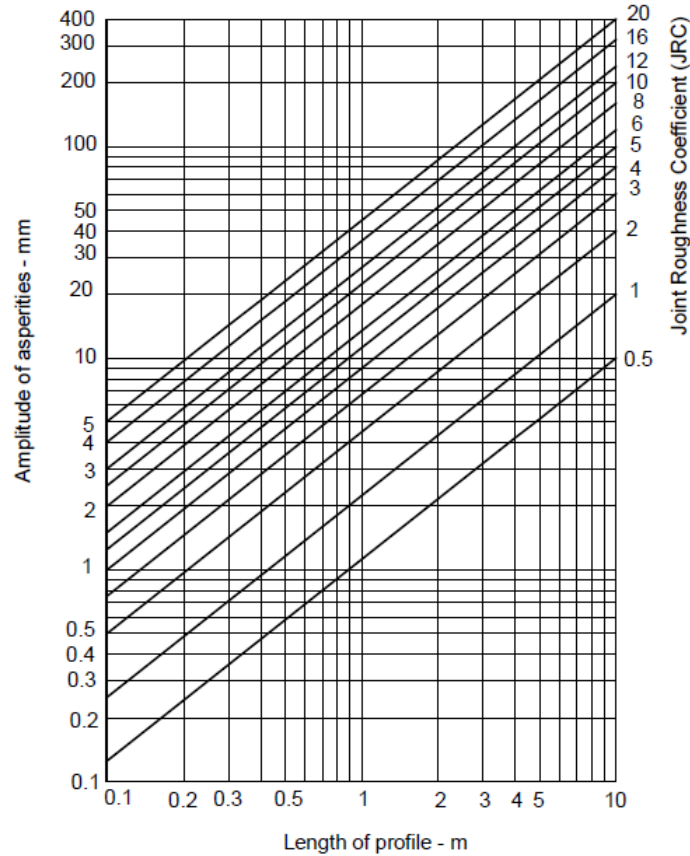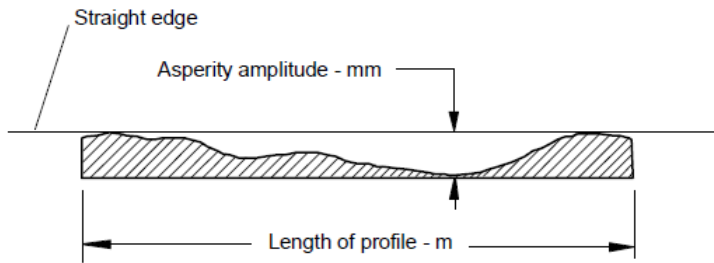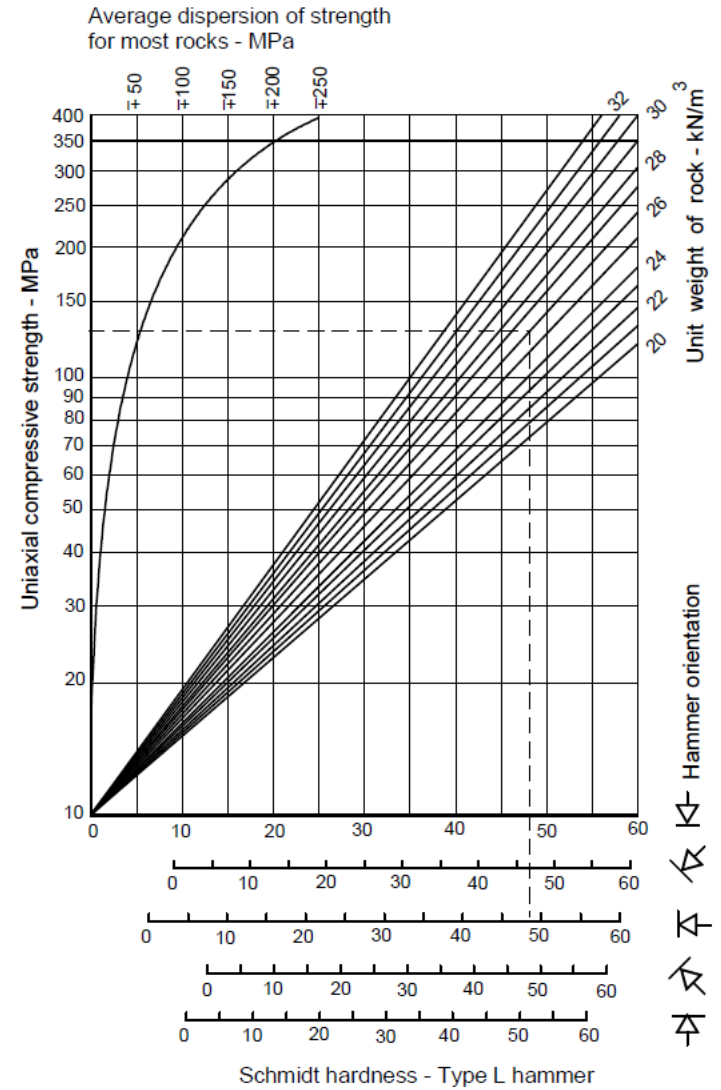Figure 7: Estimate of joint wall compressive strength from Schmidt hardness.
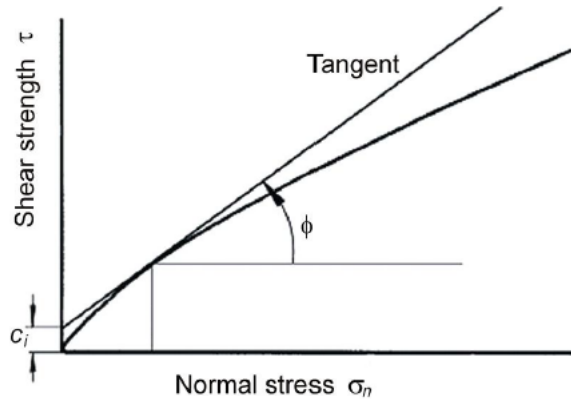
Figure 8: Definition of instantaneous cohesion c_i and instantaneous friction angle ϕ_i for a non-linear failure criterion.

Note that equation 6 is not valid for $\sigma_n = 0$ and it ceases to have any practical meaning for $\phi_r + JRC \log_{10}(JCS/\sigma_n) > 70°$. This limit can be used to determine a minimum value for σ_n. An upper limit for σ_n is given by $\sigma_n = JCS$.

In a typical practical application, a spreadsheet program can be used to solve Equation 6 and to calculate the instantaneous cohesion and friction values for a range of normal stress values. A portion of such a spreadsheet is illustrated in Figure 9. In this spreadsheet the instantaneous friction angle ϕ_i, for a normal stress of σ_n, has been calculated from the relationship

$$\phi_i = \arctan\left(\frac{\partial \tau}{\partial \sigma_n}\right) \qquad (10)$$

$$\frac{\partial \tau}{\partial \sigma_n} = \tan\left(JRC \log_{10}\frac{JCS}{\sigma_n} + \phi_r\right) - \frac{\pi JRC}{180 \ln 10}\left[\tan^2\left(JRC \log_{10}\frac{JCS}{\sigma_n} + \phi_r\right) + 1\right] \qquad (11)$$

The instantaneous cohesion c_i is calculated from:

$$c_i = \tau - \sigma_n \tan\phi_i \qquad (12)$$

In choosing the values of c_i and ϕ_i for use in a particular application, the average normal stress σ_n acting on the discontinuity planes should be estimated and used to determine the appropriate row in the spreadsheet. For many practical problems in the field, a single average value of σ_n will suffice but, where critical stability problems are being considered, this selection should be made for each important discontinuity surface.

Barton shear failure criterion

Input parameters:

Residual friction angle (PHIR) - degrees	29
Joint roughness coefficient (JRC)	16.9
Joint compressive strength (JCS)	96
Minimum normal stress (SIGNMIN)	0.360

Normal stress (SIGN) MPa	Shear strength (TAU) MPa	dTAU dSIGN (DTDS)	Friction angle (PHI) degrees	Cohesive strength (COH) MPa
0.360	0.989	1.652	58.82	0.394
0.720	1.538	1.423	54.91	0.513
1.440	2.476	1.213	50.49	0.730
2.880	4.073	1.030	45.85	1.107
5.759	6.779	0.872	41.07	1.760
11.518	11.344	0.733	36.22	2.907
23.036	18.973	0.609	31.33	4.953
46.073	31.533	0.496	26.40	8.666

Cell formulae:

SIGNMIN = 10^(LOG(JCS)-((70-PHIR)/JRC))

TAU = SIGN*TAN((PHIR+JRC*LOG(JCS/SIGN))*PI()/180)

DTDS = TAN((JRC*LOG(JCS/SIGN)+PHIR)*PI()/180)-(JRC/LN(10)) *(TAN((JRC*LOG(JCS/SIGN)+PHIR)*PI()/180)^2+1)*PI()/180

PHI = ATAN(DTDS)*180/PI()

COH = TAU-SIGN*DTDS

Figure 9 Printout of spreadsheet cells and formulae used to calculate shear strength, instantaneous friction angle and instantaneous cohesion for a range of normal stresses.

Dilatancy and Shear Strength

In the case of sliding of an unconstrained block of rock from a slope, dilatancy will accompany shearing of all but the smoothest discontinuity surfaces. If a rock block is free to dilate, then the second-order asperities will have a diminished effect on shear strength.

constant normal load

σ_n

τ

Normal deformation free to dilate

Wyllie & Mah (2004)

$i_1 = 13°$

ψ_p

0.5–2 m

$i_2 = 26°$

$i_2 = 28°$

ψ_p

50–100 mm
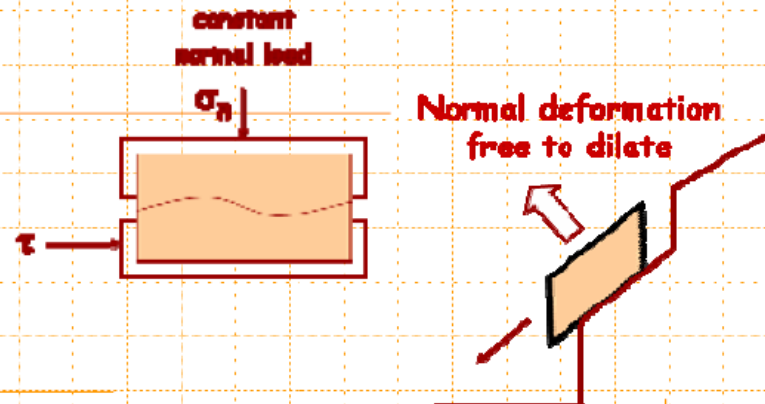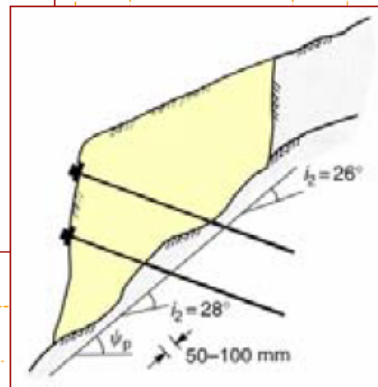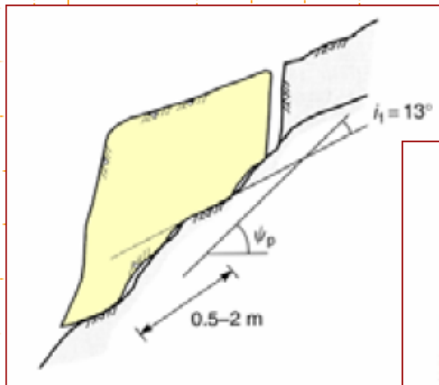
Thus, by increasing the normal force across a shear surface by adding tensioned rock bolts, dilation can be limited and interlocking along the sliding surface maintained, allowing the second-order asperities to contribute to the shear strength.

Residual Strength

For the residual strength condition, any cohesion is lost once displacement has broken the cementing action. Also, the residual friction angle is less than the peak friction angle because the shear displacement grinds the minor irregularities on the rock surface and produces a smoother, lower friction surface.
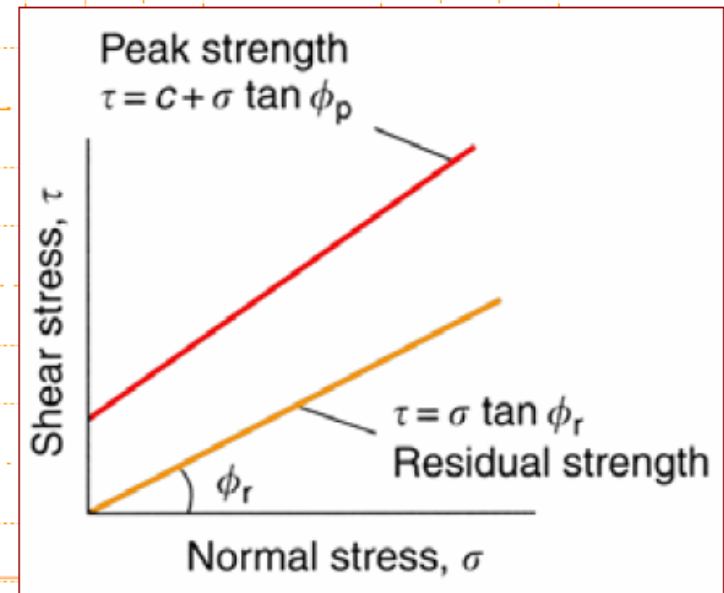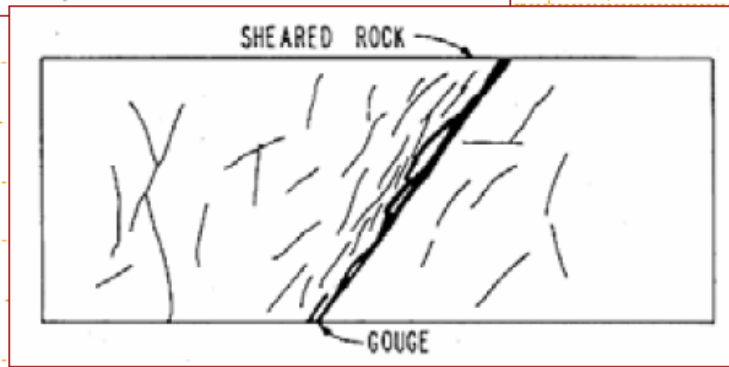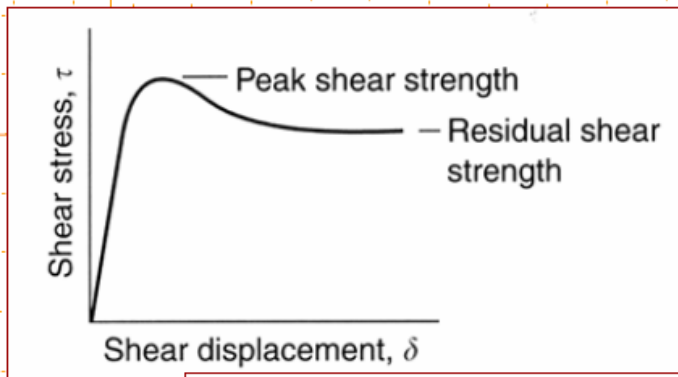
5.2 Modelli discontinui

L'ammasso roccioso, inteso come mezzo discontinuo, è costituito da una serie di blocchi di roccia intatta in mutuo contatto lungo le discontinuità: per poter descrivere il comportamento di un siffatto sistema, occorre definire separatamente il comportamento tensio-deformativo dei blocchi e delle discontinuità.

I blocchi possono essere considerati rigidi o deformabili: si utilizza la prima ipotesi se la risposta dell'ammasso roccioso è governata principalmente dalle discontinuità, ovvero quando la deformazione della roccia costituente i blocchi è trascurabile rispetto agli scorrimenti che avvengono lungo le discontinuità. Se i blocchi sono supposti deformabili, occorre definire il loro comportamento tensio-deformativo mediante uno dei modelli descritti precedentemente; è chiaro che in questo caso ci si deve riferire ai parametri di resistenza e deformabilità caratteristici della roccia intatta.

Il comportamento delle discontinuità è solitamente modellato come elasto-plastico, mediante leggi che sono legate al tipo di codice di calcolo che si utilizza per l'analisi.

La legge di plasticizzazione più comunemente usata è il criterio di resistenza di Barton-Bandis, che si esprime come segue (Bandis et al., 1983):

$$\tau = \sigma'_n \, tg\left(\varphi'_r + JRC_n \log\left(\frac{JCS_n}{\sigma'_n}\right) + i_u \right) \tag{25}$$

dove JRC_n e JCS_n sono rispettivamente i coefficienti di scabrezza e di resistenza delle pareti a contatto alla scala reale del problema, φ'_r è l'angolo di attrito residuo e i_u è l'angolo caratteristico dell'ondulazione dei giunti.

I parametri JRC_n e JCS_n sono valutati mediante correlazioni empiriche che consentono di tenere conto dell'effetto scala nell'estensione di misure eseguite su campioni di laboratorio al problema reale (Barton & Bandis, 1982); in particolare, essi sono funzione dei corrispondenti valori ottenuti sperimentalmente in laboratorio (JRC_o e JCS_o), della lunghezza caratteristica della discontinuità in laboratorio (L) e di quella reale in sito (L_n):

$$JRC_n = JRC_o \left(\frac{L_n}{L}\right)^{-0.02 JRC_O} \tag{26}$$

$$JCS_n = JCS_o \left(\frac{L_n}{L}\right)^{-0.03 JRC_O} \tag{27}$$

Il valore dell'angolo di attrito residuo φ'_r è ottenuto dall'elaborazione di prove di taglio diretto eseguite su discontinuità naturali; qualora le superfici della discontinuità si presentino lisce, piane e non alterate il valore di φ'_r può essere scelto pari al valore dell'angolo di attrito di base φ_b, a sua volta valutato elaborando i risultati di prove di scorrimento (tilt-test) o di taglio diretto eseguite su discontinuità lisce artificiali. L'angolo i_u, caratterizzante la scabrezza a grande scala (ondulosità), deve essere preferibilmente valutato con misurazioni in sito.

Nel caso in cui sia necessario utilizzare una legge di plasticizzazione lineare, si linearizza la legge di Barton-Bandis mediante il criterio di Mohr-Coulomb, nell'intervallo di valori della tensione normale σ'_n che interessano il problema in esame:

$$\tau' = \sigma'_n \, tg\varphi' + c' \tag{28}$$

ove i valori dei parametri c' e φ' sono dunque rappresentativi di un certo intervallo di σ'_n.

I contatti tra le facce delle discontinuità sono usualmente assunti deformabili; è pertanto necessario definire:

- la rigidezza normale k_n, ovvero il rapporto tra l'incremento della tensione normale $d\sigma_n$ agente all'interfaccia e l'incremento dello spostamento normale corrispondente dv. L'incremento di σ_n genera una variazione dell'apertura della discontinuità, che tende a decrescere in modo marcatamente non lineare fino ad un valore limite, e la successione di più cicli di carico e scarico genera un irrigidimento della discontinuità. La relazione tra σ_n e v può essere descritta allora, per ogni eventuale ciclo di carico, mediante un'iperbole (Bandis et al., 1983) definita esclusivamente dal valore della rigidezza iniziale k_{ni} e dal valore massimo della chiusura del giunto v_m per il ciclo di carico in esame; la dipendenza di k_n dalla storia di carico può essere espressa dall'equazione:

$$k_n = k_{ni}\left(1 - \frac{\sigma_n}{v_m k_{ni} + \sigma_n}\right)^{-2} \qquad (29)$$

Il valore di rigidezza iniziale può essere valutato mediante la relazione:

$$k_{ni} = 0.0178\left[\frac{JCS_n}{a}\right] + 1.748 JRC_n - 7.155 \qquad (30)$$

ove a rappresenta l'apertura del giunto all'inizio del ciclo di carico, ovvero per sforzo normale nullo.
Il valore di v_m è determinabile mediante la relazione:

$$v_m = A + B(JRC_n) + C\left(\frac{JCS_n}{a}\right)^D \qquad (31)$$

essendo A,B,C e D delle costanti che dipendono dalla storia di carico del giunto.

- la rigidezza tangenziale k_s, fornita dal rapporto tra l'incremento della tensione di taglio $d\tau_n$ agente sulla superficie di discontinuità ed il corrispondente scorrimento tra le facce della discontinuità du. Il valore di k_s varia dunque in funzione dello scorrimento subito dal giunto; detto u_p lo spostamento necessario per raggiungere le condizioni di resistenza a taglio di picco, si può esprimere la rigidezza tangenziale come (Bandis et al., 1983):

$$k_s = \sigma_n tg\left(\frac{0.75\varphi_r}{0.2u_p}\right)L_n \qquad \text{per } (u/u_p) < 0.20 \qquad (34)$$

$$k_s = \sigma_n tg\left(\frac{0.25\varphi_r}{0.1u_p}\right)L_n \qquad \text{per } (u/u_p) > 0.20 \qquad (35)$$

essendo φ_r l'angolo di resistenza a taglio residuo caratteristico del giunto.

3. INDAGINI E PROVE GEOTECNICHE

I mezzi di indagine, generalmente utilizzati per la caratterizzazione geologica, concorrono, insieme alle prove geotecniche di laboratorio ed in sito, alla caratterizzazione geotecnica dell'ammasso roccioso. Data la stretta connessione tra le due fasi, occorre che, nel predisporre il programma di indagini e prove, siano trattati congiuntamente gli aspetti geologici e geotecnici e le rispettive interazioni.

3.1 Indagini

La ricostruzione del profilo geologico-geotecnico lungo il tracciato di una galleria, che comprende la previsione dei litotipi incontrati, dell'assetto geologico-strutturale e delle condizioni idrogeologiche, ai fini della caratterizzazione geotecnica comporta la suddivisione in classi di qualità dell'ammasso roccioso, secondo uno o più metodi di classificazione che saranno richiamati più avanti. I principali tipi di indagine utilizzati in sede progettuale comprendono: (1) i rilievi geologico-strutturali di superficie e (2) le perforazioni di sondaggio a carotaggio (ISRM 1978a). Nel primo caso, una delle principali difficoltà incontrate riguarda, al di là della rappresentatività dell'ammasso roccioso e dell'effettiva disponibilità di affioramenti (sono frequenti i casi in cui le coperture obliterano la roccia di interesse), la condizione di disturbo e alterazione dell'ammasso roccioso in superficie. Nel secondo caso i problemi sono ovviamente connessi con la scala dell'indagine (cioè con il ridotto diametro del foro), il carattere puntuale dell'accertamento e l'inevitabile disturbo meccanico della perforazione, in particolare per i litotipi deboli.

Con riferimento alla progettazione di gallerie di grande diametro ed in condizioni particolari, si è talora dimostrato utile ricorrere al rilievo geologico-strutturale e geotecnico in cunicolo pilota, anche se non mancano al riguardo clamorosi esempi in cui l'impiego del cunicolo è risultato di gran lunga inferiore alle attese (si ricordano i casi recenti del Pinglin Tunnel a Taiwan e della galleria di valico, sull'autostrada A1). I rilievi geostrutturali sono finalizzati a dare una rappresentazione visiva, in termini qualitativi e per quanto possibile quantitativi, dell'ammasso roccioso attraversato dal cunicolo pilota e delle discontinuità via via incontrate. Si veda al riguardo l'esempio della Figura 3.

RILIEVO GEOLOGICO

DATA: 14/02/1994 RILEVATORE: PORZIO
GALLERIA: FRASNADELLO IMBOCCO: SUD/PREGALLENO
PROG. FRONTE: 232 ORIENT. FRONTE: E–W

FUORISAGOMA   VENUTA CON Q = 10 l/min

ASSE GALLERIA

PROGRESSIVA (m)   VENUTA 5–8 l/min

TIPO DI ROCCIA: DOLOMIA NERA

PROG. 128–134 INTERCALAZIONI DI COLORE BIANCO
LUNGO LA STRATIFICAZIONE (MICRO CRISTALLINO)

SISTEMA / DISCONTINUITÀ	TIPO	APERTURA (mm)	SPAZIATURA (m)	CONTINUITÀ (m)	IMMERSIONE (°)	INCLINAZIONE (°)	SCABREZZA	RIEMP./SPESS (mm)	ACQUA
1	STR	2	0.3	1	190	45	US	OXID	ASS.
2	GIU	CHI			290	70	US		ELEV.
3	GIU	CHI	1–3 cm	0.3	40	65	US		DEB.
4	GIU	CHI	0.3–0.4	0.5	60	50	US		ASS.
5	GIU	CHI	0.2	0.8	330	65	US		ASS.

COND. STRUTT. GENERALI: AMMASSO ROCCIOSO DI ASPETTO MASSIVO

COND. IDR. GENERALI: VENUTE LOCALIZZATE PR. 133 ELEVATA

DATI ULTERIORI: FUORI SAGOMA DETERMINATI DA STRATIFICAZIONE

METODOLOGIA DI SCAVO: TBM   AVANZAMENTO GIORNALIERO: 35 m
SEZIONE TIPO: _____   SOSTEGNO PROVVISORIO: _____

3.2 Prove di laboratorio

Le prove di laboratorio costituiscono parte integrante e essenziale della caratterizzazione geotecnica di un ammasso roccioso. I campioni possono essere prelevati mediante fori di sondaggio o in superficie. In entrambi i casi, massima cura va evidentemente utilizzata affinché i campioni prelevati subiscano il minor grado di disturbo possibile.

È opportuno poi che i campioni siano classificati mediante la determinazione delle seguenti proprietà indice secondo le procedure sperimentali di riferimento:

- composizione mineralogica (ISRM, 1978b);
- caratteristiche petrografiche (ISRM, 1978b);
- peso dell'unità di volume totale (ISRM, 1979a);
- peso dell'unità di volume secco (ISRM, 1979a);
- contenuto d'acqua (ISRM, 1979a);
- grado di saturazione (ISRM, 1979a);

- peso specifici dei grani (ISRM, 1979a);
- velocità sonica (ISRM, 1978c);
- resistenza a compressione monoassiale (ISRM, 1979b);
- resistenza a trazione brasiliana (ISRM, 1977);
- indice di durabilità (ISRM, 1979a).

PROVA DI...	SI EFFETTUA CON...	SI DETERMINANO...	RACCOMANDAZIONI DI RIFERIMENTO
Compressione monoassiale	misura delle deformazioni assiali, di quelle diametrali e della sollecitazione assiale. La prova viene eseguita in condizioni di gradiente di carico controllato e noto.	la resistenza a compressione monoassiale σ_c, il modulo elastico tangente E_t e il coefficiente di Poisson tangente v_t.	ISRM, 1979a
Compressione triassiale	misura delle deformazioni assiali e di quelle diametrali. La prova viene eseguita sottoponendo il campione a compressione isotropa fino al raggiungimento della pressione laterale prefissata; successivamente si incrementa il carico assiale sino a raggiungere la resistenza di picco del campione. La prova viene generalmente eseguita in condizioni di gradiente di carico controllato e noto. In particolari situazioni, ove si tratti di determinare la resistenza residua, la prova viene condotta con un'apparecchiatura in grado di imporre una deformazione assiale a gradiente controllato.	le leggi di resistenza (inviluppo di rottura) di picco e residua del tipo Mohr-Coulomb (con la determinazione dei parametri c'_p, ϕ'_p e c'_r, ϕ'_r) o Hoek e Brown (con la determinazione dei parametri σ_c, m_p e m_{res} essendo m il parametro che esprime l'incremento della resistenza al crescere della pressione di confinamento rispettivamente in condizioni di picco e residue).	ISRM, 1983
Taglio diretto su discontinuità	misura dello scorrimento e dello spostamento normale. La prova viene eseguita sottoponendo inizialmente il campione ad una sollecitazione costante normale alla superficie della discontinuità; successivamente si applica una sollecitazione di taglio, parallela a tale superficie, incrementata sino a provocarne lo scorrimento.	per le superfici artificiali lisce: l'angolo di attrito di base ϕ_b; per le superfici naturali: le leggi di resistenza di picco e residua del tipo Mohr-Coulomb (con la determinazione dei parametri c'_p, ϕ'_p e c'_r, ϕ'_r); la legge di resistenza di Barton (con la determinazione dei parametri JRC_o, JCS_o, ϕ'_r, essendo JRC_o il coefficiente di scabrezza e JCS_o il coefficiente di resistenza di parete alla scala del campione).	ISRM, 1974

Tabella 1 – Elenco delle prove di laboratorio per la determinazione delle proprietà meccaniche (deformabilità e resistenza).

Per la determinazione della resistenza a compressione monoassiale si può ricorrere all'esecuzione della prova specifica o, in alternativa, ove appropriato, alla determinazione mediante la prova di carico puntiforme – indice di resistenza (ISRM, 1972).

Per determinare il comportamento meccanico del materiale roccia e dei fattori che lo governano, si ricorre alle convenzionali prove di compressione monoassiale e triassiale. Per le discontinuità, si utilizza comunemente la prova di taglio diretto. Tali prove sono riassunte nella Tabella 1, insieme ad alcune informazioni sulle modalità esecutive e la normativa di riferimento.

Ulteriori prove sperimentali sono necessarie in quei casi in cui gli ammassi rocciosi hanno caratteristiche particolarmente scadenti o comportamenti di tipo rigonfiante e/o spingente. Nel caso di ammassi potenzialmente rigonfianti, è opportuno effettuare le prove riassunte nella Tabella 2 nella quale sono riportate le indicazioni date dalla commissione ISRM sulle rocce rigonfianti.

PROVA DI...	SI EFFETTUA...	RACCOMANDAZIONI DI RIFERIMENTO
Analisi diffrattometrica a raggi x	allo scopo di individuare la presenza di minerali argillosi (si considera come frazione argillosa la frazione granulometrica inferiore ai 2μ) a struttura rigonfiante (montmorillonite, smectite, vermiculite e intergradi), definendone in tutti i casi la composizione percentuale, con riferimento al volume totale del campione ed alla frazione argillosa, nella quale sono ovviamente compresi i minerali argillosi di tipo inerte.	-
Indice di deformazione di rigonfiamento	in edometro. Si determina la pressione necessaria (I_{SP}) ad impedire il rigonfiamento.	ISRM, 1989
Indice di pressione di rigonfiamento	in edometro. Si determina la deformazione assiale (I_{SA}) del provino immesso in acqua, mentre si sviluppa il rigonfiamento in condizioni di deformazione radiale impedita.	Madsen, 1999
Prove di rigonfiamento libero	determinando la deformazione assiale e radiale libera.	Madsen, 1999
Determinazione della tensione di rigonfiamento assiale in funzione della deformazione assiale di rigonfiamento	in edometro. Il provino viene riconsolidato allo stato tensionale rappresentativo del sito in esame, si aggiunge acqua e si scarica il provino a gradini attendendo che il provino abbia sviluppato tutta la sua capacità rigonfiante tra un gradino e il successivo. La prova consente di tracciare una curva $\sigma - \varepsilon$ che permette di ricavare la deformazione di rigonfiamento in funzione dello stato tensionale applicato.	Madsen, 1999

Tabella 2 – Elenco delle prove di laboratorio di rigonfiamento.

Le prove sulla matrice rocciosa e sulle discontinuità in laboratorio devono essere accompagnate da un'adeguata campagna di indagini in sito. In rapporto all'importanza dell'opera ed in considerazione della complessità della situazione geologica e geotecnica evidenziata, queste prove saranno sviluppate secondo gradi diversi di approfondimento e di ampiezza, commisurati nelle varie fasi, dal progetto esecutivo alla costruzione. Le prove più comunemente eseguite sono indicate nella Tabella 4.

È opportuno ricordare che nel caso di ammassi rocciosi anisotropi (i.e. ammassi rocciosi stratificati o scistosi) le prove devono essere eseguite in direzione sia normale che parallela al piano di isotropia.

Nel caso delle prove dilatometriche poi, poiché queste prove interessano una fascia di roccia di spessore modesto, nell'immediato intorno dello stesso foro di sondaggio, i valori dei parametri possono risultare significativamente diversi da quelli dell'ammasso roccioso in sito.

Per la valutazione della resistenza al taglio delle discontinuità secondo il modello di Barton, il coefficiente di scabrezza JRC_o e la resistenza alla compressione sulla parete del giunto JCS_o vengono determinati mediante semplici prove di scivolamento in sito o tramite il pettine di Barton, nel primo caso, e ricorrendo allo sclerometro o martello di Schmidt nel secondo.

PROVA...	SI EFFETTUA...	RACCOMANDAZIONI DI RIFERIMENTO
di carico su piastra	generalmente in cunicoli esplorativi, sul fondo di pozzi verticali o sulla roccia in affioramento. La prova viene eseguita secondo lo schema di piastra flessibile e ricorrendo alla misura degli spostamenti indotti dall'applicazione del carico all'interno dell'ammasso roccioso, in un foro di sondaggio apposito. Le prove vengono di norma effettuate mediante una serie di cicli di carico-scarico, con livelli di sollecitazione gradualmente crescenti. Oltre alla determinazione del modulo di deformazione (E_d) dell'ammasso roccioso oggetto di prova e del corrispondente modulo di scarico (E_e) (modulo "elastico"), ove la prova sia eseguita mantenendo costante il carico applicato (per i livelli di carico scelti) si potranno anche trarre indicazioni circa il comportamento deformativo a carico costante (creep).	ISRM, 1979c
con martinetti piatti	generalmente sulla parete di cunicoli esplorativi. Queste prove consentono di determinare sia il modulo di deformazione (E_d) che lo stato di sollecitazione agente alla superficie dell'ammasso roccioso.	ISRM, 1979c
dilatometrica	all'interno di fori di sondaggio, allo scopo di determinare il modulo di deformazione (E_d) dell'ammasso roccioso. Poiché queste prove interessano una fascia di roccia di spessore modesto, nell'immediato intorno dello stesso foro di sondaggio sede della prova, i valori dei moduli ricavati possono risultare significativamente diversi da quelli dell'ammasso roccioso in sito. Possono essere usati dilatometri del tipo Menard, simile a quello già usato per le terre, o meglio dilatometri per prove in roccia che rilevano le variazioni diametrali del foro, sede di prova, in corrispondenza di tre diverse orientazioni e per valori noti della pressione idrostatica uniforme applicata sulla parete.	ISRM, 1987a

Tabella 4 – Elenco delle prove in sito.

3.4 Determinazione delle caratteristiche di permeabilità

Allo scopo di determinare le caratteristiche di permeabilità degli ammassi rocciosi si può ricorrere all'esecuzione di prove specifiche, generalmente in fori di sondaggio. Le prove sono riportate nella Tabella 5.

Nel caso della prova Lugeon bisogna tenere conto che i risultati sono dipendenti dalle condizioni di prova, per cui è bene parlare di coefficiente di permeabilità per una data condizione di prova.

PROVA...	SI EFFETTUA...	RACCOMANDAZIONI DI RIFERIMENTO
Lugeon	immettendo acqua in pressione in un tratto di un foro di sondaggio. La prova può essere eseguita sia durante la perforazione (a fondo foro), sia a perforazione ultimata (in risalita), in un tratto qualunque del foro	AGI, 1977
Permeabilità di grande scala	generalmente con un pozzo centrale e una serie di fori piezometrici a raggiera lungo uno o più allineamenti. Le modalità di prova e la configurazione geometrica cui ricorrere saranno definite caso per caso, in rapporto alla situazione in esame.	AGI, 1977

Tabella 5 – Elenco delle prove di permeabilità.

3.5 Determinazione dello stato tensionale in sito

La determinazione dello stato tensionale in sito viene di norma condotta mediante le prove indicate nella Tabella 6.

PROVA...	SI EFFETTUA...	RACCOMANDAZIONI DI RIFERIMENTO
CSIR Doorstopper	misurando le deformazioni che si sviluppano nella zona centrale del fondo di un foro da sonda, in seguito alla liberazione delle tensioni, ottenuta mediante sovracarotaggio.	ISRM, 1987b
CSIRO Triassiale	misurando le deformazioni che si sviluppano sulla parete di un foro da sonda, in seguito a sovracarotaggio.	ISRM, 1987b
di fratturazione idraulica	isolando una porzione di foro da sonda e applicando al suo interno una pressione idraulica. Si misurano la pressione necessaria a provocare la rottura della roccia, quella necessaria a riaprire la fessura dopo che è stata depressurizzata e quella necessaria a mantenere aperta la fessura e si combinano questi dati per calcolare lo stato di sforzo originario.	ISRM, 1987b

Tabella 6 – Elenco delle prove per la determinazione dello stato tensionale in sito.

A commento delle informazioni riportate nelle pagine precedenti nei riguardi delle indagini e prove finalizzate alla caratterizzazione dell'ammasso roccioso, la Tabella 7 presenta le acquisizioni di tipo geotecnico in relazione alla loro importanza nella progettazione di gallerie con scavo meccanizzato.

DETERMINAZIONE	IMPORTANZA
Proprietà indice	utile
Compressione monoassiale	notevole
Compressione triassiale	utile (in casi, notevole)
Taglio diretto su discontinuità	consigliata
Prove di rigonfiamento	notevole
Carico su piastra	consigliata (in casi, in corso d'opera)
Martinetti piatti	consigliata (in casi, in corso d'opera)
Dilatometriche	consigliata
Permeabilità	notevole
Stato tensionale in situ	utile (in casi, notevole)

Tabella 7 – Sintesi delle determinazioni sperimentali e livello di importanza per lo scavo di gallerie con scavo meccanizzato.
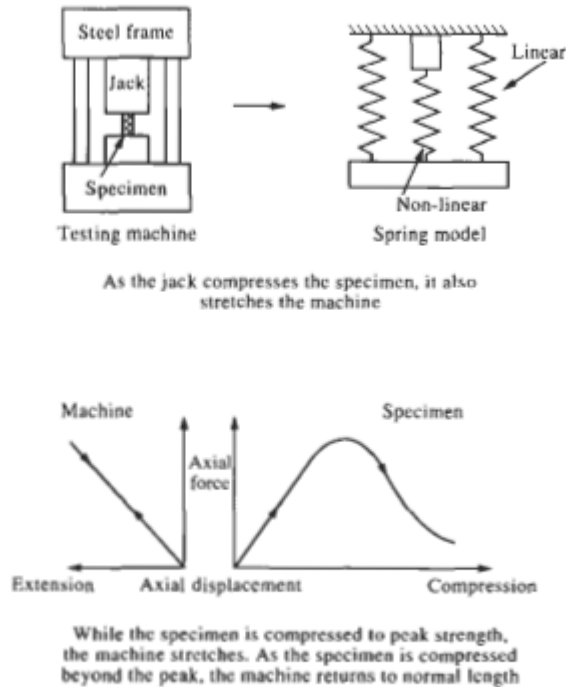
Testing machine / Spring model

As the jack compresses the specimen, it also stretches the machine

While the specimen is compressed to peak strength, the machine stretches. As the specimen is compressed beyond the peak, the machine returns to normal length

Figure 6.6 Schematic and conceptual illustration of specimen and testing machine stiffnesses.

Soft testing machine

Energy required = ABCD
Energy supplied = AECD

Stiff testing machine

Energy required = ABCD
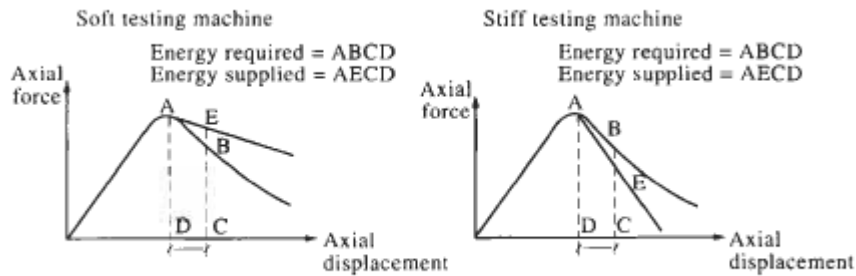Energy supplied = AECD

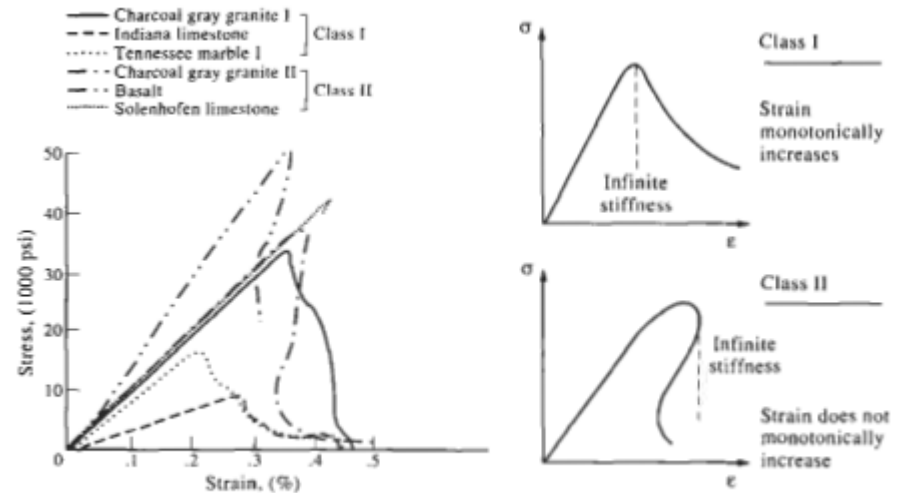**Figure 6.7** Machine stiffness and specimen stiffness in the post-peak region.

Figure 6.8 Examples of complete stress–strain curves for different rocks (from Wawersik and Fairhurst, 1970).
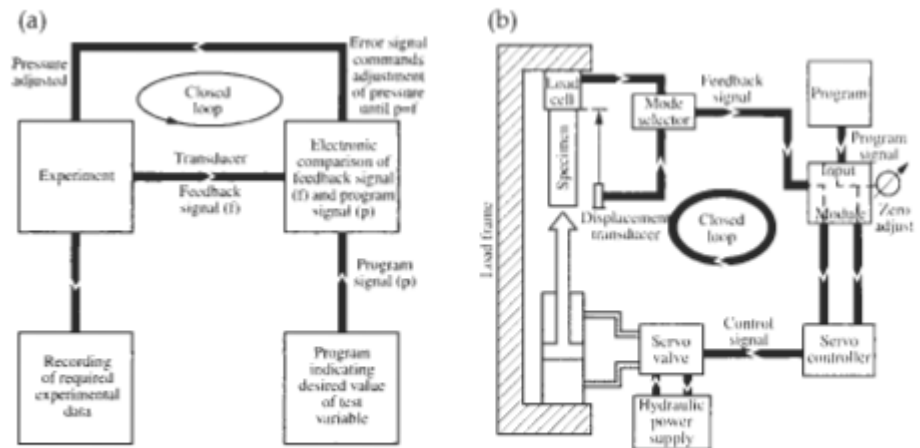

Figure 6.9 (a) Principle of closed-loop control. (b) Schematic of fast–response, closed-loop servo-controlled testing machine (courtesy MTS Systems Corp.).
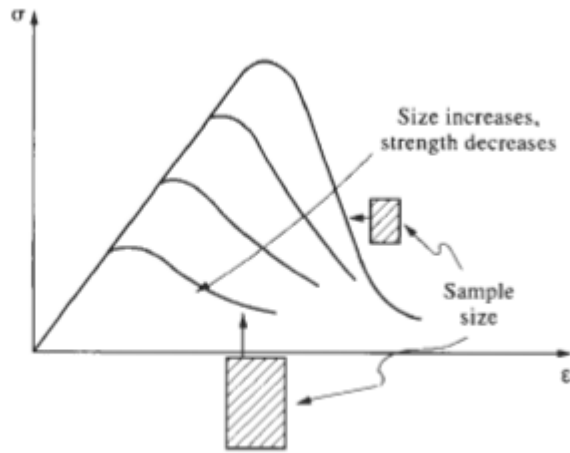
44

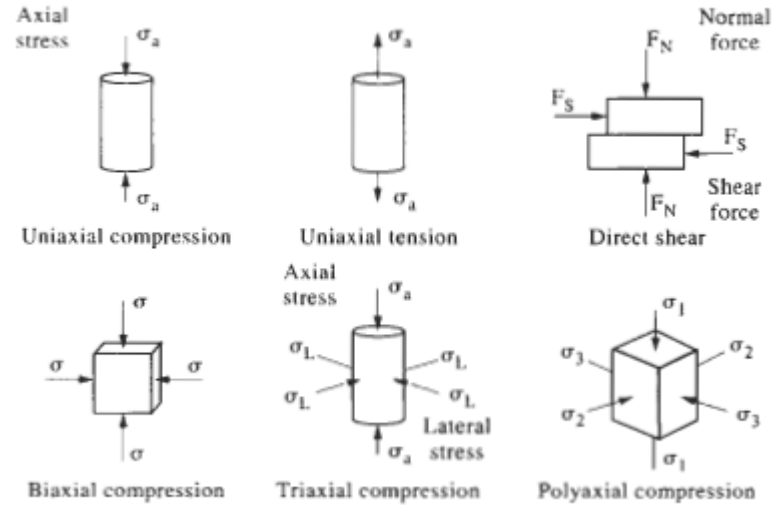**Figure 6.11** The size effect in the uniaxial complete stress–strain curve.

Figure 6.13 Specimen loading conditi ons in general laboratory use.
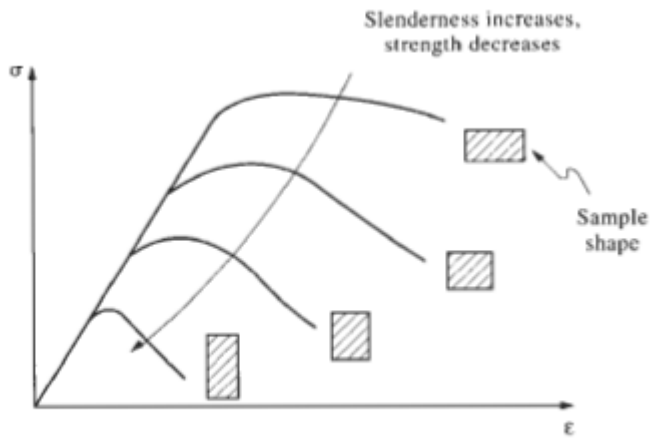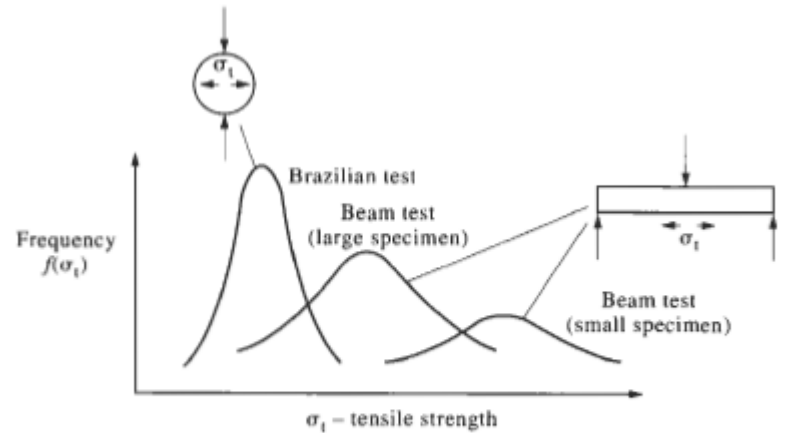

Figure 6.12 The shape effect in uniaxial compression.

Figure 6.14 Tensile strength variation as a function of specimen volume and type of test.

σ_a

Increasing
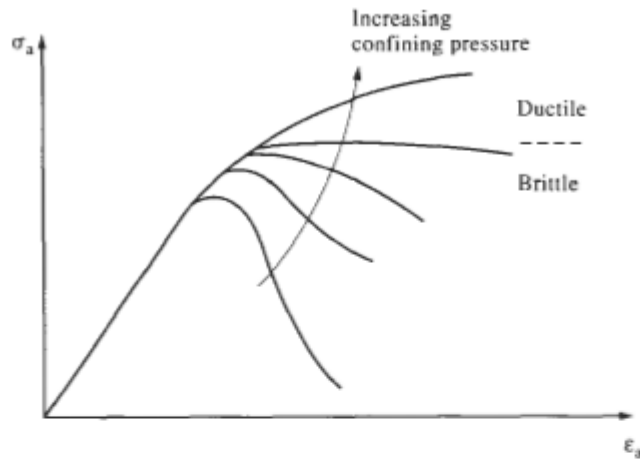confining pressure

Ductile

Brittle

ε_a

Figure 6.15 The effect of confining pressure in the triaxial test and the brittle–ductile transition.

An idea of the variability in the confining pressure associated with the transition is given in the table below (after Goodman, 1989).

Rock type	Confining pressure (MPa)
Rock salt	0
Chalk	<10
Limestone	20–100
Sandstone	>100
Granite	≫100

Time-dependent effects. We have indicated that during the complete stress–strain curve, microcracking occurs from a very early stage in the pre-peak region. For some purposes, it is convenient to assume that much of the pre-peak portion represents elastic behaviour. However, there is no time component in the theory of elasticity; yet, because of the continually increasing microstructural damage even in the 'elastic' region, we would expect some time-dependent behaviour.

There are four main time-dependent effects which are discussed here.

(a) **strain rate**—the total form of the complete stress–strain curve is a function of the applied strain rate;
(b) **creep**—a material continues to strain when the applied stress is held constant;
(c) **relaxation**—there is a decrease in stress within the material when the applied strain is held constant;
(d) **fatigue**—there is an increase in strain due to cyclical changes in stress.

These four effects are shown in Fig. 6.16 and are all manifestations of the time-dependent nature of microcrack development.

The effect of a reduced strain rate is to reduce the overall elastic modulus and the compressive strength. Creep from a point A in Fig. 6.16 is indicated by the line AC. Relaxation is indicated by the line AR. Fatigue is indicated by the stress cycles. The relation between these effects can be seen especially from the form of the complete stress–strain curve at lower and lower strain rates. Depending on whether the control variable is stress or strain, the rock will be continually creeping or relaxing, respectively, during generation of the complete stress–strain curve.

We have noted that stress cannot be used as the control variable to obtain the post-peak region of the curve; nor indeed, as indicated by the line BC in Fig. 6.16, can creep occur in the post-peak region without instantaneous failure. As indicated by the lines AR and BR, relaxation can occur on either side of the curve for a Class I curve. Also indicated in the figure are the lines
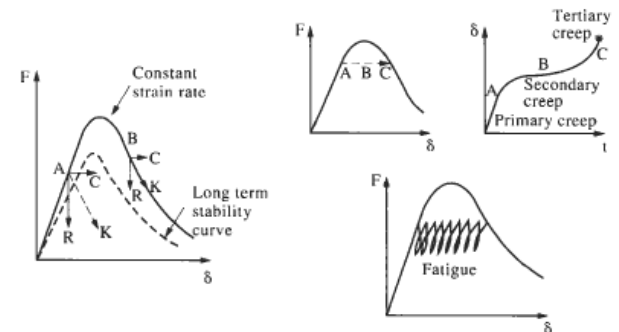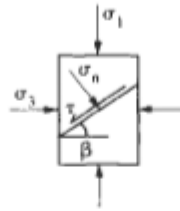

Figure 6.16 Time-dependent effects and the complete stress–strain curve.

BASIC EQUATIONS   Rock fails at a critical combination of normal and shear stresses:

$$|\tau| = \tau_0 + \mu\sigma_n$$

τ_0 = cohesion μ = coeff. of friction

$$|\tau| = \tfrac{1}{2}(\sigma_1 - \sigma_3)\sin 2\beta$$

$$\sigma_n = \tfrac{1}{2}(\sigma_1 + \sigma_3) + \tfrac{1}{2}(\sigma_1 - \sigma_3)\cos 2\beta$$

The equation for $|\tau|$ and σ_n are the equations of a circle in (σ, τ) space:

FUNDAMENTAL GEOMETRY

Tensile cutoff, T_0

Mohr envelope

$\mu = \tan\phi$
$\tau_0 = c$

At failure,
$2\beta = 90 + \phi$
$\Rightarrow \beta = 45 + \frac{\phi}{2}$

σ_t Uniaxial tension

σ_3 σ_c Uniaxial compression

2β
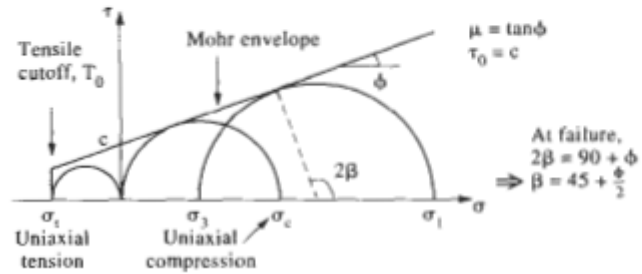
Figure 6.18 The Mohr–Coulomb failure criterion.

$m = 14.3$
$r^2 = 0.87$

$\frac{\sigma_1}{\sigma_c}$
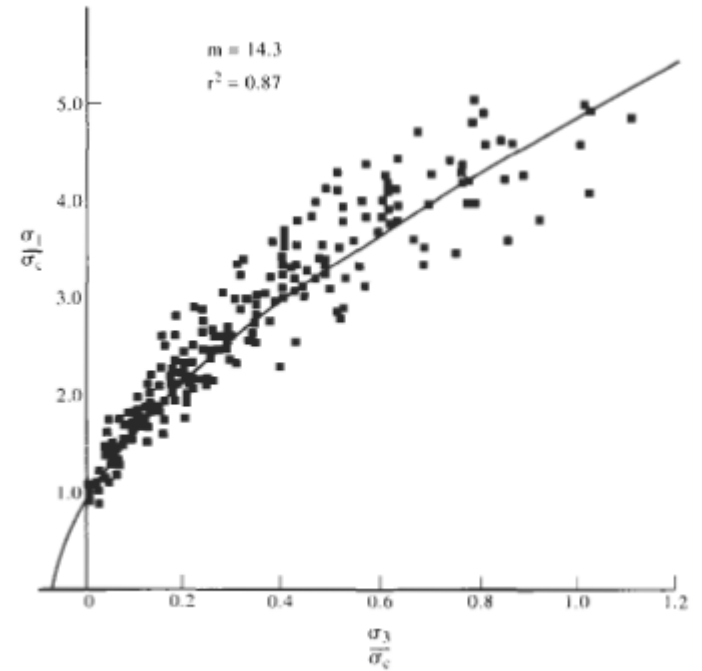
$\frac{\sigma_3}{\sigma_c}$

Figure 6.20 The Hoek–Brown empirical failure criterion.

47

4. CLASSIFICAZIONE DELL'AMMASSO ROCCIOSO

Le classificazioni consentono di assegnare una classe di qualità all'ammasso roccioso in esame, essendo ogni classe associata ad un indice numerico. L'ammasso roccioso viene concordemente suddiviso in regioni omogenee lungo il tracciato della galleria, che spesso sono delimitate da singolarità geologiche (faglie, dislocazioni, ecc.); quindi, sulla base delle risultanze dei rilievi geostrutturali e delle perforazioni di sondaggio (in casi particolari, dell'osservazione di cunicoli esplorativi), si procede alla determinazione degli indici di classificazione.

Ad oggi, i metodi più diffusamente usati per classificare gli ammassi rocciosi sono:

- RSR (Rock Structure Rating System) (Wickham et al. 1972)
- Q (Barton et al., 1974, Grimstad & Barton, 1993)
- RMR (Rock Mass Rating System) (Bieniawski, 1973, Bieniawski, 1989)
- GSI (Geological Strength Index) (Hoek, 1994, Hoek et al., 1995, Hoek et al., 1998)
- Önorm B 2203 (Lauffer, 1997).

Rock mass classification

Introduction

During the feasibility and preliminary design stages of a project, when very little detailed information is available on the rock mass and its stress and hydrologic characteristics, the use of a rock mass classification scheme can be of considerable benefit. At its simplest, this may involve using the classification scheme as a check-list to ensure that all relevant information has been considered. At the other end of the spectrum, one or more rock mass classification schemes can be used to build up a picture of the composition and characteristics of a rock mass to provide initial estimates of support requirements, and to provide estimates of the strength and deformation properties of the rock mass.

It is important to understand the limitations of rock mass classification schemes (Palmstrom and Broch, 2006) and that their use does not (and cannot) replace some of the more elaborate design procedures. However, the use of these design procedures requires access to relatively detailed information on in situ stresses, rock mass properties and planned excavation sequence, none of which may be available at an early stage in the project. As this information becomes available, the use of the rock mass classification schemes should be updated and used in conjunction with site specific analyses.

Engineering rock mass classification

Rock mass classification schemes have been developing for over 100 years since Ritter (1879) attempted to formalise an empirical approach to tunnel design, in particular for determining support requirements. While the classification schemes are appropriate for their original application, especially if used within the bounds of the case histories from which they were developed, considerable caution must be exercised in applying rock mass classifications to other rock engineering problems.

Summaries of some important classification systems are presented in this chapter, and although every attempt has been made to present all of the pertinent data from the original texts, there are numerous notes and comments which cannot be included. The interested reader should make every effort to read the cited references for a full appreciation of the use, applicability and limitations of each system.

Most of the multi-parameter classification schemes (Wickham et al (1972) Bieniawski (1973, 1989) and Barton et al (1974)) were developed from civil engineering case histories in which all of the components of the engineering geological character of the rock mass were included. In underground hard rock mining, however, especially at deep levels, rock mass weathering and the influence of water usually are not significant and may be ignored. Different classification systems place different emphases on the various parameters, and it is recommended that at least two methods be used at any site during the early stages of a project.

Terzaghi's rock mass classification

The earliest reference to the use of rock mass classification for the design of tunnel support is in a paper by Terzaghi (1946) in which the rock loads, carried by steel sets, are estimated on the basis of a descriptive classification. While no useful purpose would be served by including details of Terzaghi's classification in this discussion on the design of support, it is interesting to examine the rock mass descriptions included in his original paper, because he draws attention to those characteristics that dominate rock mass behaviour, particularly in situations where gravity constitutes the dominant driving force. The clear and concise definitions and the practical comments included in these descriptions are good examples of the type of engineering geology information, which is most useful for engineering design.

Terzaghi's descriptions (quoted directly from his paper) are:

- *Intact* rock contains neither joints nor hair cracks. Hence, if it breaks, it breaks across sound rock. On account of the injury to the rock due to blasting, spalls may drop off the roof several hours or days after blasting. This is known as a *spalling* condition. Hard, intact rock may also be encountered in the *popping* condition involving the spontaneous and violent detachment of rock slabs from the sides or roof.

- *Stratified* rock consists of individual strata with little or no resistance against separation along the boundaries between the strata. The strata may or may not be weakened by transverse joints. In such rock the spalling condition is quite common.

- *Moderately jointed* rock contains joints and hair cracks, but the blocks between joints are locally grown together or so intimately interlocked that vertical walls do not require lateral support. In rocks of this type, both spalling and popping conditions may be encountered.

- *Blocky and seamy* rock consists of chemically intact or almost intact rock fragments which are entirely separated from each other and imperfectly interlocked. In such rock, vertical walls may require lateral support.

- *Crushed* but chemically intact rock has the character of crusher run. If most or all of the fragments are as small as fine sand grains and no recementation has taken place, crushed rock below the water table exhibits the properties of a water-bearing sand.

- *Squeezing* rock slowly advances into the tunnel without perceptible volume increase. A prerequisite for squeeze is a high percentage of microscopic and sub-microscopic particles of micaceous minerals or clay minerals with a low swelling capacity.

- *Swelling* rock advances into the tunnel chiefly on account of expansion. The capacity to swell seems to be limited to those rocks that contain clay minerals such as montmorillonite, with a high swelling capacity.

Lauffer (1958) proposed that the stand-up time for an unsupported span is related to the quality of the rock mass in which the span is excavated. In a tunnel, the unsupported span is defined as the span of the tunnel or the distance between the face and the nearest support, if this is greater than the tunnel span. Lauffer's original classification has since been modified by a number of authors, notably Pacher et al (1974), and now forms part of the general tunnelling approach known as the New Austrian Tunnelling Method.

The significance of the stand-up time concept is that an increase in the span of the tunnel leads to a significant reduction in the time available for the installation of support. For example, a small pilot tunnel may be successfully constructed with minimal support, while a larger span tunnel in the same rock mass may not be stable without the immediate installation of substantial support.

The New Austrian Tunnelling Method includes a number of techniques for safe tunnelling in rock conditions in which the stand-up time is limited before failure occurs. These techniques include the use of smaller headings and benching or the use of multiple drifts to form a reinforced ring inside which the bulk of the tunnel can be excavated. These techniques are applicable in soft rocks such as shales, phyllites and mudstones in which the squeezing and swelling problems, described by Terzaghi (see previous section), are likely to occur. The techniques are also applicable when tunnelling in excessively broken rock, but great care should be taken in attempting to apply these techniques to excavations in hard rocks in which different failure mechanisms occur.

In designing support for hard rock excavations it is prudent to assume that the stability of the rock mass surrounding the excavation is not time-dependent. Hence, if a structurally defined wedge is exposed in the roof of an excavation, it will fall as soon as the rock supporting it is removed. This can occur at the time of the blast or during the subsequent scaling operation. If it is required to keep such a wedge in place, or to enhance the margin of safety, it is essential that the support be installed as early as possible, preferably before the rock supporting the full wedge is removed. On the other hand, in a highly stressed rock, failure will generally be induced by some change in the stress field surrounding the excavation. The failure may occur gradually and manifest itself as spalling or slabbing or it may occur suddenly in the form of a rock burst. In either case, the support design must take into account the change in the stress field rather than the 'stand-up' time of the excavation.

Rock quality designation index (RQD)

The Rock Quality Designation index (*RQD*) was developed by Deere (Deere et al 1967) to provide a quantitative estimate of rock mass quality from drill core logs. RQD is defined as the percentage of intact core pieces longer than 100 mm (4 inches) in the total length of core. The core should be at least NW size (54.7 mm or 2.15 inches in diameter) and should be drilled with a double-tube core barrel. The correct procedures for

measurement of the length of core pieces and the calculation of *RQD* are summarised in Figure 1.
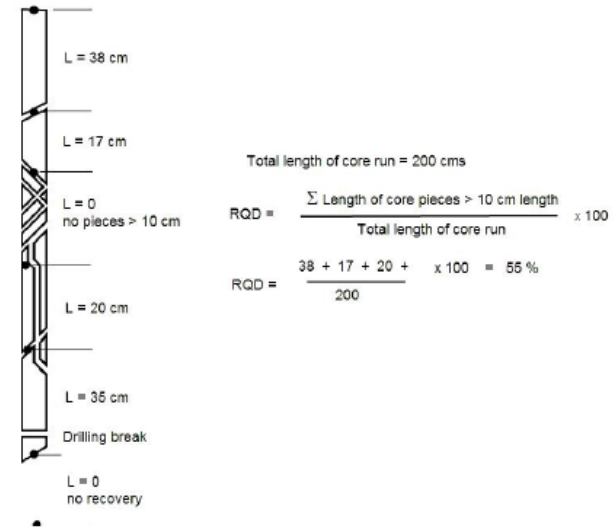

Figure 1: Procedure for measurement and calculation of *RQD* (After Deere, 1989).

Palmström (1982) suggested that, when no core is available but discontinuity traces are visible in surface exposures or exploration adits, the *RQD* may be estimated from the number of discontinuities per unit volume. The suggested relationship for clay-free rock masses is:

$$RQD = 115 - 3.3 \, J_v \qquad (1)$$

where J_v is the sum of the number of joints per unit length for all joint (discontinuity) sets known as the volumetric joint count.

RQD is a directionally dependent parameter and its value may change significantly, depending upon the borehole orientation. The use of the volumetric joint count can be quite useful in reducing this directional dependence.

RQD is intended to represent the rock mass quality in situ. When using diamond drill core, care must be taken to ensure that fractures, which have been caused by handling or the drilling process, are identified and ignored when determining the value of *RQD*.

When using Palmström's relationship for exposure mapping, blast induced fractures should not be included when estimating J_v.

Deere's *RQD* was widely used, particularly in North America, after its introduction. Cording and Deere (1972), Merritt (1972) and Deere and Deere (1988) attempted to relate *RQD* to Terzaghi's rock load factors and to rockbolt requirements in tunnels. In the context of this discussion, the most important use of *RQD* is as a component of the *RMR* and *Q* rock mass classifications covered later in this chapter.

Rock Structure Rating (RSR)

Wickham et al (1972) described a quantitative method for describing the quality of a rock mass and for selecting appropriate support on the basis of their Rock Structure Rating (*RSR*) classification. Most of the case histories, used in the development of this system, were for relatively small tunnels supported by means of steel sets, although historically this system was the first to make reference to shotcrete support. In spite of this limitation, it is worth examining the *RSR* system in some detail since it demonstrates the logic involved in developing a quasi-quantitative rock mass classification system.

The significance of the *RSR* system, in the context of this discussion, is that it introduced the concept of rating each of the components listed below to arrive at a numerical value of $RSR = A + B + C$.

1. *Parameter A, Geology:* General appraisal of geological structure on the basis of:
   a. Rock type origin (igneous, metamorphic, sedimentary).
   b. Rock hardness (hard, medium, soft, decomposed).
   c. Geologic structure (massive, slightly faulted/folded, moderately faulted/folded, intensely faulted/folded).
2. *Parameter B, Geometry:* Effect of discontinuity pattern with respect to the direction of the tunnel drive on the basis of:
   a. Joint spacing.
   b. Joint orientation (strike and dip).
   c. Direction of tunnel drive.
3. *Parameter C:* Effect of groundwater inflow and joint condition on the basis of:
   a. Overall rock mass quality on the basis of A and B combined.
   b. Joint condition (good, fair, poor).
   c. Amount of water inflow (in gallons per minute per 1000 feet of tunnel).

Note that the *RSR* classification used Imperial units and that these units have been retained in this discussion.

Three tables from Wickham et al's 1972 paper are reproduced in Tables 1, 2 and 3. These tables can be used to evaluate the rating of each of these parameters to arrive at the *RSR* value (maximum *RSR* = 100).

Table 1: Rock Structure Rating: Parameter A: General area geology

	Basic Rock Type				Geological Structure			
	Hard	Medium	Soft	Decomposed				
Igneous	1	2	3	4		Slightly	Moderately	Intensively
Metamorphic	1	2	3	4		Folded or	Folded or	Folded or
Sedimentary	2	3	4	4	Massive	Faulted	Faulted	Faulted
Type 1					30	22	15	9
Type 2					27	20	13	8
Type 3					24	18	12	7
Type 4					19	15	10	6

Table 2: Rock Structure Rating: Parameter B: Joint pattern, direction of drive

	Strike ⊥ to Axis					Strike ∥ to Axis		
	Direction of Drive					Direction of Drive		
	Both	With Dip		Against Dip		Either direction		
		Dip of Prominent Joints [a]				Dip of Prominent Joints		
Average joint spacing	Flat	Dipping	Vertical	Dipping	Vertical	Flat	Dipping	Vertical
1. Very closely jointed, < 2 in	9	11	13	10	12	9	9	7
2. Closely jointed, 2-6 in	13	16	19	15	17	14	14	11
3. Moderately jointed, 6-12 in	23	24	28	19	22	23	23	19
4. Moderate to blocky, 1-2 ft	30	32	36	25	28	30	28	24
5. Blocky to massive, 2-4 ft	36	38	40	33	35	36	24	28
6. Massive, > 4 ft	40	43	45	37	40	40	38	34

Table 3: Rock Structure Rating: Parameter C: Groundwater, joint condition

	Sum of Parameters A + B					
	13 - 44			45 - 75		
Anticipated water inflow	Joint Condition [b]					
gpm/1000 ft of tunnel	Good	Fair	Poor	Good	Fair	Poor
None	22	18	12	25	22	18
Slight, < 200 gpm	19	15	9	23	19	14
Moderate, 200-1000 gpm	15	22	7	21	16	12
Heavy, > 1000 gp	10	8	6	18	14	10

[a] Dip: flat: 0-20°; dipping: 20-50°; and vertical: 50-90°

[b] Joint condition: good = tight or cemented; fair = slightly weathered or altered; poor = severely weathered, altered or open

For example, a hard metamorphic rock which is slightly folded or faulted has a rating of $A = 22$ (from Table 1). The rock mass is moderately jointed, with joints striking perpendicular to the tunnel axis which is being driven east-west, and dipping at between 20° and 50°.

Table 2 gives the rating for $B = 24$ for driving with dip (defined below).
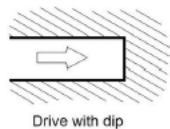
Drive with dip

The value of $A + B = 46$ and this means that, for joints of fair condition (slightly weathered and altered) and a moderate water inflow of between 200 and 1,000 gallons per minute, Table 3 gives the rating for $C = 16$. Hence, the final value of the rock structure rating $RSR = A + B + C = 62$.
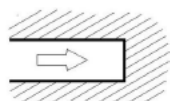
Drive against dip

A typical set of prediction curves for a 24 foot diameter tunnel are given in Figure 2 which shows that, for the RSR value of 62 derived above, the predicted support would be 2 inches of shotcrete and 1 inch diameter rockbolts spaced at 5 foot centres. As indicated in the figure, steel sets would be spaced at more than 7 feet apart and would not be considered a practical solution for the support of this tunnel.
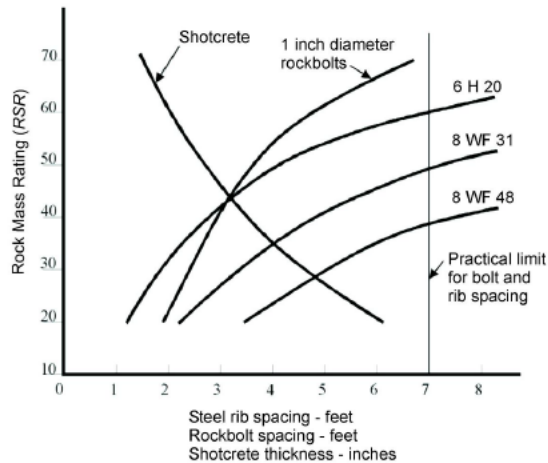

Figure 2: RSR support estimates for a 24 ft. (7.3 m) diameter circular tunnel. Note that rockbolts and shotcrete are generally used together. (After Wickham et al 1972).

For the same size tunnel in a rock mass with $RSR = 30$, the support could be provided by 8 WF 31 steel sets (8 inch deep wide flange I section weighing 31 lb per foot) spaced 3 feet apart, or by 5 inches of shotcrete and 1 inch diameter rockbolts spaced at 2.5 feet centres. In this case it is probable that the steel set solution would be cheaper and more effective than the use of rockbolts and shotcrete.

Although the RSR classification system is not widely used today, Wickham et al's work played a significant role in the development of the classification schemes discussed in the remaining sections of this chapter.

Geomechanics Classification

Bieniawski (1976) published the details of a rock mass classification called the Geomechanics Classification or the Rock Mass Rating (RMR) system. Over the years, this system has been successively refined as more case records have been examined and the reader should be aware that Bieniawski has made significant changes in the ratings assigned to different parameters. The discussion which follows is based upon the 1989 version of the classification (Bieniawski, 1989). Both this version and the 1976 version deal with estimating the strength of rock masses. The following six parameters are used to classify a rock mass using the RMR system:

1. Uniaxial compressive strength of rock material.
2. Rock Quality Designation (RQD).
3. Spacing of discontinuities.
4. Condition of discontinuities.
5. Groundwater conditions.
6. Orientation of discontinuities.

In applying this classification system, the rock mass is divided into a number of structural regions and each region is classified separately. The boundaries of the structural regions usually coincide with a major structural feature such as a fault or with a change in rock type. In some cases, significant changes in discontinuity spacing or characteristics, within the same rock type, may necessitate the division of the rock mass into a number of small structural regions.

The Rock Mass Rating system is presented in Table 4, giving the ratings for each of the six parameters listed above. These ratings are summed to give a value of RMR. The following example illustrates the use of these tables to arrive at an RMR value.

A tunnel is to be driven through slightly weathered granite with a dominant joint set dipping at 60° against the direction of the drive. Index testing and logging of diamond drilled core give typical Point-load strength index values of 8 MPa and average RQD values of 70%. The slightly rough and slightly weathered joints with a separation of < 1 mm, are spaced at 300 mm. Tunnelling conditions are anticipated to be wet.
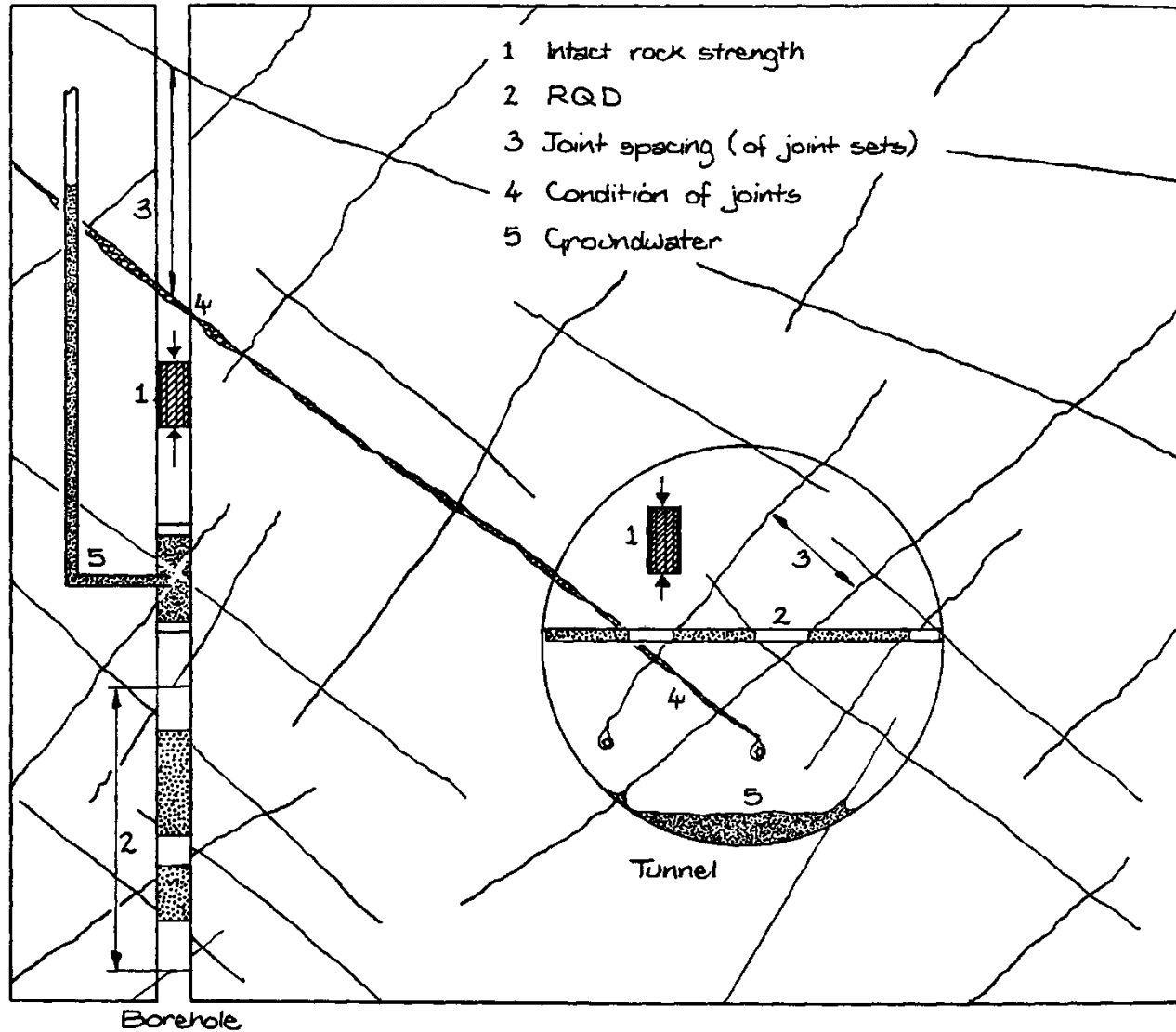
Rock Mass Rating System

1 Intact rock strength
2 RQD
3 Joint spacing (of joint sets)
4 Condition of joints
5 Groundwater

Borehole

Tunnel

Table 4: Rock Mass Rating System (After Bieniawski 1989).

A. CLASSIFICATION PARAMETERS AND THEIR RATINGS

	Parameter				Range of values				
1	Strength of intact rock material	Point-load strength index	>10 MPa	4 - 10 MPa	2 - 4 MPa	1 - 2 MPa	For this low range - uniaxial compressive test is preferred		
		Uniaxial comp. strength	>250 MPa	100 - 250 MPa	50 - 100 MPa	25 - 50 MPa	5 - 25 MPa	1 - 5 MPa	< 1 MPa
	Rating		15	12	7	4	2	1	0
2	Drill core Quality RQD		90% - 100%	75% - 90%	50% - 75%	25% - 50%	< 25%		
	Rating		20	17	13	8	3		
3	Spacing of discontinuities		> 2 m	0.6 - 2 . m	200 - 600 mm	60 - 200 mm	< 60 mm		
	Rating		20	15	10	8	5		
4	Condition of discontinuities (See E)		Very rough surfaces Not continuous No separation Unweathered wall rock	Slightly rough surfaces Separation < 1 mm Slightly weathered walls	Slightly rough surfaces Separation < 1 mm Highly weathered walls	Slickensided surfaces or Gouge < 5 mm thick or Separation 1-5 mm Continuous	Soft gouge >5 mm thick or Separation > 5 mm Continuous		
	Rating		30	25	20	10	0		
5	Groundwater	Inflow per 10 m tunnel length (l/m)	None	< 10	10 - 25	25 - 125	> 125		
		(Joint water press)/ (Major principal σ)	0	< 0.1	0.1, - 0.2	0.2 - 0.5	> 0.5		
		General conditions	Completely dry	Damp	Wet	Dripping	Flowing		
	Rating		15	10	7	4	0		

B. RATING ADJUSTMENT FOR DISCONTINUITY ORIENTATIONS (See F)

Strike and dip orientations		Very favourable	Favourable	Fair	Unfavourable	Very Unfavourable
Ratings	Tunnels & mines	0	-2	-5	-10	-12
	Foundations	0	-2	-7	-15	-25
	Slopes	0	-5	-25	-50	

C. ROCK MASS CLASSES DETERMINED FROM TOTAL RATINGS

Rating	100 ← 81	80 ← 61	60 ← 41	40 ← 21	< 21
Class number	I	II	III	IV	V
Description	Very good rock	Good rock	Fair rock	Poor rock	Very poor rock

D. MEANING OF ROCK CLASSES

Class number	I	II	III	IV	V
Average stand-up time	20 yrs for 15 m span	1 year for 10 m span	1 week for 5 m span	10 hrs for 2.5 m span	30 min for 1 m span
Cohesion of rock mass (kPa)	> 400	300 - 400	200 - 300	100 - 200	< 100
Friction angle of rock mass (deg)	> 45	35 - 45	25 - 35	15 - 25	< 15

E. GUIDELINES FOR CLASSIFICATION OF DISCONTINUITY conditions

	< 1 m	1 - 3 m	3 - 10 m	10 - 20 m	> 20 m
Discontinuity length (persistence) Rating	6	4	2	1	0
Separation (aperture)	None	< 0.1 mm	0.1 - 1.0 mm	1 - 5 mm	> 5 mm
Rating	6	5	4	1	0
Roughness	Very rough	Rough	Slightly rough	Smooth	Slickensided
Rating	6	5	3	1	0
Infilling (gouge)	None	Hard filling < 5 mm	Hard filling > 5 mm	Soft filling < 5 mm	Soft filling > 5 mm
Rating	6	4	2	2	0
Weathering	Unweathered	Slightly weathered	Moderately weathered	Highly weathered	Decomposed
Ratings	6	5	3	1	0

F. EFFECT OF DISCONTINUITY STRIKE AND DIP ORIENTATION IN TUNNELLING**

Strike perpendicular to tunnel axis				Strike parallel to tunnel axis	
Drive with dip - Dip 45 - 90°	Drive with dip - Dip 20 - 45°		Dip 45 - 90°	Dip 20 - 45°	
Very favourable	Favourable		Very unfavourable	Fair	
Drive against dip - Dip 45-90°	Drive against dip - Dip 20-45°		Dip 0-20 - Irrespective of strike°		
Fair	Unfavourable		Fair		

* Some conditions are mutually exclusive . For example, if infilling is present, the roughness of the surface will be overshadowed by the influence of the gouge. In such cases use A.4 directly.

** Modified after Wickham et al (1972).

The *RMR* value for the example under consideration is determined as follows:

Table	Item	Value	Rating
4: A.1	Point load index	8 MPa	12
4: A.2	*RQD*	70%	13
4: A.3	Spacing of discontinuities	300 mm	10
4: E.4	Condition of discontinuities	Note 1	22
4: A.5	Groundwater	Wet	7
4: B	Adjustment for joint orientation	Note 2	-5
		Total	59

Note 1. For slightly rough and altered discontinuity surfaces with a separation of < 1 mm, Table 4.A.4 gives a rating of 25. When more detailed information is available, Table 4.E can be used to obtain a more refined rating. Hence, in this case, the rating is the sum of: 4 (1-3 m discontinuity length), 4 (separation 0.1-1.0 mm), 3 (slightly rough), 6 (no infilling) and 5 (slightly weathered) = 22.

Note 2. Table 4.F gives a description of 'Fair' for the conditions assumed where the tunnel is to be driven against the dip of a set of joints dipping at 60°. Using this description for 'Tunnels and Mines' in Table 4.B gives an adjustment rating of -5.

Bieniawski (1989) published a set of guidelines for the selection of support in tunnels in rock for which the value of *RMR* has been determined. These guidelines are reproduced in Table 4. Note that these guidelines have been published for a 10 m span horseshoe shaped tunnel, constructed using drill and blast methods, in a rock mass subjected to a vertical stress < 25 MPa (equivalent to a depth below surface of <900 m).

For the case considered earlier, with *RMR* = 59, Table 4 suggests that a tunnel could be excavated by top heading and bench, with a 1.5 to 3 m advance in the top heading. Support should be installed after each blast and the support should be placed at a maximum distance of 10 m from the face. Systematic rock bolting, using 4 m long 20 mm diameter fully grouted bolts spaced at 1.5 to 2 m in the crown and walls, is recommended. Wire mesh, with 50 to 100 mm of shotcrete for the crown and 30 mm of shotcrete for the walls, is recommended.

The value of *RMR* of 59 indicates that the rock mass is on the boundary between the 'Fair rock' and 'Good rock' categories. In the initial stages of design and construction, it is advisable to utilise the support suggested for fair rock. If the construction is progressing well with no stability problems, and the support is performing very well, then it should be possible to gradually reduce the support requirements to those indicated for a good rock mass. In addition, if the excavation is required to be stable for a short amount of time, then it is advisable to try the less expensive and extensive support suggested for good rock. However, if the rock mass surrounding the excavation is expected to undergo large mining induced stress changes, then more substantial support appropriate for fair rock should be installed. This example indicates that a great deal of judgement is needed in the application of rock mass classification to support design.

Table 5: Guidelines for excavation and support of 10 m span rock tunnels in accordance with the *RMR* system (After Bieniawski 1989).

Rock mass class	Excavation	Rock bolts (20 mm diameter, fully grouted)	Shotcrete	Steel sets
I - Very good rock *RMR*: 81-100	Full face, 3 m advance.	Generally no support required except spot bolting.		
II - Good rock *RMR*: 61-80	Full face , 1-1.5 m advance. Complete support 20 m from face.	Locally, bolts in crown 3 m long, spaced 2.5 m with occasional wire mesh.	50 mm in crown where required.	None.
III - Fair rock *RMR*: 41-60	Top heading and bench 1.5-3 m advance in top heading. Commence support after each blast. Complete support 10 m from face.	Systematic bolts 4 m long, spaced 1.5 - 2 m in crown and walls with wire mesh in crown.	50-100 mm in crown and 30 mm in sides.	None.
IV - Poor rock *RMR*: 21-40	Top heading and bench 1.0-1.5 m advance in top heading. Install support concurrently with excavation, 10 m from face.	Systematic bolts 4-5 m long, spaced 1-1.5 m in crown and walls with wire mesh.	100-150 mm in crown and 100 mm in sides.	Light to medium ribs spaced 1.5 m where required.
V – Very poor rock *RMR*: < 20	Multiple drifts 0.5-1.5 m advance in top heading. Install support concurrently with excavation. Shotcrete as soon as possible after blasting.	Systematic bolts 5-6 m long, spaced 1-1.5 m in crown and walls with wire mesh. Bolt invert.	150-200 mm in crown, 150 mm in sides, and 50 mm on face.	Medium to heavy ribs spaced 0.75 m with steel lagging and forepoling if required. Close invert.

It should be noted that Table 5 has not had a major revision since 1973. In many mining and civil engineering applications, steel fibre reinforced shotcrete may be considered in place of wire mesh and shotcrete.

4.2 Classificazione mediante Q

Il metodo Q, introdotto da Barton et al. (1974), prevede la definizione, per l'ammasso roccioso in esame, di sei parametri:

- recupero percentuale modificato RQD (Rock Quality Designation)
- J_n, funzione del numero di sistemi principali di discontinuità presenti
- J_r, funzione del grado di scabrezza a piccola e grande scala delle superfici di discontinuità
- J_a, funzione delle condizioni delle superfici di discontinuità (alterazione, riempimento)
- J_w, coefficiente di riduzione che tiene conto delle venute di acqua
- SRF, fattore di riduzione funzione dello stato tensionale in sito.

Noto il valore di RQD, ad ognuno degli altri parametri è associato un indice numerico; la formula (1) consente di definire un valore Q caratteristico dell'ammasso roccioso ed una relativa classe di qualità. Sono previste nove classi, per valori di Q variabili da meno di 0.01 a 1000.

$$Q = \frac{RQD}{J_n} \frac{J_r}{J_a} \frac{J_w}{SRF} \tag{1}$$

È utile ricordare che per ammassi rocciosi di buona qualità e nel campo di profondità 25-50 m, l'indice Q può essere posto in relazione con V_p, la velocità dell'onda elastica longitudinale in sito (Barton, 1996):

$$V_p = \log Q + 3.5 \tag{2}$$

dove V_p è espresso in km/s.

L'analisi della correlazione tra Q e V_P in numerosi siti costituiti da rocce tenere ha evidenziato la necessità di variare tale relazione per tener conto della resistenza a compressione e della porosità della roccia in esame, e della profondità alla quale avviene lo scavo (Barton, 1996). Quando la roccia costituente l'ammasso presenta un valore di resistenza a compressione monoassiale σ_c inferiore a 100 MPa (valore ritenuto caratteristico di una roccia di buona resistenza) occorre allora utilizzare per tale relazione l'indice Q_c (vedi formula 3), ottenuto normalizzando il valore di Q per il rapporto $\sigma_c/100$ dove σ_c è espresso in MPa:

$$Q_c = \left(\frac{RQD}{J_n} \frac{J_r}{J_a} \frac{J_w}{SRF} \right) \frac{\sigma_c}{100} \tag{3}$$

La Figura 8 pone in relazione V_p e Q_c, in ragione della profondità H considerata e della porosità n (si noti che la diagonale posta al centro del diagramma - H=25 m ed n=1% - corrisponde alla relazione $V_p = \log Q + 3.5$) e consente anche la stima del modulo di deformazione E_d dell'ammasso roccioso.

Rock Tunnelling Quality Index, Q

On the basis of an evaluation of a large number of case histories of underground excavations, Barton et al (1974) of the Norwegian Geotechnical Institute proposed a Tunnelling Quality Index (Q) for the determination of rock mass characteristics and tunnel support requirements. The numerical value of the index Q varies on a logarithmic scale from 0.001 to a maximum of 1,000 and is defined by:

$$Q = \frac{RQD}{J_n} \times \frac{J_r}{J_a} \times \frac{J_w}{SRF} \qquad (2)$$

where RQD is the Rock Quality Designation
J_n is the joint set number
J_r is the joint roughness number
J_a is the joint alteration number
J_w is the joint water reduction factor
SRF is the stress reduction factor

In explaining the meaning of the parameters used to determine the value of Q, Barton et al (1974) offer the following comments:

The first quotient (RQD/J$_n$), representing the structure of the rock mass, is a crude measure of the block or particle size, with the two extreme values (100/0.5 and 10/20) differing by a factor of 400. If the quotient is interpreted in units of centimetres, the extreme 'particle sizes' of 200 to 0.5 cm are seen to be crude but fairly realistic approximations. Probably the largest blocks should be several times this size and the smallest fragments less than half the size. (Clay particles are of course excluded).

The second quotient (J$_r$/J$_a$) represents the roughness and frictional characteristics of the joint walls or filling materials. This quotient is weighted in favour of rough, unaltered joints in direct contact. It is to be expected that such surfaces will be close to peak strength, that they will dilate strongly when sheared, and they will therefore be especially favourable to tunnel stability.

When rock joints have thin clay mineral coatings and fillings, the strength is reduced significantly. Nevertheless, rock wall contact after small shear displacements have occurred may be a very important factor for preserving the excavation from ultimate failure.

Where no rock wall contact exists, the conditions are extremely unfavourable to tunnel stability. The 'friction angles' (given in Table 6) are a little below the residual strength values for most clays, and are possibly down-graded by the fact that these clay bands or fillings may tend to consolidate during shear, at least if normal consolidation or if softening and swelling has occurred. The swelling pressure of montmorillonite may also be a factor here.

The third quotient (J_w/SRF) consists of two stress parameters. SRF is a measure of: 1) loosening load in the case of an excavation through shear zones and clay bearing rock, 2) rock stress in competent rock, and 3) squeezing loads in plastic incompetent rocks. It can be regarded as a total stress parameter. The parameter J_w is a measure of water pressure, which has an adverse effect on the shear strength of joints due to a reduction in effective normal stress. Water may, in addition, cause softening and possible out-wash in the case of clay-filled joints. It has proved impossible to combine these two parameters in terms of inter-block effective stress, because paradoxically a high value of effective normal stress may sometimes signify less stable conditions than a low value, despite the higher shear strength. The quotient (J_w/SRF) is a complicated empirical factor describing the 'active stress'.

It appears that the rock tunnelling quality Q can now be considered to be a function of only three parameters which are crude measures of:

1. Block size   (RQD/Jn)
2. Inter-block shear strength   (Jr/Ja)
3. Active stress   (Jw/SRF)

Undoubtedly, there are several other parameters which could be added to improve the accuracy of the classification system. One of these would be the joint orientation. Although many case records include the necessary information on structural orientation in relation to excavation axis, it was not found to be the important general parameter that might be expected. Part of the reason for this may be that the orientations of many types of excavations can be, and normally are, adjusted to avoid the maximum effect of unfavourably oriented major joints. However, this choice is not available in the case of tunnels, and more than half the case records were in this category. The parameters Jn, Jr and Ja appear to play a more important role than orientation, because the number of joint sets determines the degree of freedom for block movement (if any), and the frictional and dilational characteristics can vary more than the down-dip gravitational component of unfavourably oriented joints. If joint orientations had been included the classification would have been less general, and its essential simplicity lost.

Table 6 (After Barton et al 1974) gives the classification of individual parameters used to obtain the Tunnelling Quality Index Q for a rock mass.

The use of Table 6 is illustrated in the following example. A 15 m span crusher chamber for an underground mine is to be excavated in a norite at a depth of 2,100 m below surface. The rock mass contains two sets of joints controlling stability. These joints are

undulating, rough and unweathered with very minor surface staining. *RQD* values range from 85% to 95% and laboratory tests on core samples of intact rock give an average uniaxial compressive strength of 170 MPa. The principal stress directions are approximately vertical and horizontal and the magnitude of the horizontal principal stress is approximately 1.5 times that of the vertical principal stress. The rock mass is locally damp but there is no evidence of flowing water.

The numerical value of *RQD* is used directly in the calculation of *Q* and, for this rock mass, an average value of 90 will be used. Table 6.2 shows that, for two joint sets, the joint set number, $Jn = 4$. For rough or irregular joints which are undulating, Table 6.3 gives a joint roughness number of $Jr = 3$. Table 6.4 gives the joint alteration number, $Ja = 1.0$, for unaltered joint walls with surface staining only. Table 6.5 shows that, for an excavation with minor inflow, the joint water reduction factor, $Jw = 1.0$. For a depth below surface of 2,100 m the overburden stress will be approximately 57 MPa and, in this case, the major principal stress $\sigma_1 = 85$ MPa. Since the uniaxial compressive strength of the norite is approximately 170 MPa, this gives a ratio of $\sigma_c / \sigma_1 = 2$. Table 6.6 shows that, for competent rock with rock stress problems, this value of σ_c / σ_1 can be expected to produce heavy rock burst conditions and that the value of *SRF* should lie between 10 and 20. A value of $SRF = 15$ will be assumed for this calculation. Using these values gives:

$$Q = \frac{90}{4} \times \frac{3}{1} \times \frac{1}{15} = 4.5$$

In relating the value of the index *Q* to the stability and support requirements of underground excavations, Barton et al (1974) defined an additional parameter which they called the Equivalent Dimension, *De*, of the excavation. This dimension is obtained by dividing the span, diameter or wall height of the excavation by a quantity called the Excavation Support Ratio, *ESR*. Hence:

$$D_e = \frac{\text{Excavation span, diameter or height (m)}}{\text{Excavation Support Ratio } ESR}$$

The value of *ESR* is related to the intended use of the excavation and to the degree of security which is demanded of the support system installed to maintain the stability of the excavation. Barton et al (1974) suggest the following values:

Excavation category		ESR
A	Temporary mine openings.	3-5
B	Permanent mine openings, water tunnels for hydro power (excluding high pressure penstocks), pilot tunnels, drifts and headings for large excavations.	1.6
C	Storage rooms, water treatment plants, minor road and railway tunnels, surge chambers, access tunnels.	1.3
D	Power stations, major road and railway tunnels, civil defence chambers, portal intersections.	1.0
E	Underground nuclear power stations, railway stations, sports and public facilities, factories.	0.8

Table 6: Classification of individual parameters used in the Tunnelling Quality Index *Q*

DESCRIPTION	VALUE	NOTES
1. ROCK QUALITY DESIGNATION	*RQD*	
A. Very poor	0 - 25	1. Where *RQD* is reported or measured as ≤ 10 (including 0),
B. Poor	25 - 50	a nominal value of 10 is used to evaluate *Q*.
C. Fair	50 - 75	
D. Good	75 - 90	2. *RQD* intervals of 5, i.e. 100, 95, 90 etc. are sufficiently
E. Excellent	90 - 100	accurate.
2. JOINT SET NUMBER	J_n	
A. Massive, no or few joints	0.5 - 1.0	
B. One joint set	2	
C. One joint set plus random	3	
D. Two joint sets	4	
E. Two joint sets plus random	6	
F. Three joint sets	9	1. For intersections use ($3.0 \times J_n$)
G. Three joint sets plus random	12	
H. Four or more joint sets, random,	15	2. For portals use ($2.0 \times J_n$)
heavily jointed, 'sugar cube', etc.		
J. Crushed rock, earthlike	20	
3. JOINT ROUGHNESS NUMBER	J_r	
a. Rock wall contact		
b. Rock wall contact before 10 cm shear		
A. Discontinuous joints	4	
B. Rough and irregular, undulating	3	
C. Smooth undulating	2	
D. Slickensided undulating	1.5	1. Add 1.0 if the mean spacing of the relevant joint set is
E. Rough or irregular, planar	1.5	greater than 3 m.
F. Smooth, planar	1.0	
G. Slickensided, planar	0.5	2. $J_r = 0.5$ can be used for planar, slickensided joints having
c. No rock wall contact when sheared		lineations, provided that the lineations are oriented for
H. Zones containing clay minerals thick	1.0	minimum strength.
enough to prevent rock wall contact	(nominal)	
J. Sandy, gravely or crushed zone thick	1.0	
enough to prevent rock wall contact	(nominal)	
4. JOINT ALTERATION NUMBER	J_a	φr degrees (approx.)
a. Rock wall contact		
A. Tightly healed, hard, non-softening,	0.75	1. Values of φr, the residual friction angle,
impermeable filling		are intended as an approximate guide
B. Unaltered joint walls, surface staining only	1.0	25 - 35	to the mineralogical properties of the
C. Slightly altered joint walls, non-softening	2.0	25 - 30	alteration products, if present.
mineral coatings, sandy particles, clay-free		
disintegrated rock, etc.		
D. Silty-, or sandy-clay coatings, small clay-	3.0	20 - 25	
fraction (non-softening)		
E. Softening or low-friction clay mineral coatings,	4.0	8 - 16	
i.e. kaolinite, mica. Also chlorite, talc, gypsum		
and graphite etc., and small quantities of swelling		
clays. (Discontinuous coatings, 1 - 2 mm or less)		

Table 6: (cont'd.) Classification of individual parameters used in the Tunnelling Quality Index Q (After Barton et al 1974).

4. JOINT ALTERATION NUMBER	J_a	ϕ_r degrees (approx.)	
b. Rock wall contact before 10 cm shear			
F. Sandy particles, clay-free, disintegrating rock etc.	4.0	25 - 30	
G. Strongly over-consolidated, non-softening clay mineral fillings (continuous < 5 mm thick)	6.0	16 - 24	
H. Medium or low over-consolidation, softening clay mineral fillings (continuous < 5 mm thick)	8.0	12 - 16	
J. Swelling clay fillings, i.e. montmorillonite, (continuous < 5 mm thick). Values of J_a depend on percent of swelling clay-size particles, and access to water.	8.0 - 12.0	6 - 12	
c. No rock wall contact when sheared			
K. Zones or bands of disintegrated or crushed	6.0		
L. rock and clay (see G, H and J for clay	8.0		
M. conditions)	8.0 - 12.0	6 - 24	
N. Zones or bands of silty- or sandy-clay, small clay fraction, non-softening	5.0		
O. Thick continuous zones or bands of clay	10.0 - 13.0		
P. & R. (see G.H and J for clay conditions)	6.0 - 24.0		
5. JOINT WATER REDUCTION	J_w	approx. water pressure (kgf/cm^2)	
A. Dry excavation or minor inflow i.e. < 5 l/m locally	1.0	< 1.0	
B. Medium inflow or pressure, occasional outwash of joint fillings	0.66	1.0 - 2.5	
C. Large inflow or high pressure in competent rock with unfilled joints	0.5	2.5 - 10.0	1. Factors C to F are crude estimates; increase J_w if drainage installed.
D. Large inflow or high pressure	0.33	2.5 - 10.0	
E. Exceptionally high inflow or pressure at blasting, decaying with time	0.2 - 0.1	> 10	2. Special problems caused by ice formation are not considered.
F. Exceptionally high inflow or pressure	0.1 - 0.05	> 10	
6. STRESS REDUCTION FACTOR		SRF	
a. Weakness zones intersecting excavation, which may cause loosening of rock mass when tunnel is excavated			
A. Multiple occurrences of weakness zones containing clay or chemically disintegrated rock, very loose surrounding rock any depth)	10.0		1. Reduce these values of SRF by 25 - 50% but only if the relevant shear zones influence do not intersect the excavation
B. Single weakness zones containing clay, or chemically disintegrated rock (excavation depth < 50 m)	5.0		
C. Single weakness zones containing clay, or chemically disintegrated rock (excavation depth > 50 m)	2.5		
D. Multiple shear zones in competent rock (clay free), loose surrounding rock (any depth)	7.5		
E. Single shear zone in competent rock (clay free). (depth of excavation < 50 m)	5.0		
F. Single shear zone in competent rock (clay free). (depth of excavation > 50 m)	2.5		
G. Loose open joints, heavily jointed or 'sugar cube', (any depth)	5.0		

Table 6: (cont'd.) Classification of individual parameters in the Tunnelling Quality Index Q (After Barton et al 1974).

DESCRIPTION		VALUE		NOTES
6. STRESS REDUCTION FACTOR			SRF	
b. Competent rock, rock stress problems				
	σ_c/σ_1	σ_t/σ_1		2. For strongly anisotropic virgin stress field
H. Low stress, near surface	> 200	> 13	2.5	(if measured): when $5 \le \sigma_1/\sigma_3 \le 10$, reduce σ_c
J. Medium stress	200 - 10	13 - 0.66	1.0	to $0.8\sigma_c$ and σ_t to $0.8\sigma_t$. When σ_1/σ_3 > 10,
K. High stress, very tight structure (usually favourable to stability, may be unfavourable to wall stability)	10 - 5	0.66 - 0.33	0.5 - 2	reduce σ_c and σ_t to $0.6\sigma_c$ and $0.6\sigma_t$, where σ_c = unconfined compressive strength, and σ_t = tensile strength (point load) and σ_1 and
L. Mild rockburst (massive rock)	5 - 2.5	0.33 - 0.16	5 - 10	σ_3 are the major and minor principal stresses.
M. Heavy rockburst (massive rock)	< 2.5	< 0.16	10 - 20	3. Few case records available where depth of
c. Squeezing rock, plastic flow of incompetent rock under influence of high rock pressure				crown below surface is less than span width. Suggest SRF increase from 2.5 to 5 for such
N. Mild squeezing rock pressure			5 - 10	cases (see H).
O. Heavy squeezing rock pressure			10 - 20	
d. Swelling rock, chemical swelling activity depending on presence of water				
P. Mild swelling rock pressure			5 - 10	
R. Heavy swelling rock pressure			10 - 15	

ADDITIONAL NOTES ON THE USE OF THESE TABLES

When making estimates of the rock mass Quality (Q), the following guidelines should be followed in addition to the notes listed in the tables:

1. When borehole core is unavailable, RQD can be estimated from the number of joints per unit volume, in which the number of joints per metre for each joint set are added. A simple relationship can be used to convert this number to RQD for the case of clay free rock masses: $RQD = 115 - 3.3 J_v$ (approx.), where J_v = total number of joints per m^3 ($0 < RQD < 100$ for $35 > J_v > 4.5$).

2. The parameter J_n representing the number of joint sets will often be affected by foliation, schistosity, slaty cleavage or bedding etc. If strongly developed, these parallel 'joints' should obviously be counted as a complete joint set. However, if there are few 'joints' visible, or if only occasional breaks in the core are due to these features, then it will be more appropriate to count them as 'random' joints when evaluating J_n.

3. The parameters J_r and J_a (representing shear strength) should be relevant to the weakest significant joint set or clay filled discontinuity in the given zone. However, if the joint set or discontinuity with the minimum value of J_r/J_a is favourably oriented for stability, then a second, less favourably oriented joint set or discontinuity may sometimes be more significant, and its higher value of J_r/J_a should be used when evaluating Q. The value of J_r/J_a should in fact relate to the surface most likely to allow failure to initiate.

4. When a rock mass contains clay, the factor SRF appropriate to loosening loads should be evaluated. In such cases the strength of the intact rock is of little interest. However, when jointing is minimal and clay is completely absent, the strength of the intact rock may become the weakest link, and the stability will then depend on the ratio rock-stress/rock-strength. A strongly anisotropic stress field is unfavourable for stability and is roughly accounted for as in note 2 in the table for stress reduction factor evaluation.

5. The compressive and tensile strengths (σ_c and σ_t) of the intact rock should be evaluated in the saturated condition if this is appropriate to the present and future in situ conditions. A very conservative estimate of the strength should be made for those rocks that deteriorate when exposed to moist or saturated conditions.

The crusher station discussed earlier falls into the category of permanent mine openings and is assigned an excavation support ratio ESR = 1.6. Hence, for an excavation span of 15 m, the equivalent dimension, De = 15/1.6 = 9.4.

The equivalent dimension, De, plotted against the value of Q, is used to define a number of support categories in a chart published in the original paper by Barton et al (1974). This chart has recently been updated by Grimstad and Barton (1993) to reflect the increasing use of steel fibre reinforced shotcrete in underground excavation support. Figure 3 is reproduced from this updated chart.

From Figure 3, a value of De of 9.4 and a value of Q of 4.5 places this crusher excavation in category (4) which requires a pattern of rockbolts (spaced at 2.3 m) and 40 to 50 mm of unreinforced shotcrete.

Because of the mild to heavy rock burst conditions which are anticipated, it may be prudent to destress the rock in the walls of this crusher chamber. This is achieved by using relatively heavy production blasting to excavate the chamber and omitting the smooth blasting usually used to trim the final walls of an excavation such as an underground powerhouse at shallower depth. Caution is recommended in the use of destress blasting and, for critical applications, it may be advisable to seek the advice of a blasting specialist before embarking on this course of action.

Løset (1992) suggests that, for rocks with $4 < Q < 30$, blasting damage will result in the creation of new 'joints' with a consequent local reduction in the value of Q for the rock surrounding the excavation. He suggests that this can be accounted for by reducing the RQD value for the blast damaged zone.

Assuming that the RQD value for the destressed rock around the crusher chamber drops to 50 %, the resulting value of Q = 2.9. From Figure 3, this value of Q, for an equivalent dimension, De of 9.4, places the excavation just inside category (5) which requires rockbolts, at approximately 2 m spacing, and a 50 mm thick layer of steel fibre reinforced shotcrete.

Barton et al (1980) provide additional information on rockbolt length, maximum unsupported spans and roof support pressures to supplement the support recommendations published in the original 1974 paper.

The length L of rockbolts can be estimated from the excavation width B and the Excavation Support Ratio ESR:

$$L = 2 + \frac{0.15B}{ESR}$$

(3)

The maximum unsupported span can be estimated from:

$$\text{Maximum span (unsupported)} = 2\,ESR\,Q^{0.4}$$

(4)

Based upon analyses of case records, Grimstad and Barton (1993) suggest that the relationship between the value of Q and the permanent roof support pressure P_{roof} is estimated from:

$$P_{roof} = \frac{2\sqrt{Jn}\,Q^{-\frac{1}{3}}}{3Jr}$$

(5)

RMR $\approx$ 9 lnQ+44   (Bieniawski, 1989) $Q \approx e^{\frac{(RMR-44)}{9}}$ [1]

RMR $\approx$ 15 logQ+50   (Barton, 1995) $Q \approx 10^{\frac{(RMR-50)}{15}}$ [2]

[1] RMR $\approx$ −18.2   2.6   23.3   44   56.5 64.7   77.2 85.4   97.9 106.2

[2] RMR $\approx$ 5   **V**   20   **IV** 35   50 **III** 59   65 **II** 74   80   89 **I** 95

Rock mass quality $Q = \dfrac{RQD}{J_n} \times \dfrac{J_r}{J_a} \times \dfrac{J_w}{SRF}$

Qc		Vp		M
Rock mass quality		Seismic velocity		Deformation modulus

$V_p \approx \log Q_c + 3.5$ (km/sec.) $E_{mass} \approx 10 \cdot Q_c^{1/3}$ (GPa) $E_{mass} \approx 10 \cdot 10^{\left(\frac{V_p - 3.5}{3}\right)}$ (GPa)
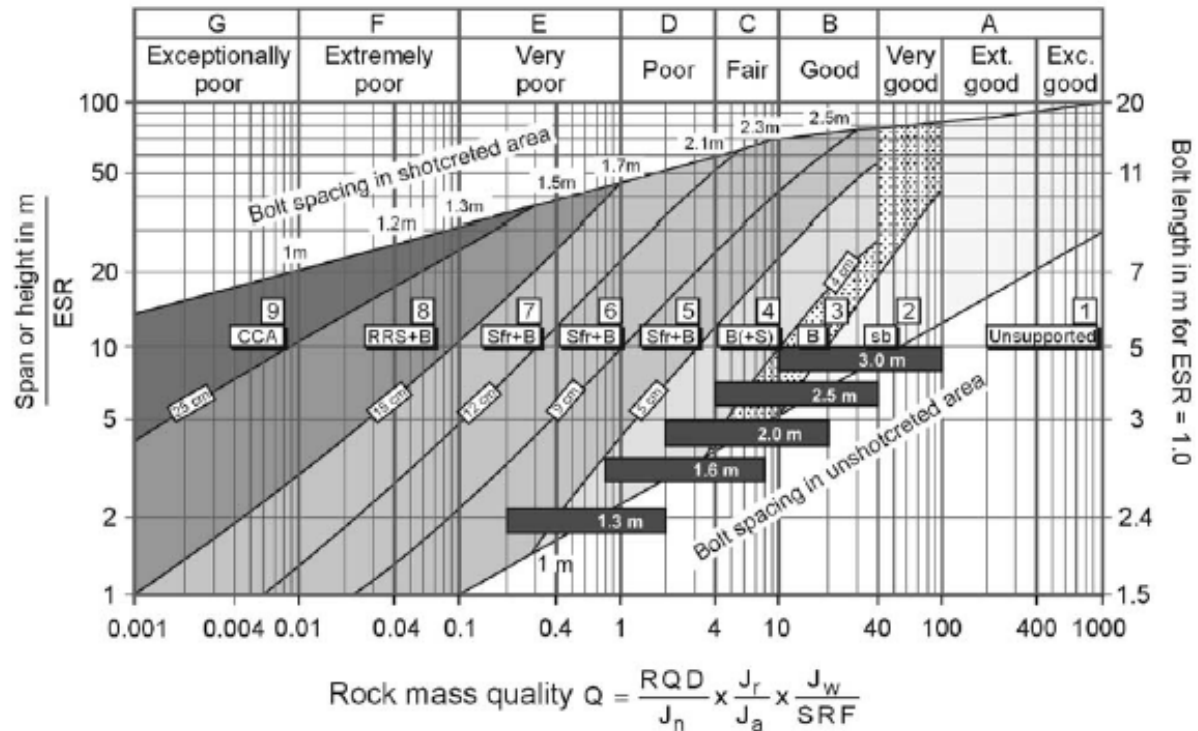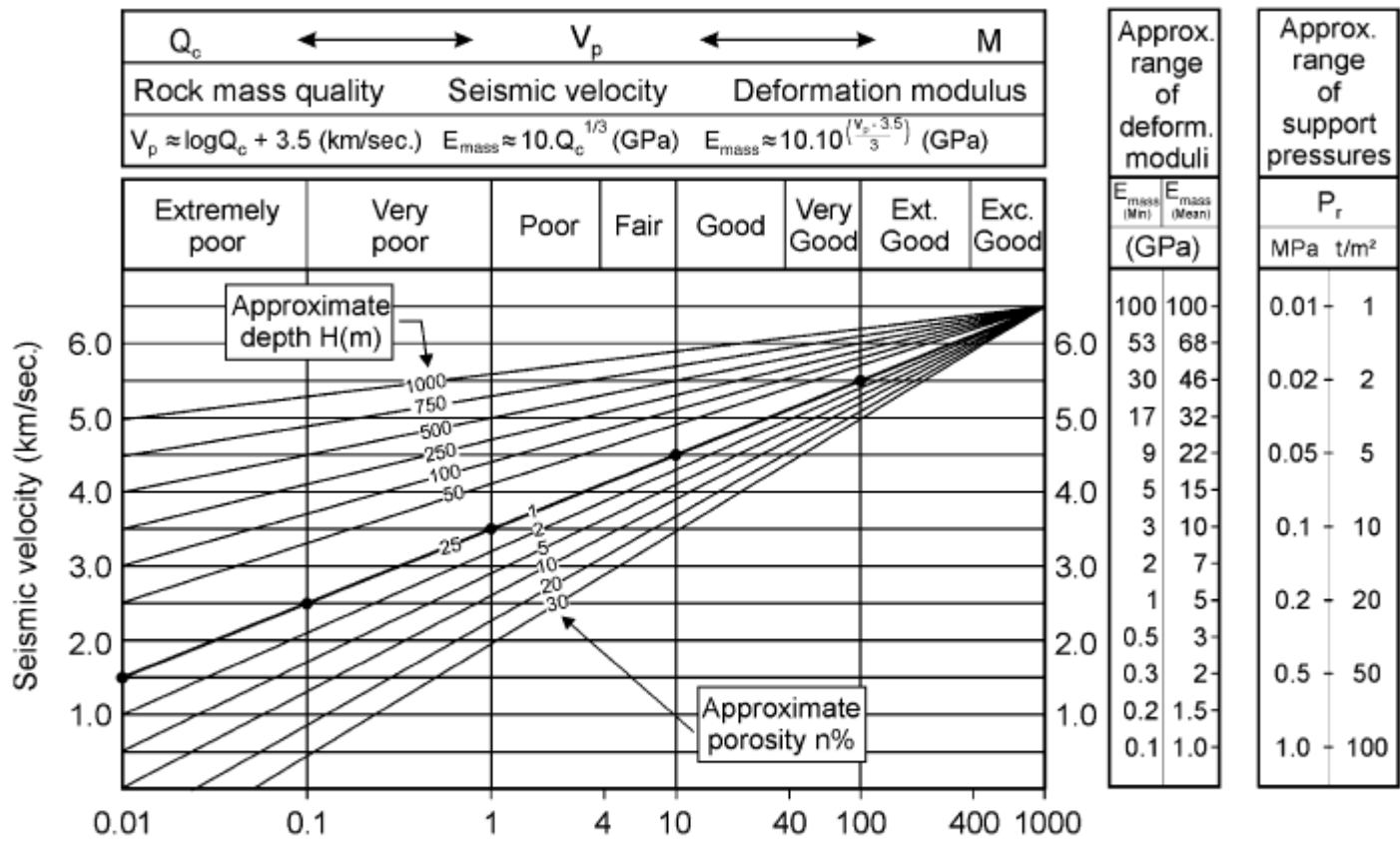
$$Q_c = \left[\frac{RQD}{J_n} \times \frac{J_r}{J_a} \times \frac{J_w}{SRF} \right] \frac{\sigma_c}{100}$$
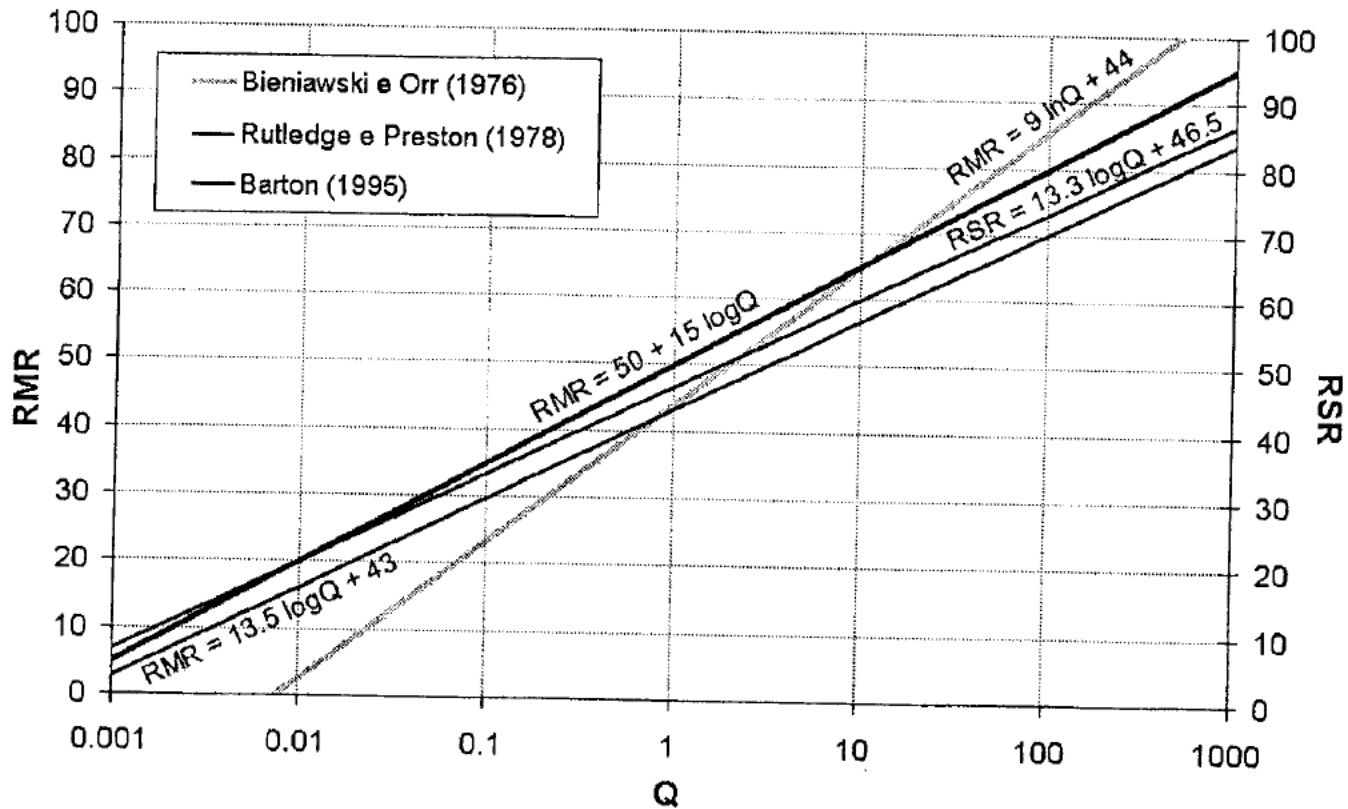
Figura 10 - Relazioni tra gli indici di classificazione Q, RMR e RSR.

Prediction of in-situ deformation modulus E_m
from rock mass classifications

Tunnel Quality Index Q

In situ modulus of deformation Em - GPa

Case histories:

● Serafim and Pereira (1983)

■ Bieniawski (1978)

$Em = 10^{(RMR - 10)/40}$

$Em = 2\,RMR - 100$

$Em = 25\,Log_{10}\,Q$

Geomechanics Rock Mass Rating RMR

64
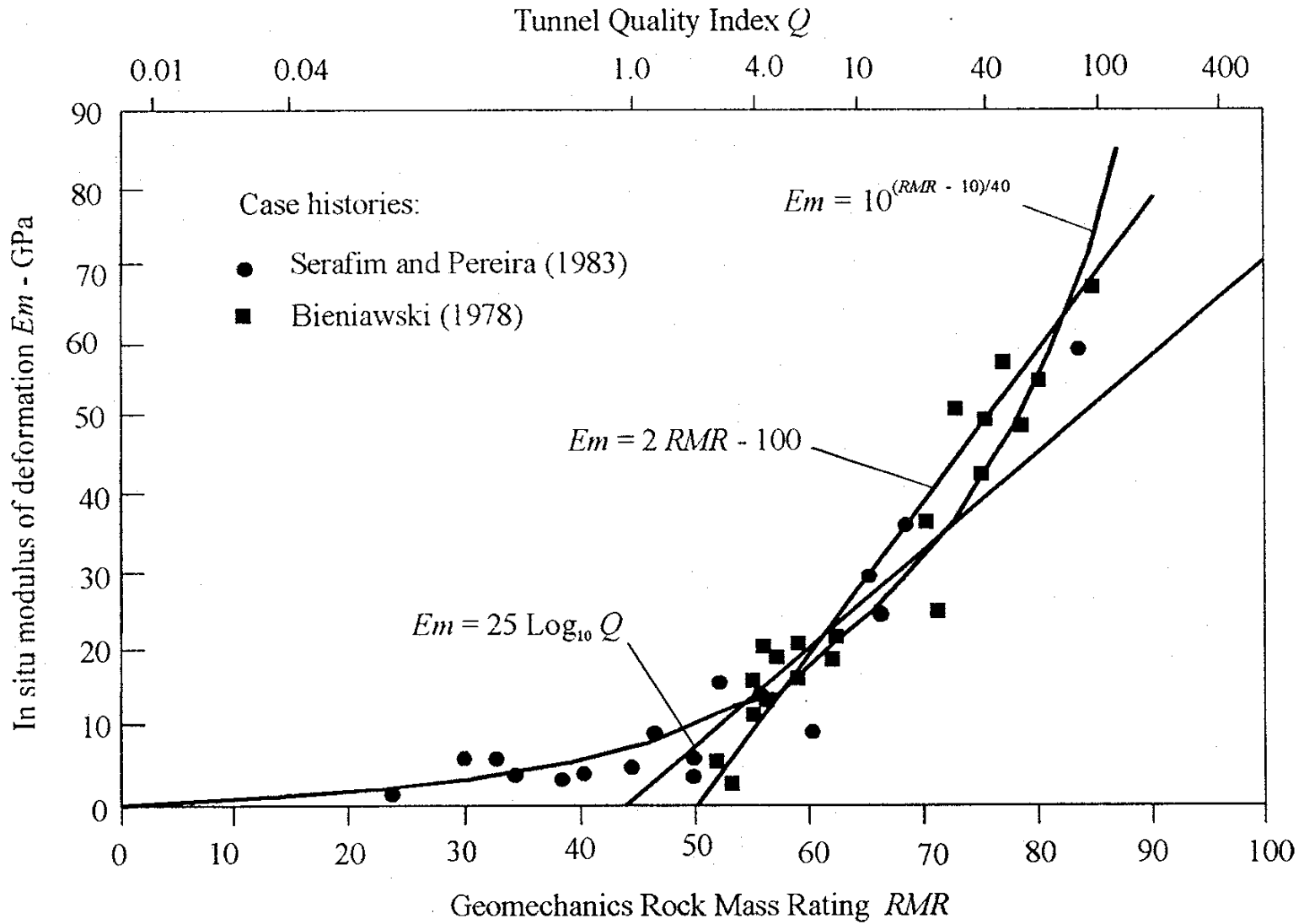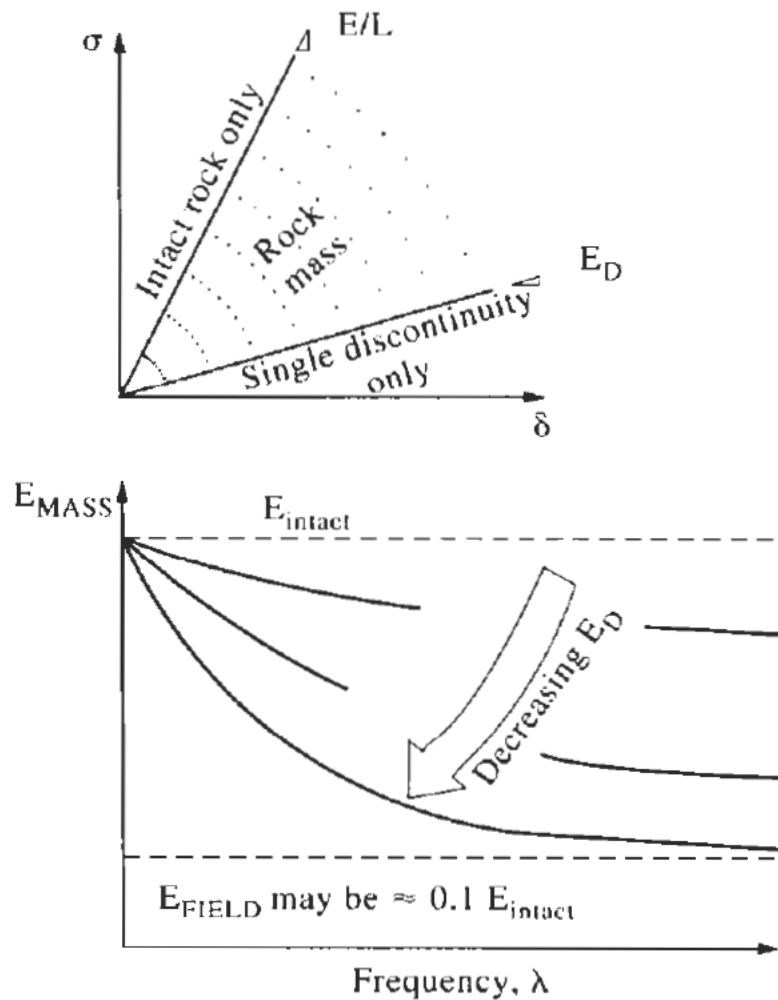
Figure 8.2 Variation of *in situ* rock deformability as a function of the discontinuities (idealized case for a single set of discontinuities).

Geological strength Index

The strength of a jointed rock mass depends on the properties of the intact rock pieces and also upon the freedom of these pieces to slide and rotate under different stress conditions. This freedom is controlled by the geometrical shape of the intact rock pieces as well as the condition of the surfaces separating the pieces. Angular rock pieces with clean, rough discontinuity surfaces will result in a much stronger rock mass than one which contains rounded particles surrounded by weathered and altered material.

The Geological Strength Index (GSI), introduced by Hoek (1994) and Hoek, Kaiser and Bawden (1995) provides a number which, when combined with the intact rock properties, can be used for estimating the reduction in rock mass strength for different geological conditions. This system is presented in Table 5, for blocky rock masses, and Table 6 for heterogeneous rock masses such as flysch. Table 6 has also been extended to deal with molassic rocks (Hoek et al 2006) and ophiolites (Marinos et al, 2005).

Before the introduction of the GSI system in 1994, the application of the Hoek-Brown criterion in the field was based on a correlation with the 1976 version of Bieniawski's Rock Mass Rating, with the Groundwater rating set to 10 (dry) and the Adjustment for Joint Orientation set to 0 (very favourable) (Bieniawski, 1976). If the 1989 version of Bieniawski's RMR classification (Bieniawski, 1989) is used, then the Groundwater rating set to 15 and the Adjustment for Joint Orientation set to zero.

During the early years of the application of the GSI system the value of GSI was estimated directly from RMR. However, this correlation has proved to be unreliable, particularly for poor quality rock masses and for rocks with lithological peculiarities that cannot be accommodated in the RMR classification. Consequently, it is recommended that GSI should be estimated directly by means of the charts presented in Tables 5 and 6 and not from the RMR classification.

Experience shows that most geologists and engineering geologists are comfortable with the descriptive and largely qualitative nature of the GSI tables and generally have little difficulty in arriving at an estimated value. On the other hand, many engineers feel the need for a more quantitative system in which they can "measure" some physical dimension. Conversely, these engineers have little difficulty understanding the importance of the intact rock strength σ_{ci} and its incorporation in the assessment of the rock mass properties. Many geologists tend to confuse intact and rock mass strength and consistently underestimate the intact strength.

An additional practical question is whether borehole cores can be used to estimate the GSI value behind the visible faces? Borehole cores are the best source of data at depth but it has to be recognized that it is necessary to extrapolate the one dimensional information provided by core to the three-dimensional rock mass. However, this is a common problem in borehole investigation and most experienced engineering geologists are comfortable with this extrapolation process. Multiple boreholes and inclined boreholes are of great help the interpretation of rock mass characteristics at depth.

The most important decision to be made in using the GSI system is whether or not it should be used. If the discontinuity spacing is large compared with the dimensions of the tunnel or slope under consideration then, as shown in Figure 5, the GSI tables and the Hoek-Brown criterion should not be used and the discontinuities should be treated individually. Where the discontinuity spacing is small compared with the size of the structure (Figure 5) then the GSI tables can be used with confidence.

Table 5: Characterisation of blocky rock masses on the basis of interlocking and joint conditions.
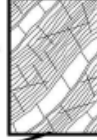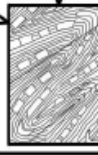

GEOLOGICAL STRENGTH INDEX FOR JOINTED ROCKS (Hoek and Marinos, 2000)

From the lithology, structure and surface conditions of the discontinuities, estimate the average value of GSI. Do not try to be too precise. Quoting a range from 33 to 37 is more realistic than stating that GSI = 35. Note that the table does not apply to structurally controlled failures. Where weak planar structural planes are present in an unfavourable orientation with respect to the excavation face, these will dominate the rock mass behaviour. The shear strength of surfaces in rocks that are prone to deterioration as a result of changes in moisture content will be reduced is water is present. When working with rocks in the fair to very poor categories, a shift to the right may be made for wet conditions. Water pressure is dealt with by effective stress analysis.

SURFACE CONDITIONS

DECREASING SURFACE QUALITY →

STRUCTURE	VERY GOOD — Very rough, fresh unweathered surfaces	GOOD — Rough, slightly weathered, iron stained surfaces	FAIR — Smooth, moderately weathered and altered surfaces	POOR — Slickensided, highly weathered surfaces with compact coatings or fillings or angular fragments	VERY POOR — Slickensided, highly weathered surfaces with soft clay coatings or fillings
INTACT OR MASSIVE - intact rock specimens or massive in situ rock with few widely spaced discontinuities	90 / 80			N/A	N/A
BLOCKY - well interlocked un-disturbed rock mass consisting of cubical blocks formed by three intersecting discontinuity sets		70 / 60			
VERY BLOCKY- interlocked, partially disturbed mass with multi-faceted angular blocks formed by 4 or more joint sets			50		
BLOCKY/DISTURBED/SEAMY - folded with angular blocks formed by many intersecting discontinuity sets. Persistence of bedding planes or schistosity			40	30	
DISINTEGRATED - poorly inter-locked, heavily broken rock mass with mixture of angular and rounded rock pieces				20	
LAMINATED/SHEARED - Lack of blockiness due to close spacing of weak schistosity or shear planes	N/A	N/A			10

DECREASING INTERLOCKING OF ROCK PIECES

GSI FOR HETEROGENEOUS ROCK MASSES SUCH AS FLYSCH
(Marinos.P and Hoek. E, 2000)

From a description of the lithology, structure and surface conditions (particularly of the bedding planes), choose a box in the chart. Locate the position in the box that corresponds to the condition of the discontinuities and estimate the average value of GSI from the contours. Do not attempt to be too precise. Quoting a range from 33 to 37 is more realistic than giving GSI = 35. Note that the Hoek-Brown criterion does not apply to structurally controlled failures. Where unfavourably oriented continuous weak planar discontinuities are present, these will dominate the behaviour of the rock mass. The strength of some rock masses is reduced by the presence of groundwater and this can be allowed for by a slight shift to the right in the columns for fair, poor and very poor conditions. Water pressure does not change the value of GSI and it is dealt with by using effective stress analysis.

COMPOSITION AND STRUCTURE

SURFACE CONDITIONS OF DISCONTINUITIES (Predominantly bedding planes)

	VERY GOOD - Very rough, fresh unweathered surfaces	GOOD - Rough, slightly weathered surfaces	FAIR - Smooth, moderately weathered and altered surfaces	POOR - Very smooth, occasionally slickensided surfaces with compact coatings or fillings with angular fragments	VERY POOR - Very smooth slickensided or highly weathered surfaces with soft clay coatings or fillings

A. Thick bedded, very blocky sandstone
The effect of pelitic coatings on the bedding planes is minimized by the confinement of the rock mass. In shallow tunnels or slopes these bedding planes may cause structurally controlled instability.

70
60
A

B. Sandstone with thin interlayers of siltstone

C. Sandstone and siltstone in similar amounts

D. Siltstone or silty shale with sandstone layers

E. Weak siltstone or clayey shale with sandstone layers

50
40
B C D E

C,D, E and G - may be more or less folded than Illustrated but this does not change the strength. Tectonic deformation, faulting and loss of continuity moves these categories to F and H.

F. Tectonically deformed, intensively folded/faulted, sheared clayey shale or siltstone with broken and deformed sandstone layers forming an almost chaotic structure

30
20
F

G. Undisturbed silty or clayey shale with or without a few very thin sandstone layers

H. Tectonically deformed silty or clayey shale forming a chaotic structure with pockets of clay. Thin layers of sandstone are transformed into small rock pieces.

G H 10

→ : Means deformation after tectonic disturbance

Table 7: Most common GSI range of typical limestone.*

Table 11: Common GSI range for typical schist.*

1. Massive
2. Thin bedded
3. Brecciated

1. Strong (e.g. micaschists, calcitic schists)
2. Weak (e.g. chloritic schists, phyllites)
3. Sheared schist

5. DETERMINAZIONE DEI PARAMETRI DI RESISTENZA E DEFORMABILITÀ

I parametri che caratterizzano la resistenza e la deformabilità dell'ammasso roccioso sono scelti in funzione del modello geotecnico che meglio rappresenta le condizioni reali del caso in esame, che a sua volta pilota la scelta del metodo di analisi da adottare in sede di progetto. Per gli ammassi rocciosi, si fa generalmente riferimento alla distinzione classica tra modelli continui, continui equivalenti e discontinui, basata essenzialmente sulla struttura dell'ammasso roccioso e sulle caratteristiche dei litotipi che lo costituiscono.

Il modello continuo viene ad esempio applicato ad ammassi costituiti da rocce tenere; in questo caso si fa usualmente riferimento ad un modello di comportamento valido per la roccia intatta. Quando il litotipo costituente l'ammasso ha caratteristiche di resistenza più elevate, si ricorre invece ai modelli continuo equivalente o discontinuo. In particolare, si modellano come mezzi continui equivalenti gli ammassi rocciosi nei quali la risposta deformativa dipende principalmente dalle caratteristiche globali del sistema roccia intatta-discontinuità: è il caso di ammassi nei quali la spaziatura caratteristica dei sistemi di discontinuità è sufficientemente bassa da poter considerare molto piccolo il volume rappresentativo della roccia in confronto alla dimensione del cavo. In questo caso, il modello di comportamento da adottare dovrà tenere implicitamente conto del grado di fratturazione del mezzo.
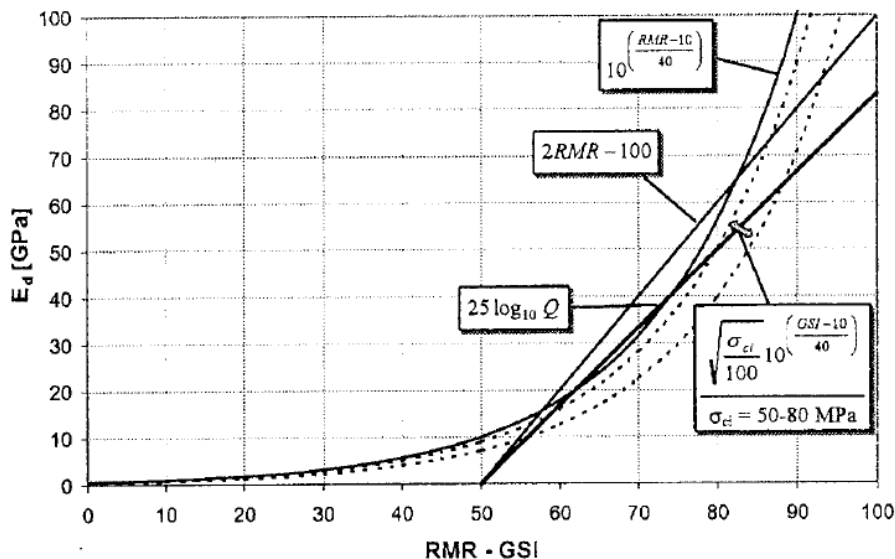
5.1 Modelli continui e continui-equivalenti

Generalmente, ad un ammasso roccioso considerato come mezzo continuo equivalente o continuo e interessato dallo scavo di una galleria, viene assegnato uno dei modelli di comportamento descritti nel seguito.

5.1.1 Elastico lineare, isotropo

Un mezzo a comportamento elastico lineare manifesta degli incrementi di deformazione reversibile al variare dello stato tensionale agente; la relazione che lega sforzi $[\sigma]$ e deformazioni $[\varepsilon]$ è di tipo lineare:

$$[\sigma] = [C] \, [\varepsilon] \qquad (10)$$

dove $[C]$ è la matrice delle costanti elastiche.

Per modellare un comportamento di questo tipo occorre quindi definire il modulo di elasticità E ed il coefficiente di Poisson ν. I valori di questi parametri sono ottenuti, nel caso di mezzo continuo, dalle prove a compressione monoassiale di laboratorio e, nel caso di mezzo continuo-equivalente, dalle opportune prove in sito (dilatometriche, di carico su piastra e con martinetti piatti) o mediante le formule empiriche che correlano il modulo di deformabilità dell'ammasso con gli indici di classificazione. A questo riguardo, esistono leggi empiriche basate sul valore di RMR, di GSI e di Q (Figura 13).

5.1.2 Elastico lineare, anisotropo

L'anisotropia si manifesta negli ammassi rocciosi principalmente in termini di isotropia trasversale; in questo caso le costanti elastiche indipendenti sono cinque. Detto s il piano di isotropia ed n la direzione ad esso perpendicolare (asse di simmetria di rotazione), occorre determinare: i moduli di elasticità e di Poisson associati ad s; il modulo di elasticità associato ad n; il coefficiente di Poisson che esprime l'influenza delle deformazioni relative al piano s su quelle relative ad n; il modulo di taglio G indipendente che associa le deformazioni angolari alle tensioni tangenziali agenti in un piano qualsiasi passante per n. È chiaro che i cinque parametri devono essere valutati sulla base di prove in sito, ove tali prove vengano eseguite nelle direzioni parallela e perpendicolare al piano di isotropia, dovendo comunque introdurre un'ipotesi semplificativa per valutare G. Le relazioni empiriche basate sugli indici di classificazione, che sono valide essenzialmente per mezzi isotropi, forniscono valori dei parametri di deformabilità da usare con prudenza, ove il mezzo in esame sia fortemente anisotropo.

5.1.3 Elastico-plastico

La risposta di un mezzo a comportamento elasto-plastico ad una variazione tensionale consiste nella somma di un incremento di deformazione elastica reversibile $(d\varepsilon_{ij})^{el}$ ed un incremento di deformazione plastica irreversibile $(d\varepsilon_{ij})^{pl}$:

$$d\varepsilon_{ij} = (d\varepsilon_{ij})^{el} + (d\varepsilon_{ij})^{pl} \tag{16}$$

La descrizione del comportamento elasto-plastico richiede la definizione di:
- Legge costitutiva in campo elastico, per la quale sono necessari i parametri già discussi per i mezzi elastici.
- Legge di plasticizzazione, che definisce una soglia tensionale oltre la quale il mezzo si deforma irreversibilmente. Nel caso più generale tale legge si esprime con l'equazione di una superficie nel riferimento spaziale delle tensioni, funzione dello stato tensionale σ_{ij} e della deformazione plastica ε_{ij}^{pl}:

$$f(\sigma_{ij}, \varepsilon_{ij}^{pl}) = 0 \tag{17}$$

Uno stato tensionale per cui f<0 genera una risposta elastica del mezzo, mentre la condizione f=0 implica la sua plasticizzazione. Dopo la plasticizzazione iniziale, lo stato tensionale per il quale si generano le successive deformazioni plastiche dipende dal livello di deformazione plastica raggiunto. Nel caso più generale, cioè, la superficie di plasticizzazione può variare in forma e dimensione al progredire della deformazione plastica.
- Legge di flusso plastico che presuppone l'esistenza di una funzione di potenziale plastico $g(\sigma_{ij}, \varepsilon_{ij}^{pl})$, alla quale il vettore dell'incremento di deformazione plastica è ortogonale. La legge di flusso può essere espressa come:

$$(d\varepsilon_{ij})^{pl} = \lambda \frac{\partial g}{\partial \sigma_{ij}} \tag{18}$$

essendo λ una costante di proporzionalità, detta moltiplicatore plastico.
Se la funzione di potenziale plastico coincide con quella di plasticizzazione, cioè se g = f, la (18) è detta di tipo associato; diversamente si ha una legge di tipo non associato.
I modelli di uso più frequente, schematizzati in Figura 14 (Hoek e Brown, 1997), sono:
- idealmente plastico, per ammassi rocciosi con condizioni di qualità da scadente a molto scadente (Figura 14a);
- rammollente, per ammassi rocciosi con condizioni di qualità medie (Figura 14b);
- idealmente fragile, per ammassi rocciosi con caratteristiche di qualità molto buone (Figura 14c).
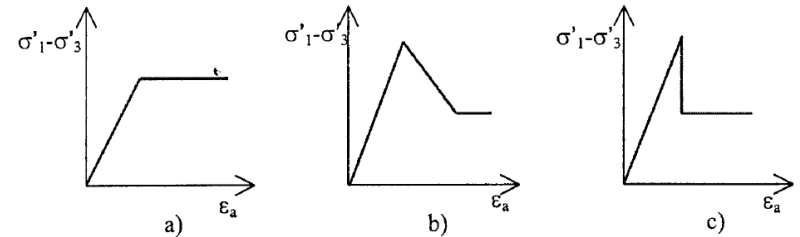

Figura 14 - Comportamenti elasto-plastici: a) idealmente plastico, b) rammollente, c) idealmente fragile

Per definire la soglia tensionale oltre la quale il mezzo si deforma irreversibilmente, si fa generalmente riferimento ai criteri di resistenza ricordati in quanto segue.

Rock mass properties

Introduction

Reliable estimates of the strength and deformation characteristics of rock masses are required for almost any form of analysis used for the design of slopes, foundations and underground excavations. Hoek and Brown (1980a, 1980b) proposed a method for obtaining estimates of the strength of jointed rock masses, based upon an assessment of the interlocking of rock blocks and the condition of the surfaces between these blocks. This method was modified over the years in order to meet the needs of users who were applying it to problems that were not considered when the original criterion was developed (Hoek 1983, Hoek and Brown 1988). The application of the method to very poor quality rock masses required further changes (Hoek, Wood and Shah 1992) and, eventually, the development of a new classification called the Geological Strength Index (Hoek, Kaiser and Bawden 1995, Hoek 1994, Hoek and Brown 1997, Hoek, Marinos and Benissi, 1998, Marinos and Hoek, 2001). A major revision was carried out in 2002 in order to smooth out the curves, necessary for the application of the criterion in numerical models, and to update the methods for estimating Mohr Coulomb parameters (Hoek, Carranza-Torres and Corkum, 2002). A related modification for estimating the deformation modulus of rock masses was made by Hoek and Diederichs (2006).

This chapter presents the most recent version of the Hoek-Brown criterion in a form that has been found practical in the field and that appears to provide the most reliable set of results for use as input for methods of analysis in current use in rock engineering.

Generalised Hoek-Brown criterion

The Generalised Hoek-Brown failure criterion for jointed rock masses is defined by:

$$\sigma_1' = \sigma_3' + \sigma_{ci}\left(m_b \frac{\sigma_3'}{\sigma_{ci}} + s\right)^a \tag{1}$$

where σ_1' and σ_3' are the maximum and minimum effective principal stresses at failure,
  m_b is the value of the Hoek-Brown constant m for the rock mass,
  s and a are constants which depend upon the rock mass characteristics, and
  σ_{ci} is the uniaxial compressive strength of the intact rock pieces.

Normal and shear stresses are related to principal stresses by the equations published by Balmer[1] (1952).

$$\sigma_n' = \frac{\sigma_1' + \sigma_3'}{2} - \frac{\sigma_1' - \sigma_3'}{2} \cdot \frac{d\sigma_1'/d\sigma_3' - 1}{d\sigma_1'/d\sigma_3' + 1} \tag{2}$$

$$\tau = (\sigma_1' - \sigma_3')\frac{\sqrt{d\sigma_1'/d\sigma_3'}}{d\sigma_1'/d\sigma_3' + 1} \tag{3}$$

where

$$d\sigma_1'/d\sigma_3' = 1 + am_b\left(m_b\sigma_3'/\sigma_{ci} + s\right)^{a-1} \tag{4}$$

In order to use the Hoek-Brown criterion for estimating the strength and deformability of jointed rock masses, three 'properties' of the rock mass have to be estimated. These are:

- uniaxial compressive strength σ_{ci} of the intact rock pieces,
- value of the Hoek-Brown constant m_i for these intact rock pieces, and
- value of the Geological Strength Index GSI for the rock mass.

Intact rock properties

For the intact rock pieces that make up the rock mass, equation (1) simplifies to:

$$\sigma_1' = \sigma_3' + \sigma_{ci}\left(m_i \frac{\sigma_3'}{\sigma_{ci}} + 1\right)^{0.5} \tag{5}$$

The relationship between the principal stresses at failure for a given rock is defined by two constants, the uniaxial compressive strength σ_{ci} and a constant m_i. Wherever possible the values of these constants should be determined by statistical analysis of the results of a set of triaxial tests on carefully prepared core samples.

Note that the range of minor principal stress (σ_3') values over which these tests are carried out is critical in determining reliable values for the two constants. In deriving the original values of σ_{ci} and m_i, Hoek and Brown (1980a) used a range of $0 < \sigma_3' < 0.5\sigma_{ci}$ and, in order to be consistent, it is essential that the same range be used in any laboratory triaxial tests on intact rock specimens. At least five well spaced data points should be included in the analysis.

One type of triaxial cell that can be used for these tests is illustrated in Figure 1. This cell, described by Franklin and Hoek (1970), does not require draining between tests and is convenient for the rapid testing on a large number of specimens. More sophisticated cells are available for research purposes but the results obtained from the cell illustrated in Figure 1 are adequate for the rock strength estimates required for estimating σ_{ci} and m_i. This cell has the additional advantage that it can be used in the field when testing materials such as coals or mudstones that are extremely difficult to preserve during transportation and normal specimen preparation for laboratory testing.

Laboratory tests should be carried out at moisture contents as close as possible to those which occur in the field. Many rocks show a significant strength decrease with increasing moisture content and tests on samples, which have been left to dry in a core shed for several months, can give a misleading impression of the intact rock strength.

Once the five or more triaxial test results have been obtained, they can be analysed to determine the uniaxial compressive strength σ_{ci} and the Hoek-Brown constant m_i as described by Hoek and Brown (1980a). In this analysis, equation (5) is re-written in the form:

$$y = m\sigma_{ci}x + s\sigma_{ci} \tag{6}$$

where $x = \sigma_3'$ and $y = (\sigma_1' - \sigma_3')^2$

For n specimens the uniaxial compressive strength σ_{ci}, the constant and m_i the coefficient of determination r^2 are calculated from:

$$\sigma_{ci}^2 = \frac{\sum y}{n} - \left[\frac{\sum xy - (\sum x \sum y/n)}{\sum x^2 - ((\sum x)^2/n)}\right]\frac{\sum x}{n} \tag{7}$$

$$m_i = \frac{1}{\sigma_{ci}}\left[\frac{\sum xy - (\sum x \sum y/n)}{\sum x^2 - ((\sum x)^2/n)}\right] \tag{8}$$

$$r^2 = \frac{[\sum xy - (\sum x \sum y/n)]^2}{[\sum x^2 - (\sum x)^2/n][\sum y^2 - (\sum y)^2/n]} \tag{9}$$

A spreadsheet for the analysis of triaxial test data is given in Table 1. Note that high quality triaxial test data will usually give a coefficient of determination r^2 of greater than 0.9. These calculations, together with many more related to the Hoek-Brown criterion can also be performed by the program RocLab that can be downloaded (free) from www.rocscience.com.

When laboratory tests are not possible, Table 2 and Table 3 can be used to obtain estimates of σ_{ci} and m_i.

Figure 1:   Cut-away view of a triaxial cell for testing rock specimens.

Labels in figure:
- Hardened and ground steel spherical seats
- Clearance gap for strain gauge wires
- Mild steel cell body
- Rock specimen with ground ends and a length to diameter ratio of 2
- Oil inlet - maximum pressure 700 MPa
- Strain gauges - if required
- Rubber sealing sleeve

Table 1: Spreadsheet for the calculation of σ_{ci} and m_i from triaxial test data

Triaxial test data

x		y	xy	xsq	ysq
sig3	sig1				
0	38.3	1466.89	0.0	0.0	2151766
5	72.4	4542.76	22713.8	25.0	20636668
7.5	80.5	5329.00	39967.5	56.3	28398241
15	115.6	10120.36	151805.4	225.0	102421687
20	134.3	13064.49	261289.8	400.0	170680899
47.5	441.1	34523.50	475776.5	706.3	324289261
sumx		sumy	sumxy	sumxsq	sumysq

Calculation results

Number of tests   n =   5
Uniaxial strength   sigci =   37.4
Hoek-Brown constant   mi =   15.50
Hoek-Brown constant   s =   1.00
Coefficient of determination   r2 =   0.997

Cell formulae

y = (sig1-sig3)^2
sigci = SQRT(sumy/n - (sumxy-sumx*sumy/n)/(sumxsq-(sumx^2)/n)*sumx/n)
mi = (1/sigci)*((sumxy-sumx*sumy/n)/(sumxsq-(sumx^2)/n))
r2 = ((sumxy-(sumx*sumy/n))^2)/((sumxsq-(sumx^2)/n)*(sumysq-(sumy^2)/n))

Note: These calculations, together with many other calculations related to the Hoek-Brown criterion, can also be carried out using the program RocLab that can be downloaded (free) from www.rocscience.com.

Figure 3. Summary of equations with the non-linear failure criterion proposed by Hoek & Brown (1980b)

Triaxial compression
$$\sigma_1' = \sigma_3' + (m\,\sigma_c\,\sigma_3' + s\,\sigma_c^2)^{1/2}$$

Uniaxial compression
$$\sigma_{cm} = (s\sigma_c^2)^{1/2}$$

Uniaxial tension
$$\sigma_{tm} = \tfrac{1}{2}\sigma_c\,(m - (m^2 + 4s)^{1/2})$$

Major principal stress σ_1'

Minor principal stress σ_1'

Mohr envelope
$$\tau = (\text{Cot }\phi_i' - \text{Cos }\phi_i')\frac{m\sigma_c}{8}$$

Shear stress τ

Effective normal stress σ'

$$\phi_i' = \text{Arctan }(4h\,\text{Cos}^2\,(30 + \tfrac{1}{3}\,\text{Arcsin }h^{-3/2}) - 1)^{-1/2}$$
$$\text{where } h = 1 + \frac{16\,(m\sigma' + s\sigma_c)}{3m^2\,\sigma_c}$$

$$c_i' = \tau - \sigma'\,\text{Tan }\phi_i'$$

Instantaneous friction angle ϕ_i'

Instantaneous cohesion c_i'

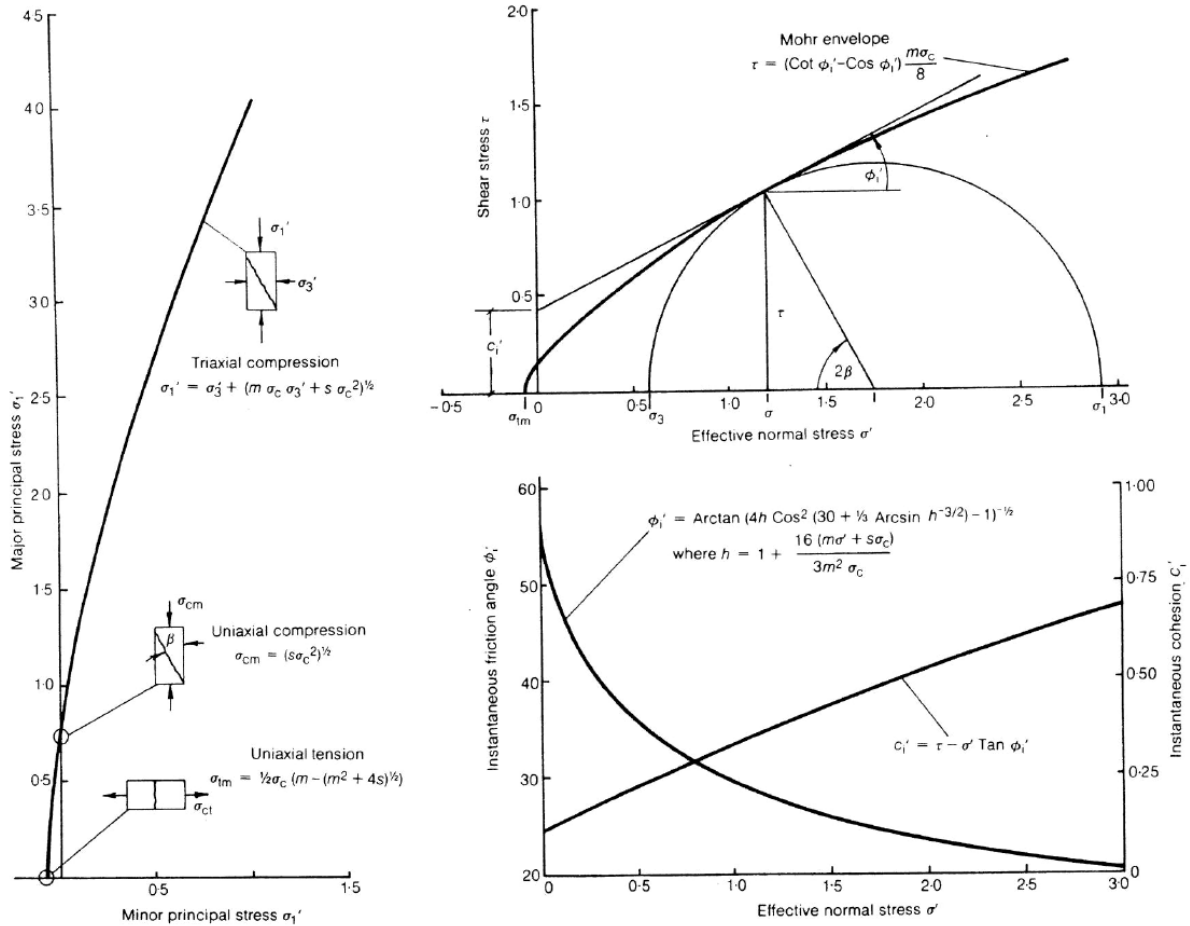Effective normal stress σ'

75

Table 2: Field estimates of uniaxial compressive strength.

Grade*	Term	Uniaxial Comp. Strength (MPa)	Point Load Index (MPa)	Field estimate of strength	Examples
R6	Extremely Strong	> 250	>10	Specimen can only be chipped with a geological hammer	Fresh basalt, chert, diabase, gneiss, granite, quartzite
R5	Very strong	100 - 250	4 - 10	Specimen requires many blows of a geological hammer to fracture it	Amphibolite, sandstone, basalt, gabbro, gneiss, granodiorite, limestone, marble, rhyolite, tuff
R4	Strong	50 - 100	2 - 4	Specimen requires more than one blow of a geological hammer to fracture it	Limestone, marble, phyllite, sandstone, schist, shale
R3	Medium strong	25 - 50	1 - 2	Cannot be scraped or peeled with a pocket knife, specimen can be fractured with a single blow from a geological hammer	Claystone, coal, concrete, schist, shale, siltstone
R2	Weak	5 - 25	**	Can be peeled with a pocket knife with difficulty, shallow indentation made by firm blow with point of a geological hammer	Chalk, rocksalt, potash
R1	Very weak	1 - 5	**	Crumbles under firm blows with point of a geological hammer, can be peeled by a pocket knife	Highly weathered or altered rock
R0	Extremely weak	0.25 - 1	**	Indented by thumbnail	Stiff fault gouge

* Grade according to Brown (1981).

** Point load tests on rocks with a uniaxial compressive strength below 25 MPa are likely to yield highly ambiguous results.

Table 3: Values of the constant m_i for intact rock, by rock group. Note that values in parenthesis are estimates.

Rock type	Class	Group	Texture: Coarse	Texture: Medium	Texture: Fine	Texture: Very fine
SEDIMENTARY	Clastic		Conglomerates* (21 ± 3) Breccias (19 ± 5)	Sandstones 17 ± 4	Siltstones 7 ± 2 Greywackes (18 ± 3)	Claystones 4 ± 2 Shales (6 ± 2) Marls (7 ± 2)
	Non-Clastic	Carbonates	Crystalline Limestone (12 ± 3)	Sparitic Limestones (10 ± 2)	Micritic Limestones (9 ± 2)	Dolomites (9 ± 3)
		Evaporites		Gypsum 8 ± 2	Anhydrite 12 ± 2	
		Organic				Chalk 7 ± 2
METAMORPHIC	Non Foliated		Marble 9 ± 3	Hornfels (19 ± 4) Metasandstone (19 ± 3)	Quartzites 20 ± 3	
	Slightly foliated		Migmatite (29 ± 3)	Amphibolites 26 ± 6		
	Foliated**		Gneiss 28 ± 5	Schists 12 ± 3	Phyllites (7 ± 3)	Slates 7 ± 4
IGNEOUS	Plutonic	Light	Granite 32 ± 3 Diorite 25 ± 5 Granodiorite (29 ± 3)			
		Dark	Gabbro 27 ± 3 Norite 20 ± 5	Dolerite (16 ± 5)		
	Hypabyssal		Porphyries (20 ± 5)		Diabase (15 ± 5)	Peridotite (25 ± 5)
	Volcanic	Lava		Rhyolite (25 ± 5) Andesite 25 ± 5	Dacite (25 ± 3) Basalt (25 ± 5)	Obsidian (19 ± 3)
		Pyroclastic	Agglomerate (19 ± 3)	Breccia (19 ± 5)	Tuff (13 ± 5)	

* Conglomerates and breccias may present a wide range of m_i values depending on the nature of the cementing material and the degree of cementation, so they may range from values similar to sandstone to values used for fine grained sediments.

* *These values are for intact rock specimens tested normal to bedding or foliation. The value of m_i will be significantly different if failure occurs along a weakness plane.

Anisotropic and foliated rocks such as slates, schists and phyllites, the behaviour of which is dominated by closely spaced planes of weakness, cleavage or schistosity, present particular difficulties in the determination of the uniaxial compressive strengths.

Salcedo (1983) has published the results of a set of directional uniaxial compressive tests on a graphitic phyllite from Venezuela. These results are summarised in Figure 2. It will be noted that the uniaxial compressive strength of this material varies by a factor of about 5, depending upon the direction of loading.
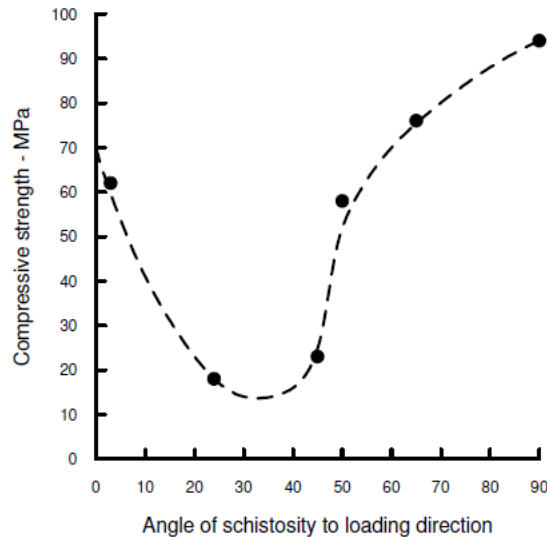
Figure 2: Influence of loading direction on the strength of graphitic phyllite tested by Salcedo (1983).

In deciding upon the value of σ_{ci} for foliated rocks, a decision has to be made on whether to use the highest or the lowest uniaxial compressive strength obtained from results such as those given in Figure 2. Mineral composition, grain size, grade of metamorphism and tectonic history all play a role in determining the characteristics of the rock mass. The author cannot offer any precise guidance on the choice of σ_{ci} but some insight into the role of schistosity in rock masses can be obtained by considering the case of the Yacambú-Quibor tunnel in Venezuela.

Strength of schistose rock

In the earlier part of these notes, the discussion on the strength of intact rock was based upon the assumption that the rock was isotropic, i.e. its strength was the same in all directions. A common problem encountered in rock mechanics involves the determination of the strength of schistose or layered rocks such as slates or shales.

If it is assumed that the shear strength of the discontinuity surfaces in such rocks is defined by an instantaneous friction angle ϕ'_i and an instantaneous cohesion c'_i (see figure 3), then the axial strength σ'_1 of a triaxial specimen containing inclined discontinuities is given by the following equation (see Jaeger and Cook (1969), pages 65 to 68):

$$\sigma'_1 = \sigma'_3 + \frac{2(c'_i + \sigma'_3 \, Tan\phi'_i)}{(1 - Tan\phi'_i \, Tan\,\beta) \, Sin\,2\beta} \qquad (14)$$

where σ'_3 is the minimum principal stress or confining pressure,
and β is the inclination of the discontinuity surfaces to the direction of the major principal stress σ_1 as shown in figure 11a.

Equation 14 can only be solved for values of β within about 25° of the friction angle ϕ'. Very small values of β will give very high values for σ'_1, while values of β close to 90° will give negative (and hence meaningless) values for σ'_1. The physical significance of these results is that slip on the discontinuity surfaces is not possible, and failure will occur through the intact material as predicted by equation 3. A typical plot of the axial strength σ'_1 versus the angle β is given in figure 11b.

If it is to be assumed that the shear strength of the discontinuity surfaces can be defined by equations 6 and 7, as discussed in the previous section, then in order to determine the values of ϕ'_i and c'_i for substitution into equation 14, the effective normal stress σ' acting across the discontinuity must be known. This is found from:

$$\sigma' = \frac{1}{2}(\sigma'_1 + \sigma'_3) - \frac{1}{2}(\sigma'_1 - \sigma'_3) \, Cos\,2\beta \qquad (15)$$

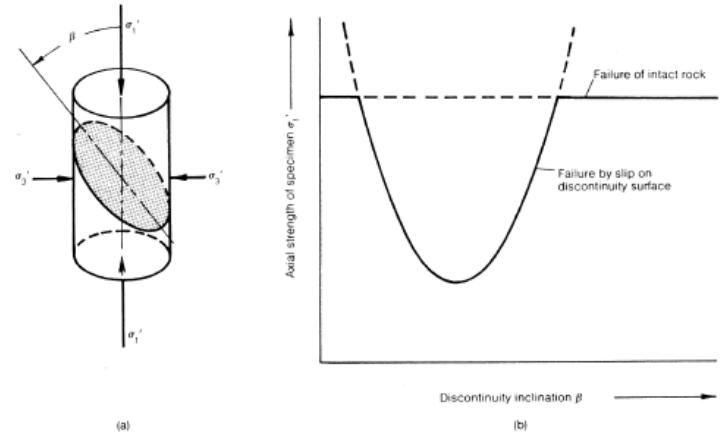(a)   (b)

Figure 11 :   (a) Configuration of triaxial test specimens containing a pre-existing discontinuity;(b) strength of specimen predicted by means of equations 14 and15.

However, since σ'_1 is the strength to be determined, the following iterative process can be used:

a) Calculate the strength σ'_{1i} of the intact material by means of equation 3, using the appropriate values of σ_c, m and s.

b) Determine values of m_j and s_j for the joint (discontinuity) surfaces from direct shear or triaxial test data. Note that the value of σ_c, the unconfined compressive strength, is the same for the intact material and the discontinuity surfaces in this analysis.

c) Use the value σ'_{1i}, calculated in step 1, to obtain the first estimate of the effective normal stress σ' from equation 15.

d) Calculate τ, ϕ'_i and c'_i from equations 7, 6 and 8, using the value of m_j and s_j from step b, and the value of σ' from step c.

e) Calculate the axial strength σ'_{1j} from equation 14.

f) If σ'_{1j} is negative or greater than σ'_{1i}, the failure of the intact material occurs in preference to slip on the discontinuity, and the strength of the specimen is defined by equation 3.

g) If σ'_{1j} is less than σ'_{1i} then failure occurs as a result of slip on the discontinuity. In this case, return to step c and use the axial strength calculated in step 5 to calculate a new value for the effective normal stress σ'.

h) Continue this iteration until the difference between successive values of σ'_{1j} in step e is less than 1%. It will be found that only three or four iterations are required to achieve this level of accuracy.

Influence of sample size

The influence of sample size upon rock strength has been widely discussed in geotechnical literature and it is generally assumed that there is a significant reduction in strength with increasing sample size. Based upon an analysis of published data, Hoek and Brown (1980a) have suggested that the uniaxial compressive strength σ_{cd} of a rock specimen with a diameter of d mm is related to the uniaxial compressive strength σ_{c50} of a 50 mm diameter sample by the following relationship:

$$\sigma_{cd} = \sigma_{c50} \left(\frac{50}{d} \right)^{0.18} \tag{10}$$

This relationship, together with the data upon which it was based, is shown in Figure 4.

It is suggested that the reduction in strength is due to the greater opportunity for failure through and around grains, the 'building blocks' of the intact rock, as more and more of these grains are included in the test sample. Eventually, when a sufficiently large number of grains are included in the sample, the strength reaches a constant value.

The Hoek-Brown failure criterion, which assumes isotropic rock and rock mass behaviour, should only be applied to those rock masses in which there are a sufficient number of closely spaced discontinuities, with similar surface characteristics, that isotropic behaviour involving failure on discontinuities can be assumed. When the structure being analysed is large and the block size small in comparison, the rock mass can be treated as a Hoek-Brown material.

Where the block size is of the same order as that of the structure being analysed or when one of the discontinuity sets is significantly weaker than the others, the Hoek-Brown criterion should not be used. In these cases, the stability of the structure should be analysed by considering failure mechanisms involving the sliding or rotation of blocks and wedges defined by intersecting structural features.

It is reasonable to extend this argument further and to suggest that, when dealing with large scale rock masses, the strength will reach a constant value when the size of individual rock pieces is sufficiently small in relation to the overall size of the structure being considered. This suggestion is embodied in Figure 5 which shows the transition
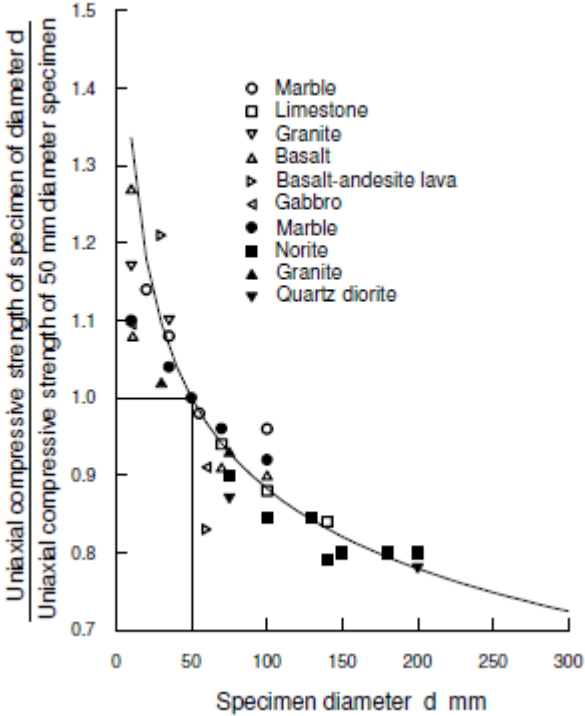
One of the practical problems that arises when assessing the value of GSI in the field is related to blast damage. As illustrated in Figure 6, there is a considerable difference in the appearance of a rock face which has been excavated by controlled blasting and a face which has been damaged by bulk blasting. Wherever possible, the undamaged face should be used to estimate the value of GSI since the overall aim is to determine the properties of the undisturbed rock mass.

Figure 6: Comparison between the results achieved using controlled blasting (on the left) and normal bulk blasting for a surface excavation in gneiss.

The influence of blast damage on the near surface rock mass properties has been taken into account in the 2002 version of the Hoek-Brown criterion (Hoek, Carranza-Torres and Corkum, 2002) as follows:

$$m_b = m_i \exp\left(\frac{GSI-100}{28-14D}\right)$$ (11)

$$s = \exp\left(\frac{GSI-100}{9-3D}\right)$$ (12)

and

$$a = \frac{1}{2} + \frac{1}{6}\left(e^{-GSI/15} - e^{-20/3}\right)$$ (13)

D is a factor which depends upon the degree of disturbance due to blast damage and stress relaxation. It varies from 0 for undisturbed in situ rock masses to 1 for very disturbed rock masses. Guidelines for the selection of D are presented in Table 7.

Note that the factor D applies only to the blast damaged zone and it should not be applied to the entire rock mass. For example, in tunnels the blast damage is generally limited to a 1 to 2 m thick zone around the tunnel and this should be incorporated into numerical models as a different and weaker material than the surrounding rock mass. Applying the blast damage factor D to the entire rock mass is inappropriate and can result in misleading and unnecessarily pessimistic results.

The uniaxial compressive strength of the rock mass is obtained by setting $\sigma_3' = 0$ in equation 1, giving:

$$\sigma_c = \sigma_{ci}.s^a$$ (14)
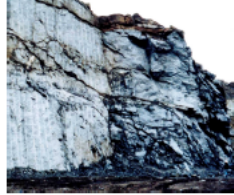
and, the tensile strength of the rock mass is:

$$\sigma_t = -\frac{s\sigma_{ci}}{m_b}$$ (15)

Equation 15 is obtained by setting $\sigma_1' = \sigma_3' = \sigma_t$ in equation 1. This represents a condition of biaxial tension. Hoek (1983) showed that, for brittle materials, the uniaxial tensile strength is equal to the biaxial tensile strength.

Note that the "switch" at GSI = 25 for the coefficients s and a (Hoek and Brown, 1997) has been eliminated in equations 11 and 12 which give smooth continuous transitions for the entire range of GSI values. The numerical values of s and a, given by these equations, are very close to those given by the previous equations and it is not necessary for readers to revisit and make corrections to old calculations.

Table 7: Guidelines for estimating disturbance factor D

Appearance of rock mass	Description of rock mass	Suggested value of D
	Excellent quality controlled blasting or excavation by Tunnel Boring Machine results in minimal disturbance to the confined rock mass surrounding a tunnel.	D = 0
	Mechanical or hand excavation in poor quality rock masses (no blasting) results in minimal disturbance to the surrounding rock mass. Where squeezing problems result in significant floor heave, disturbance can be severe unless a temporary invert, as shown in the photograph, is placed.	D = 0 D = 0.5 No invert
	Very poor quality blasting in a hard rock tunnel results in severe local damage, extending 2 or 3 m, in the surrounding rock mass.	D = 0.8
	Small scale blasting in civil engineering slopes results in modest rock mass damage, particularly if controlled blasting is used as shown on the left hand side of the photograph. However, stress relief results in some disturbance.	D = 0.7 Good blasting D = 1.0 Poor blasting
	Very large open pit mine slopes suffer significant disturbance due to heavy production blasting and also due to stress relief from overburden removal. In some softer rocks excavation can be carried out by ripping and dozing and the degree of damage to the slopes is less.	D = 1.0 Production blasting D = 0.7 Mechanical excavation

Estimation of constants based upon rock mass structure and discontinuity surface conditions

GENERALISED HOEK-BROWN CRITERION

$$\sigma_1' = \sigma_3' + \sigma_c \left(m_b \frac{\sigma_3'}{\sigma_c} + s \right)^a$$

σ_1' = major principal effective stress at failure

σ_3' = minor principal effective stress at failure

σ_c = uniaxial compressive strength of *intact* pieces of rock

m_b, s and a are constants which depend on the composition, structure and surface conditions of the rock mass

STRUCTURE

	SURFACE CONDITION	VERY GOOD Very rough, unweathered surfaces	GOOD Rough, slightly weathered, iron stained surfaces	FAIR Smooth, moderately weathered or altered surfaces	POOR Slickensided, highly weathered surfaces with compact coatings or fillings containing angular rock fragments	VERY POOR Slickensided, highly weathered surfaces with soft clay coatings or fillings
BLOCKY -very well interlocked undisturbed rock mass consisting of cubical blocks formed by three orthogonal discontinuity sets	m_b/m_i	0.60	0.40	0.26	0.16	0.08
	s	0.190	0.062	0.015	0.003	0.0004
	a	0.5	0.5	0.5	0.5	0.5
	E_m	75,000	40,000	20,000	9,000	3,000
	v	0.2	0.2	0.25	0.25	0.25
	GSI	85	75	62	48	34
VERY BLOCKY-interlocked, partially disturbed rock mass with multifaceted angular blocks formed by four or more discontinuity sets	m_b/m_i	0.40	0.29	0.16	0.11	0.07
	s	0.062	0.021	0.003	0.001	0
	a	0.5	0.5	0.5	0.5	0.53
	E_m	40,000	24,000	9,000	5,000	2,500
	v	0.2	0.25	0.25	0.25	0.3
	GSI	75	65	48	38	25
BLOCKY/SEAMY-folded and faulted with many intersecting discontinuities forming angular blocks	m_b/m_i	0.24	0.17	0.12	0.08	0.06
	s	0.012	0.004	0.001	0	0
	a	0.5	0.5	0.5	0.5	0.55
	E_m	18,000	10,000	6,000	3,000	2,000
	v	0.25	0.25	0.25	0.3	0.3
	GSI	60	50	40	30	20
CRUSHED-poorly interlocked, heavily broken rock mass with a mixture of angular and rounded blocks	m_b/m_i	0.17	0.12	0.08	0.06	0.04
	s	0.004	0.001	0	0	0
	a	0.5	0.5	0.5	0.55	0.60
	E_m	10,000	6,000	3,000	2,000	1,000
	v	0.25	0.25	0.3	0.3	0.3
	GSI	50	40	30	20	10

PARAMETRI GEOTECNICI PER UN'ANALISI TENSO-DEFORMATIVA (FEM – FDM) DERIVATI DALL'INDICE "GEOLOGICAL STRENGTH INDEX (HOEK, 1997)"

CRITERIO DI ROTTURA DI HOEK (2002)

$$\sigma_1 = \sigma_3 + \sigma_{ci} \cdot \left(m_b \cdot \frac{\sigma_3}{\sigma_{ci}} + s \right)^a$$

m_b è il fattore riduttivo della costante del litotipo definito dalla

$$m_b = m_i \exp\left(\frac{G.S.I. - 100}{28 - 14D} \right)$$

s ed a sono costanti che dipendono dalle caratteristiche dell'ammasso roccioso attraverso le

$$s = \exp\left(\frac{G.S.I. - 100}{9 - 3D} \right)$$

$$a = \frac{1}{2} + \frac{1}{6}\left(e^{-\frac{G.S.I.}{15}} - e^{-\frac{20}{3}} \right)$$

D è il fattore di disturbo" correlato al grado di disturbo conseguente alla metodologia di scavo e al grado di rilassamento dell'ammasso roccioso

MODULO DI DEFORMABILITA' DELL'AMMASSO (GPa)

$$E_m(GPa) = \left(1 - \frac{D}{2} \right) \sqrt{\frac{\sigma_{ci}}{100}} \, 10^{\left(\frac{G.S.I. - 10}{40} \right)}$$

Per $\sigma_{ci} \leq 100 MPa$

$$E_m(GPa) = \left(1 - \frac{D}{2} \right) \cdot 10^{\left(\frac{G.S.I. - 10}{40} \right)}$$

Per $\sigma_{ci} > 100 MPa$

PARAMETRI GEOTECNICI NECESSARI PER UN'ANALISI TENSO-DEFORMATIVA (FEM – FDM) CON CRITERIO DI ROTTURA DEL MEZZO ALLA "MOHR –COULOMB"

$$\tau = c + \sigma_n \tan\varphi$$

-	PESO DI VOLUME	γ
-	PARAMETRI DI RESISTENZA	Φ, c, ψ (ANGOLO DI DILATANZA)
-	PARAMETRI DI DEFORMABILITÀ	E, ν
-	STATO TENSIONALE (NELL'IPOTESI $\sigma_1' = \sigma_v'$) $K_0 = \sigma_h' / \sigma_v'$	
-	PRESSIONE NEUTRA	u
-	PERMEABILITÀ	k

DEFINIZIONE DEI PARAMETRI DI RESISTENZA DI PICCO E RESIDUI

DEFINIZIONE DELLE RELATIVE SOGLIE DI DEFORMAZIONE (TAGLIO)

Mohr-Coulomb parameters

Since many geotechnical software programs are written in terms of the Mohr-Coulomb failure criterion, it is sometimes necessary to determine equivalent angles of friction and cohesive strengths for each rock mass and stress range. This is done by fitting an average linear relationship to the curve generated by solving equation 1 for a range of minor principal stress values defined by $\sigma_t < \sigma_3 < \sigma_{3max}$, as illustrated in Figure 7. The fitting process involves balancing the areas above and below the Mohr-Coulomb plot. This results in the following equations for the angle of friction ϕ' and cohesive strength c' :

$$\phi' = \sin^{-1}\left[\frac{6am_b(s+m_b\sigma'_{3n})^{a-1}}{2(1+a)(2+a)+6am_b(s+m_b\sigma'_{3n})^{a-1}}\right] \tag{16}$$

$$c' = \frac{\sigma_{ci}\left[(1+2a)s+(1-a)m_b\sigma'_{3n}\right](s+m_b\sigma'_{3n})^{a-1}}{(1+a)(2+a)\sqrt{1+\left(6am_b(s+m_b\sigma'_{3n})^{a-1}\right)/((1+a)(2+a))}} \tag{17}$$

where $\sigma_{3n} = \sigma'_{3max}/\sigma_{ci}$

Note that the value of σ'_{3max}, the upper limit of confining stress over which the relationship between the Hoek-Brown and the Mohr-Coulomb criteria is considered, has to be determined for each individual case. Guidelines for selecting these values for slopes as well as shallow and deep tunnels are presented later.

The Mohr-Coulomb shear strength τ, for a given normal stress σ, is found by substitution of these values of c' and ϕ' in to the equation:

$$\tau = c' + \sigma \tan\phi' \tag{18}$$

The equivalent plot, in terms of the major and minor principal stresses, is defined by:

$$\sigma'_1 = \frac{2c'\cos\phi'}{1-\sin\phi'} + \frac{1+\sin\phi'}{1-\sin\phi'}\sigma'_3 \tag{19}$$
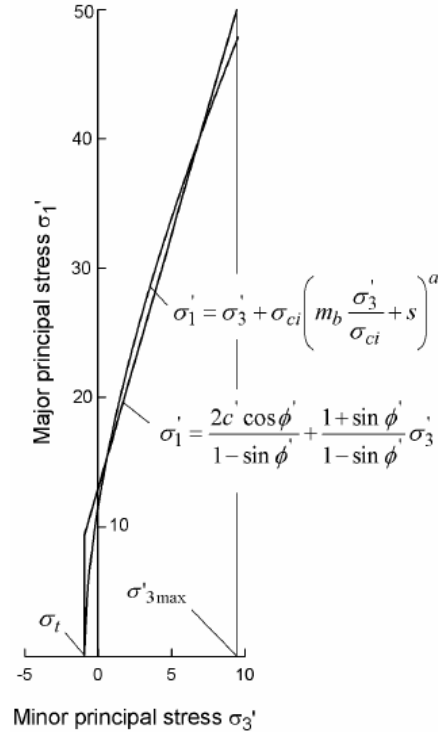

Figure 7: Relationships between major and minor principal stresses for Hoek-Brown and equivalent Mohr-Coulomb criteria.

Rock mass strength

The uniaxial compressive strength of the rock mass σ_c is given by equation 14. Failure initiates at the boundary of an excavation when σ_c is exceeded by the stress induced on that boundary. The failure propagates from this initiation point into a biaxial stress field and it eventually stabilizes when the local strength, defined by equation 1, is higher than the induced stresses σ_1 and σ_3. Most numerical models can follow this process of fracture propagation and this level of detailed analysis is very important when considering the stability of excavations in rock and when designing support systems.

However, there are times when it is useful to consider the overall behaviour of a rock mass rather than the detailed failure propagation process described above. For example, when considering the strength of a pillar, it is useful to have an estimate of the overall strength of the pillar rather than a detailed knowledge of the extent of fracture propagation in the pillar. This leads to the concept of a global "rock mass strength" and Hoek and Brown (1997) proposed that this could be estimated from the Mohr-Coulomb relationship:

$$\sigma'_{cm} = \frac{2c' \cos\phi'}{1 - \sin\phi'} \tag{20}$$

with c' and ϕ' determined for the stress range $\sigma_t < \sigma'_3 < \sigma_{ci}/4$ giving

$$\sigma'_{cm} = \sigma_{ci} \cdot \frac{(m_b + 4s - a(m_b - 8s))(m_b/4 + s)^{a-1}}{2(1+a)(2+a)} \tag{21}$$

Determination of $\sigma'_{3\max}$

The issue of determining the appropriate value of $\sigma'_{3\max}$ for use in equations 16 and 17 depends upon the specific application. Two cases will be investigated:

Tunnels – where the value of $\sigma'_{3\max}$ is that which gives equivalent characteristic curves for the two failure criteria for deep tunnels or equivalent subsidence profiles for shallow tunnels.

Slopes – here the calculated factor of safety and the shape and location of the failure surface have to be equivalent.

For the case of deep tunnels, closed form solutions for both the Generalized Hoek-Brown and the Mohr-Coulomb criteria have been used to generate hundreds of solutions and to find the value of $\sigma'_{3\max}$ that gives equivalent characteristic curves.

For shallow tunnels, where the depth below surface is less than 3 tunnel diameters, comparative numerical studies of the extent of failure and the magnitude of surface subsidence gave an identical relationship to that obtained for deep tunnels, provided that caving to surface is avoided.

The results of the studies for deep tunnels are plotted in Figure 8 and the fitted equation for both deep and shallow tunnels is:

$$\frac{\sigma'_{3\max}}{\sigma'_{cm}} = 0.47 \left(\frac{\sigma'_{cm}}{\gamma H}\right)^{-0.94} \tag{22}$$

where σ'_{cm} is the rock mass strength, defined by equation 21, γ is the unit weight of the rock mass and H is the depth of the tunnel below surface. In cases where the horizontal stress is higher than the vertical stress, the horizontal stress value should be used in place of γH.
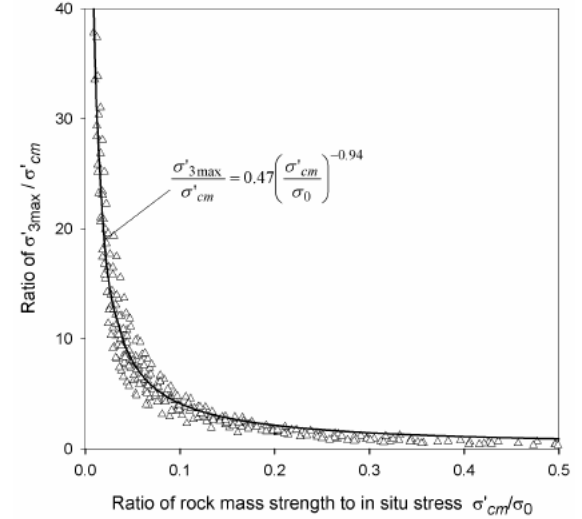
Figure 8: Relationship for the calculation of $\sigma'_{3\max}$ for equivalent Mohr-Coulomb and Hoek-Brown parameters for tunnels.

Equation 22 applies to all underground excavations, which are surrounded by a zone of failure that does not extend to surface. For studies of problems such as block caving in mines it is recommended that no attempt should be made to relate the Hoek-Brown and Mohr-Coulomb parameters and that the determination of material properties and subsequent analysis should be based on only one of these criteria.

Similar studies for slopes, using Bishop's circular failure analysis for a wide range of slope geometries and rock mass properties, gave:

$$\frac{\sigma'_{3\max}}{\sigma'_{cm}} = 0.72 \left(\frac{\sigma'_{cm}}{\gamma H}\right)^{-0.91} \tag{23}$$

where H is the height of the slope.

Deformation modulus

Hoek and Diederichs (2005) re-examined existing empirical methods for estimating rock mass deformation modulus and concluded that none of these methods provided reliable estimates over the whole range of rock mass conditions encountered. In particular, large errors were found for very poor rock masses and, at the other end of the spectrum, for massive strong rock masses. Fortunately, a new set of reliable measured data from China and Taiwan was available for analyses and it was found that the equation which gave the best fit to this data is a sigmoid function having the form:

$$y = c + \frac{a}{1 + e^{-((x - x_0)/b)}} \qquad (24)$$

Using commercial curve fitting software, Equation 24 was fitted to the Chinese and Taiwanese data and the constants a and b in the fitted equation were then replaced by expressions incorporating GSI and the disturbance factor D. These were adjusted to give the equivalent average curve and the upper and lower bounds into which > 90% of the data points fitted. Note that the constant a = 100 000 in Equation 25 is a scaling factor and it is not directly related to the physical properties of the rock mass.

The following best-fit equation was derived:

$$E_{rm}\,(MPa) = 100000 \left(\frac{1 - D/2}{1 + e^{((75+25D-GSI)/11)}} \right) \qquad (25)$$

The rock mass deformation modulus data from China and Taiwan includes information on the geology as well as the uniaxial compressive strength (σ_{ci}) of the intact rock This information permits a more detailed analysis in which the ratio of mass to intact modulus (E_{rm}/E_i) can be included. Using the modulus ratio MR proposed by Deere (1968) (modified by the authors based in part on this data set and also on additional correlations from Palmstrom and Singh (2001)) it is possible to estimate the intact modulus from:

$$E_i = MR \cdot \sigma_{ci} \qquad (26)$$

This relationship is useful when no direct values of the intact modulus (E_i) are available or where completely undisturbed sampling for measurement of E_i is difficult. A detailed analysis of the Chinese and Taiwanese data, using Equation (26) to estimate E_i resulted in the following equation:

$$E_{rm} = E_i \left(0.02 + \frac{1 - D/2}{1 + e^{((60+15D-GSI)/11)}} \right) \qquad (27)$$

This equation incorporates a finite value for the parameter c (Equation 24) to account for the modulus of broken rock (transported rock, aggregate or soil) described by GSI = 0. This equation is plotted against the average normalized field data from China and Taiwan in Figure 9.
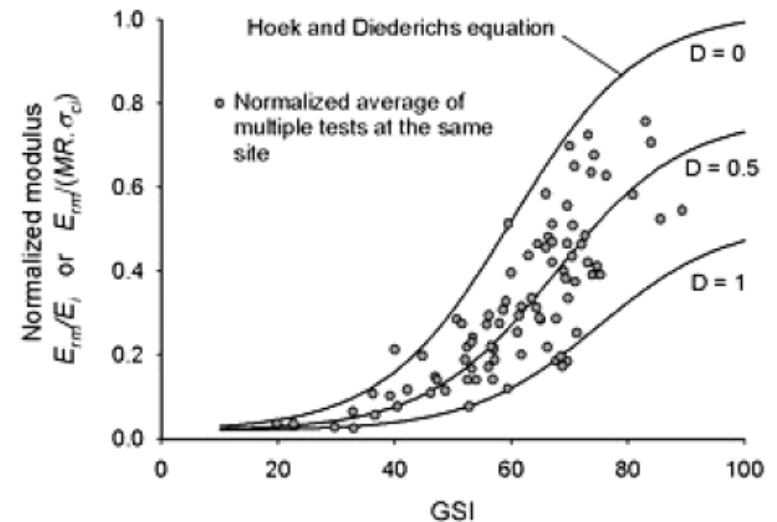

Figure 9: Plot of normalized in situ rock mass deformation modulus from China and Taiwan against Hoek and Diederichs Equation (27). Each data point represents the average of multiple tests at the same site in the same rock mass.

Table 8: Guidelines for the selection of modulus ratio (MR) values in Equation (26) - based on Deere (1968) and Palmstrom and Singh (2001)

Class	Group	Texture			
		Coarse	Medium	Fine	Very fine
SEDIMENTARY — Clastic		Conglomerates 300-400 Breccias 230-350	Sandstones 200-350	Siltstones 350-400 Greywackes 350	Claystones 200-300 Shales 150-250 * Marls 150-200
SEDIMENTARY — Non-Clastic	Carbonates	Crystalline Limestone 400-600	Sparitic Limestones 600-800	Micritic Limestones 800-1000	Dolomites 350-500
	Evaporites		Gypsum (350)**	Anhydrite (350)**	
	Organic				Chalk 1000+
METAMORPHIC — Non Foliated		Marble 700-1000	Hornfels 400-700 Metasandstone 200-300	Quartzites 300-450	
METAMORPHIC — Slightly foliated		Migmatite 350-400	Amphibolites 400-500	Gneiss 300-750*	
METAMORPHIC — Foliated*			Schists 250-1100*	Phyllites /Mica Schist 300-800*	Slates 400-600*
IGNEOUS — Plutonic — Light		Granite+ 300-550 Diorite+ 300-350 Granodiorite+ 400-450			
IGNEOUS — Plutonic — Dark		Gabbro 400-500 Dolerite 300-400 Norite 350-400			
IGNEOUS — Hypabyssal		Porphyries (400)**		Diabase 300-350	Peridotite 250-300
IGNEOUS — Volcanic — Lava			Rhyolite 300-500 Andesite 300-500	Dacite 350-450 Basalt 250-450	
IGNEOUS — Volcanic — Pyroclastic		Agglomerate 400-600	Volcanic breccia (500) **	Tuff 200-400	

* Highly anisotropic rocks: the value of MR will be significantly different if normal strain and/or loading occurs parallel (high MR) or perpendicular (low MR) to a weakness plane. Uniaxial test loading direction should be equivalent to field application.

+ Felsic Granitoids: Coarse Grained or Altered (high MR), fined grained (low MR).

** No data available, estimated on the basis of geological logic.

Table 8, based on the modulus ratio (MR) values proposed by Deere (1968) can be used for calculating the intact rock modulus E_i. In general, measured values of E_i are seldom available and, even when they are, their reliability is suspect because of specimen damage. This specimen damage has a greater impact on modulus than on strength and, hence, the intact rock strength, when available, can usually be considered more reliable.

Post-failure behaviour

When using numerical models to study the progressive failure of rock masses, estimates of the post-peak or post-failure characteristics of the rock mass are required. In some of these models, the Hoek-Brown failure criterion is treated as a yield criterion and the analysis is carried out using plasticity theory. No definite rules for dealing with this problem can be given but, based upon experience in numerical analysis of a variety of practical problems, the post-failure characteristics, illustrated in Figure 10, are suggested as a starting point.
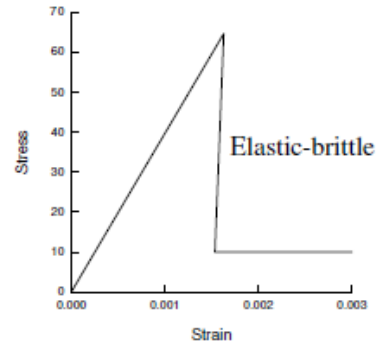
Reliability of rock mass strength estimates

The techniques described in the preceding sections of this chapter can be used to estimate the strength and deformation characteristics of isotropic jointed rock masses. When applying this procedure to rock engineering design problems, most users consider only the 'average' or mean properties. In fact, all of these properties exhibit a distribution about the mean, even under the most ideal conditions, and these distributions can have a significant impact upon the design calculations.

In the text that follows, a slope stability calculation and a tunnel support design calculation are carried out in order to evaluate the influence of these distributions. In each case the strength and deformation characteristics of the rock mass are estimated by means of the Hoek-Brown procedure, assuming that the three input parameters are defined by normal distributions.

Input parameters

Figure 11 has been used to estimate the value of the value of GSI from field observations of blockiness and discontinuity surface conditions. Included in this figure is a crosshatched circle representing the 90% confidence limits of a GSI value of 25 ± 5 (equivalent to a standard deviation of approximately 2.5). This represents the range of values that an experienced geologist would assign to a rock mass described as BLOCKY/DISTURBED or DISINTEGRATED and POOR. Typically, rocks such as flysch, schist and some phyllites may fall within this range of rock mass descriptions.

(a) Very good quality hard rock mass

(b) Average quality rock mass

(c) Very poor quality soft rock mass

Figure 10: Suggested post failure characteristics for different quality rock masses.

Figure 11: Estimate of Geological Strength Index GSI based on geological descriptions.

GEOLOGICAL STRENGTH INDEX FOR BLOCKY JOINTED ROCKS

From a description of the structure and surface conditions of the rock mass, pick an appropriate box in this chart. Estimate the average value of GSI from the contours. Do not attempt to be too precise. Quoting a range from 36 to 42 is more realistic than stating that GSI = 38. It is also important to recognize that the Hoek-Brown criterion should only be applied to rock masses where the size of individual blocks or pieces is small compared with the size of the excavation under consideration. When the individual block size is more than about one quarter of the excavation size, the failure will be structurally controlled and the Hoek-Brown criterion should not be used.

SURFACE CONDITIONS

DECREASING SURFACE QUALITY ⟹

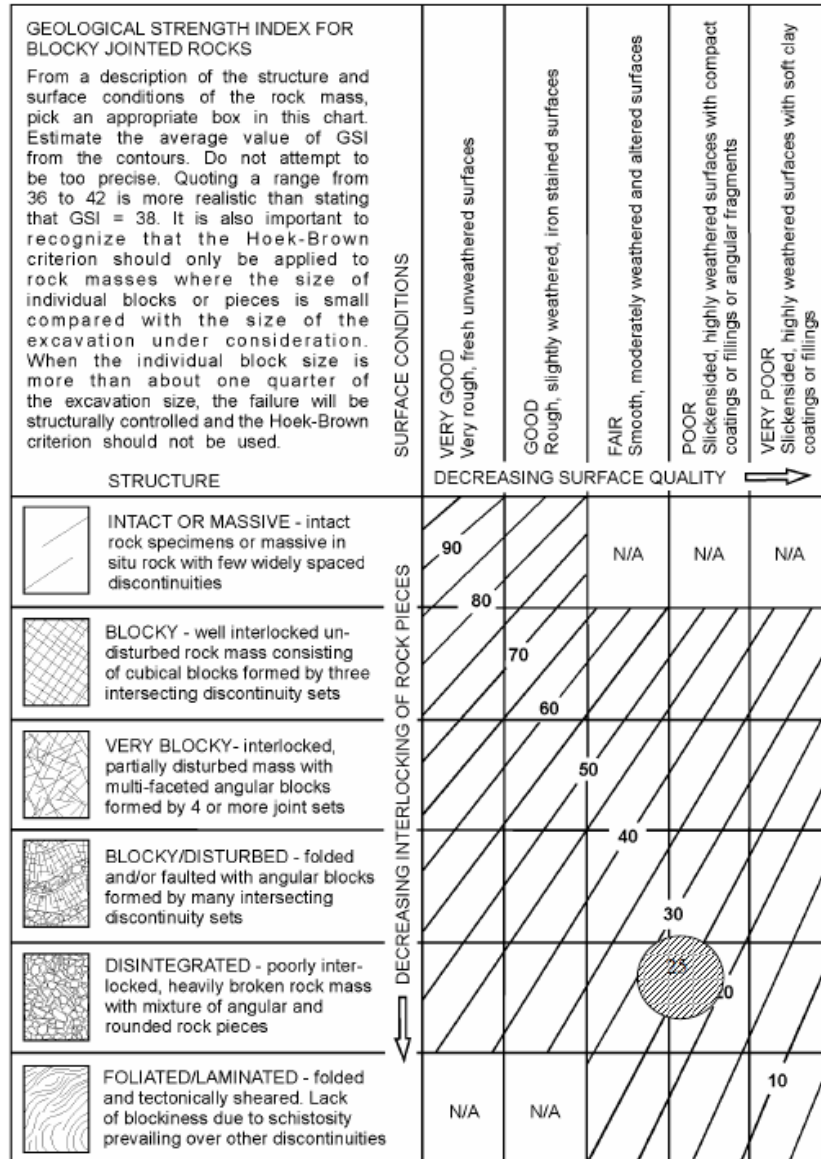| STRUCTURE		VERY GOOD — Very rough, fresh unweathered surfaces	GOOD — Rough, slightly weathered, iron stained surfaces	FAIR — Smooth, moderately weathered and altered surfaces	POOR — Slickensided, highly weathered surfaces with compact coatings or fillings or angular fragments	VERY POOR — Slickensided, highly weathered surfaces with soft clay coatings or fillings
INTACT OR MASSIVE - intact rock specimens or massive in situ rock with few widely spaced discontinuities		90		N/A	N/A	N/A
		80				
BLOCKY - well interlocked un-disturbed rock mass consisting of cubical blocks formed by three intersecting discontinuity sets			70			
			60			
VERY BLOCKY- interlocked, partially disturbed mass with multi-faceted angular blocks formed by 4 or more joint sets				50		
BLOCKY/DISTURBED - folded and/or faulted with angular blocks formed by many intersecting discontinuity sets				40		
					30	
DISINTEGRATED - poorly inter-locked, heavily broken rock mass with mixture of angular and rounded rock pieces					20	
FOLIATED/LAMINATED - folded and tectonically sheared. Lack of blockiness due to schistosity prevailing over other discontinuities		N/A	N/A			10

DECREASING INTERLOCKING OF ROCK PIECES

Practical examples of rock mass property estimates

The following examples are presented in order to illustrate the range of rock mass properties that can be encountered in the field and to give the reader some insight of how the estimation of rock mass properties was tackled in a number of actual projects.

Massive weak rock

Karzulovic and Diaz (1994) have described the results of a program of triaxial tests on a cemented breccia known as Braden Breccia from the El Teniente mine in Chile. In order to design underground openings in this rock, attempts were made to classify the rock mass in accordance with Bieniawski's RMR system. However, as illustrated in Figure 19, this rock mass has very few discontinuities and so assigning realistic numbers to terms depending upon joint spacing and condition proved to be very difficult. Finally, it was decided to treat the rock mass as a weak but homogeneous 'almost intact' rock, similar to a weak concrete, and to determine its properties by means of triaxial tests on large diameter specimens.

A series of triaxial tests was carried out on 100 mm diameter core samples, illustrated in Figure 20. The results of these tests were analysed by means of the regression analysis using the program RocLab[4]. Back analysis of the behaviour of underground openings in this rock indicate that the in-situ GSI value is approximately 75. From RocLab the following parameters were obtained:

Intact rock strength	σ_{ci}	51 MPa	Hoek-Brown constant	m_b	6.675
Hoek-Brown constant	m_i	16.3	Hoek-Brown constant	s	0.062
Geological Strength Index	GSI	75	Hoek-Brown constant	a	0.501
			Deformation modulus	E_m	15000 MPa

Figure 19: Braden Breccia at El Teniente Mine in Chile. This rock is a cemented breccia with practically no joints. It was dealt with in a manner similar to weak concrete and tests were carried out on 100 mm diameter specimens illustrated in Figure 20.

Fig. 20. 100 mm diameter by 200 mm long specimens of Braden Breccia from the El Teniente mine in Chile

Massive strong rock masses

The Rio Grande Pumped Storage Project in Argentina includes a large underground powerhouse and surge control complex and a 6 km long tailrace tunnel. The rock mass surrounding these excavations is massive gneiss with very few joints. A typical core from this rock mass is illustrated in Figure 21. The appearance of the rock at the surface was illustrated earlier in Figure 6, which shows a cutting for the dam spillway.

Figure 21: Excellent quality core with very few discontinuities from the massive gneiss of the Rio Grande project in Argentina.

The rock mass can be described as BLOCKY/VERY GOOD and the GSI value, from Table 5, is 75. Typical characteristics for the rock mass are as follows:

Intact rock strength	σ_{ci}	110 MPa	Hoek-Brown constant	m_b	11.46
Hoek-Brown constant	m_i	28	Hoek-Brown constant	s	0.062
Geological Strength Index	GSI	75	Constant	a	0.501
			Deformation modulus	E_m	45000 MPa

Figure 21 illustrates the 8 m high 12 m span top heading for the tailrace tunnel. The final tunnel height of 18 m was achieved by blasting two 5 m benches. The top heading was excavated by full-face drill and blast and, because of the excellent quality of the rock mass and the tight control on blasting quality, most of the top heading did not require any support.

Figure 21: Top heading of the 12 m span, 18 m high tailrace tunnel for the Rio Grande Pumped Storage Project.

Average quality rock mass

The partially excavated powerhouse cavern in the Nathpa Jhakri Hydroelectric project in Himachel Pradesh, India is illustrated in Figure 22. The rock is a jointed quartz mica schist, which has been extensively evaluated by the Geological Survey of India as described by Jalote et al (1996). An average GSI value of 65 was chosen to estimate the rock mass properties which were used for the cavern support design. Additional support, installed on the instructions of the Engineers, was placed in weaker rock zones.

The assumed rock mass properties are as follows:

Intact rock strength	σ_{ci}	30 MPa	Hoek-Brown constant	m_b	4.3
Hoek-Brown constant	m_i	15	Hoek-Brown constant	s	0.02
Geological Strength Index	GSI	65	Constant	a	0.5
			Deformation modulus	E_m	10000 MPa

Two and three dimensional stress analyses of the nine stages used to excavate the cavern were carried out to determine the extent of potential rock mass failure and to provide guidance in the design of the support system. An isometric view of one of the three dimensional models is given in Figure 23.

Figure 22: Partially completed 20 m span, 42.5 m high underground powerhouse cavern of the Nathpa Jhakri Hydroelectric Project in Himachel Pradesh, India. The cavern is approximately 300 m below the surface.
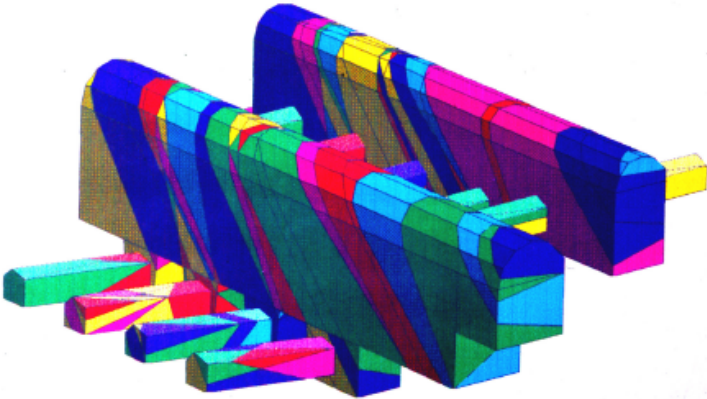

Figure 23: Isometric view of the 3DEC5 model of the underground powerhouse cavern and transformer gallery of the Nathpa Jhakri Hydroelectric Project, analysed by Dr. B. Dasgupta[6].

The support for the powerhouse cavern consists of rockbolts and mesh reinforced shotcrete. Alternating 6 and 8 m long 32 mm diameter bolts on 1 x 1 m and 1.5 x 1.5 m centres are used in the arch. Alternating 9 and 7.5 m long 32 mm diameter bolts were used in the upper and lower sidewalls with alternating 9 and 11 m long 32 mm rockbolts in the centre of the sidewalls, all at a grid spacing of 1.5 m. Shotcrete consists of two 50 mm thick layers of plain shotcrete with an interbedded layer of weldmesh. The support provided by the shotcrete was not included in the support design analysis, which relies upon the rockbolts to provide all the support required.

In the headrace tunnel, some zones of sheared quartz mica schist have been encountered and these have resulted in large displacements as illustrated in Figure 24. This is a common problem in hard rock tunnelling where the excavation sequence and support system have been designed for 'average' rock mass conditions. Unless very rapid changes in the length of blast rounds and the installed support are made when an abrupt change to poor rock conditions occurs, for example when a fault is encountered, problems with controlling tunnel deformation can arise.

Figure 24: Large displacements in the top heading of the headrace tunnel of the Nathpa Jhakri Hydroelectric project. These displacements are the result of deteriorating rock mass quality when tunnelling through a fault zone.

The only effective way to anticipate this type of problem is to keep a probe hole ahead of the advancing face at all times. Typically, a long probe hole is percussion drilled during a maintenance shift and the penetration rate, return water flow and chippings are constantly monitored during drilling. Where significant problems are indicated by this percussion drilling, one or two diamond-drilled holes may be required to investigate these problems in more detail. In some special cases, the use of a pilot tunnel may be more effective in that it permits the ground properties to be defined more accurately than is possible with probe hole drilling. In addition, pilot tunnels allow pre-drainage and pre-reinforcement of the rock ahead of the development of the full excavation profile.

Poor quality rock mass at shallow depth

Kavvadas et al (1996) have described some of the geotechnical issues associated with the construction of 18 km of tunnels and the 21 underground stations of the Athens Metro. These excavations are all shallow with typical depths to tunnel crown of between 15 and 20 m. The principal problem is one of surface subsidence rather than failure of the rock mass surrounding the openings.

The rock mass is locally known as Athenian schist which is a term used to describe a sequence of Upper Cretaceous flysch-type sediments including thinly bedded clayey and calcareous sandstones, siltstones (greywackes), slates, shales and limestones. During the Eocene, the Athenian schist formations were subjected to intense folding and thrusting. Later extensive faulting caused extensional fracturing and widespread weathering and alteration of the deposits.

The GSI values range from about 15 to about 45. The higher values correspond to the intercalated layers of sandstones and limestones, which can be described as BLOCKY/DISTURBED and POOR (Table 5). The completely decomposed schist can be described as DISINTEGRATED and VERY POOR and has GSI values ranging from 15 to 20. Rock mass properties for the completely decomposed schist, using a GSI value of 20, are as follows:

Intact rock strength - MPa	σ_{ci}	5-10	Hoek-Brown constant	m_b	0.55
Hoek-Brown constant	m_i	9.6	Hoek-Brown constant	s	0.0001
Geological Strength Index	GSI	20	Hoek-Brown constant	a	0.544
			Deformation modulus MPa	E_m	600

The Academia, Syntagma, Omonia and Olympion stations were constructed using the New Austrian Tunnelling Method twin side drift and central pillar method as illustrated in Figure 25. The more conventional top heading and bench method, illustrated in Figure 26, was used for the excavation of the Ambelokipi station. These stations are all 16.5 m wide and 12.7 m high. The appearance of the rock mass in one of the Olympion station side drift excavations is illustrated in Figures 27 and 28.
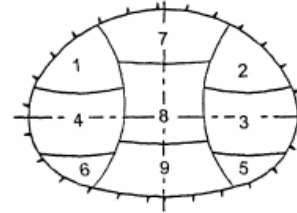

Figure 25: Twin side drift and central pillar excavation method. Temporary support consists of double wire mesh reinforced 250 - 300 mm thick shotcrete shells with embedded lattice girders or HEB 160 steel sets at 0.75 - 1 m spacing.
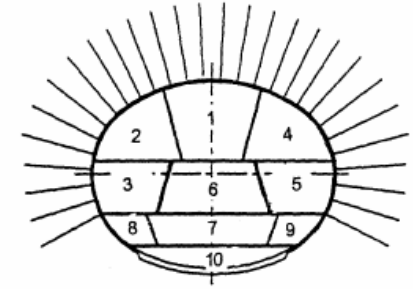
Figure 26: Top heading and bench method of excavation. Temporary support consists of a 200 mm thick shotcrete shell with 4 and 6 m long untensioned grouted rockbolts at 1.0 - 1.5 m spacing

Figure 27: Side drift in the Athens Metro Olympion station excavation that was excavated by the method illustrated in Figure 25. The station has a cover depth of approximately 10 m over the crown.
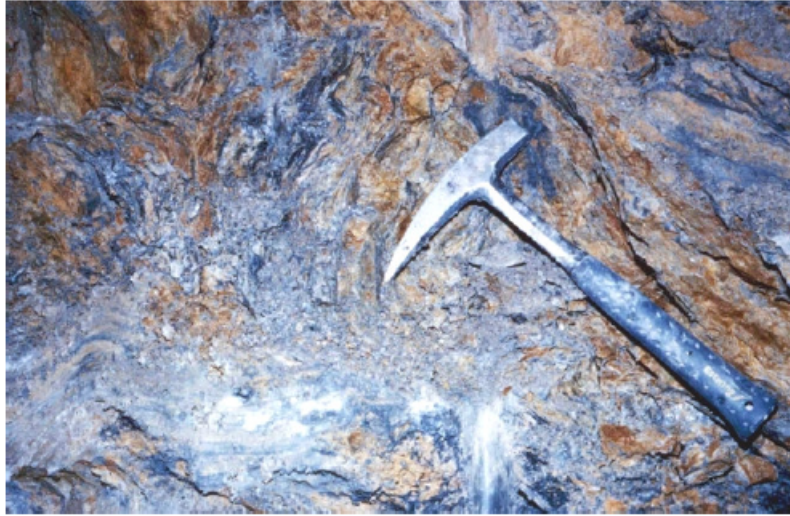
Figure 28: Appearance of the very poor quality Athenian Schist at the face of the side heading illustrated in Figure 27.

Numerical analyses of the two excavation methods showed that the twin side drift method resulted in slightly less rock mass failure in the crown of the excavation. However, the final surface displacements induced by the two excavation methods were practically identical.

Maximum vertical displacements of the surface above the centre-line of the Omonia station amounted to 51 mm. Of this, 28 mm occurred during the excavation of the side drifts, 14 mm during the removal of the central pillar and a further 9 mm occurred as a time dependent settlement after completion of the excavation. According to Kavvadas et al (1996), this time dependent settlement is due to the dissipation of excess pore water pressures which were built up during excavation. In the case of the Omonia station, the excavation of recesses towards the eastern end of the station, after completion of the station excavation, added a further 10 to 12 mm of vertical surface displacement at this end of the station.

Poor quality rock mass under high stress

The Yacambú Quibor tunnel in Venezuela is considered to be one of the most difficult tunnels in the world. This 25 km long water supply tunnel through the Andes is being excavated in sandstones and phyllites at depths of up to 1200 m below surface. The

graphitic phyllite is a very poor quality rock and gives rise to serious squeezing problems which, without adequate support, result in complete closure of the tunnel. A full-face tunnel-boring machine was completely destroyed in 1979 when trapped by squeezing ground conditions.

The graphitic phyllite has an average unconfined compressive strength of about 50 MPa and the estimated GSI value is about 25 (see Figures 2 and 3). Typical rock mass properties are as follows:

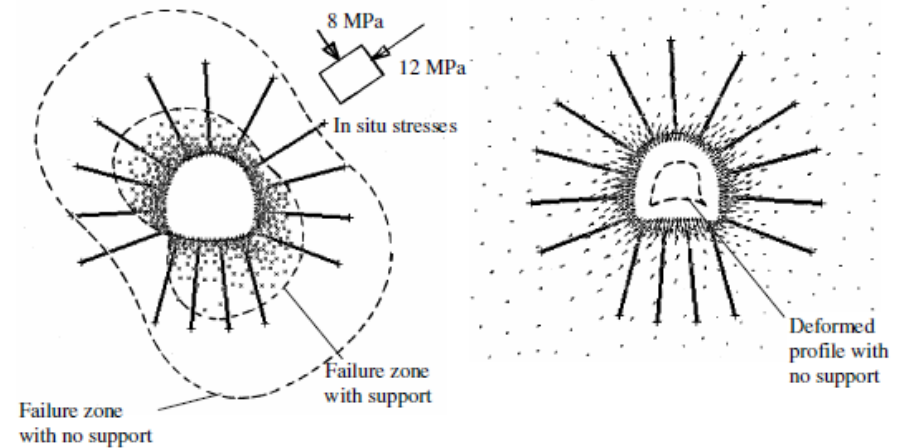| Intact rock strength MPa	σ_{ci}	50	Hoek-Brown constant	m_b	0.481
Hoek-Brown constant	mi	10	Hoek-Brown constant	s	0.0002
Geological Strength Index	GSI	25	Hoek-Brown constant	a	0.53
			Deformation modulus MPa	E_m	1000

Figure 29: Results of a numerical analysis of the failure of the rock mass surrounding the Yacambu-Quibor tunnel when excavated in graphitic phyllite at a depth of about 600 m below surface.

Figure 30: Displacements in the rock mass surrounding the Yacambu-Quibor tunnel. The maximum calculated displacement is 258 mm with no support and 106 mm with support.

Various support methods have been used on this tunnel and only one will be considered here. This was a trial section of tunnel, at a depth of about 600 m, constructed in 1989. The support of the 5.5 m span tunnel was by means of a complete ring of 5 m long, 32 mm diameter untensioned grouted dowels with a 200 mm thick shell of reinforced shotcrete. This support system proved to be very effective but was later abandoned in favour of yielding steel sets (steel sets with sliding joints) because of construction schedule considerations. In fact, at a depth of 1200 m below surface (2004-2006) it is doubtful if the rockbolts would have been effective because of the very large deformations that could only be accommodated by steel sets with sliding joints.

Examples of the results of a typical numerical stress analysis of this trial section, carried out using the program PHASE2[7], are given in Figures 29 and 30. Figure 29 shows the extent of failure, with and without support, while Figure 30 shows the displacements in the rock mass surrounding the tunnel. Note that the criteria used to judge the effectiveness of the support design are that the zone of failure surrounding the tunnel should lie within the envelope of the rockbolt support, the rockbolts should not be stressed to failure and the displacements should be of reasonable magnitude and should be uniformly distributed around the tunnel. All of these objectives were achieved by the support system described earlier.